doi : 10.17596/0003716

R/V Mirai Cruise Report

MR99-K03
"Nauru99"

8 June - 17 July, 1999

Japan Marine Science and Technology Center
(JAMSTEC)

Nauru99ers on board R/V Mirai

MR99-K03 Cruise Report

[Contents]

1. Introduction

The R/V MIRAI MR99-K03 cruise was meant for the participation into the international field experiment Nauru99, that is a collaborative research campaign of three agencies ; the U.S. Department of Energy (DOE), the U.S. National Oceanic and Atmospheric Administration (NOAA), and the Japan Marine Science and Technology Center (JAMSTEC) for the better understanding of the influence of the tropics onto the global climate. Especially, Tropical Western Pacific, where the warmest sea surface temperature exists and is called the "warm water pool", is thought to play the role of heat engine for the climate variations of the entire globe. DOE's Atmospheric Radiation Measurement (ARM) Program, which is the sponsoring agency of Nauru99, has deployed and started to operate the Atmospheric Radiation and Cloud Station (ARCS) on Nauru island from November 1998. The island of Nauru is located just eastern edge of the warm water pool. The main objective of Nauru99 is to improve our understanding of radiant heat transfer and the effects of clouds on the ocean weather processes through land-, air-, and ocean-based measurements. In addition to the ARCS on Nauru island, JAMSTEC's R/V MIRAI and NOAA's R/V Ronald H. Brown served as platforms for taking intensive and simultaneous measurements. The Cessna aircraft from Flinders University of Australia and NOAA's TAO buoys were also playing key measurement roles.

The R/V MIRAI kept the position at three different phases for each particular purpose. From 17 through 19 June, we kept just off Nauru within 1 mile for the intercomparison of ship- and land-measurements. As second phase, we made stationary observation at (0, 165E) where TAO buoy is deployed to form the apex of "large triangle configuration" with Nauru ARCS site and R/V Ronald H. Brown (2S, 165E) from 20 through 30 June. This large triangle configuration was meant to provide the necessary data for a single column model, in addition to study the meso-scale phenomena and intercomparison with buoy data. Finally, as third phase we kept the position at (0.18S, 166.85E) to form the "small triangle configuration" while R/V Ronald H. Brown was at (0.52S, 166.72E) for the dual Doppler radar observation from 1 through 4 July. However, unfortunately, we had no significant rainfall during this small triangle phase. So, on 3 July, R/V Ronald H. Brown came to close R/V MIRAI and did an intercomparison of ship-to-ship measurement.

In this cruise report, we describe what measurements were done for the above purposes. We summed up briefly the personnel, objectives, measured parameters, methods, and preliminary results. Further detailed study will be carried out immediately and all data set will be open to the public according to the Nauru99 data protocol.

2. Cruise Summary

2.1 Ship

Name	R/V MIRAI
L×B×D	128.6 m × 19.0 m × 13.2 m
Gross Tonnage	8,672 tons
Call sign	JNSR
Mother Port	Mutsu, Aomori Pref.

2.2 Cruise Code

MR99-K03

2.3 Project Name

The Study of Air-Sea Interaction in the Tropics
and International field experiment Nauru99

2.4 Undertaking Institute

Japan Marine Science and Technology Center (JAMSTEC)
2-15, Natsushima, Yokosuka 237-0061, JAPAN

2.5 Chief Scientist

Kunio Yoneyama (Ocean Research Department / JAMSTEC)

2.6 Periods and Ports of call

Leg - 1	From 08 June 1999 (Yokohama)	to 13 June 1999 (Chuuk, F.S.M.)
Leg - 2	From 14 June 1999 (Chuuk)	to 06 July 1999 (Majuro, Marshall Islands)
	calling at Nauru from 17 through 19 June 1999	
Leg - 3	From 07 July 1999 (Majuro)	to 17 July 1999 (Tsuruga)
	stopping at Guam, U.S.A. as emergency call on 11 July 1999	

2.7 Observation Summary

C-band Doppler radar	continuously
Radiosonde launching	179 times
Wind Profiler with RASS	continuously
Ceilometer	continuously
Total Sky Imager	continuously
LIDAR	continuously
Surface Meteorology	continuously
Skin Sea Surface Temperature	continuously
Turbulent Measurement	continuously
Disdrometer	continuously
Aerosol sampling	continuously
CTD	129 castings
ADCP	continuously
Sea Surface Water Monitoring	continuously
pCO2 measurement	continuously
Greenhouse effect gas measurement	continuously

3. List of Instruments

3.1 General Meteorological Observation

(1) JAMSTEC

Koshin Denki anemometer KE-500
Koshin Denki thermometer FT
Koshin Denki dew point meter DW-1
Yokogawa barometer F-451
R.M. Young rain gauge 50202
SCTI optical rain gauge ORG-115DR
Tsurumi-seiki wave height meter MW-2
Yankee Engineering System total sky imager

(2) NCAR and NOAA/ETL

R.M.Young Wind Head
Vaisala Temperature R/H Sensor
Vaisala Pressure Sensor

(3) BNL

Volunteer Ship Observing System (VSOS) Meteorological Package

R.M. Young wind monitor
STI optical rain gauge (mini-ORG)
R.M. Young rain gauge
Vaisala T/RH sensor with R.M. Young aspirator
R.M. Young barometer
Sea Snake (PRT temperature sensor with 4-20 mA interface)
Zeno data logger

3.2 Radiosonde Observation

(1) JAMSTEC

Vaisala GPS radiosonde RS80-GH
Vaisala DigiCORA MW11

3.3 Doppler Radar Observation

(1) JAMSTEC

Mitsubishi Electric C-band Doppler radar RC-52B
Sigmet signal processor RVP-6
Sigmet antenna controller RCP-02
Sigmet IRIS/Open
Honeywell inertial navigation unit DRUH

3.4 Disdrometer

(1) Yamaguchi Univ.

Portable disdrometer

3.5 Vertical Profilers

(1) JAMSTEC

Vaisala Ceilometer CT-25K

(2) NCAR and NOAA/ETL

DBS 915MHz Wind Profiling Radar

MAPR 915MHz Wind Profiling Radar

RASS [Radio Acoustic Sounding System]

S-BAND Cloud Profiling Radar

3.6 Lidar Observation

(1) NIES and Tohoku Institute of Technology

Compact Mie Scattering Lidar

3.7 Surface Flux Measurement

(1) Okayama Univ. and MUK

Supersonic Thermoanemometer

IR Hygrometer

Greenhouse Effect Gases Measuring Unit

3.8 Radiative Flux Measurement

(1) JAMSTEC

Eiko Seiki short wave radiometer MS-801 (upward and downward)

Eiko Seiki long wave radiometer MS-200 (upward and downward)

(2) MUK and MRI

Sun photometer

Pyrheliometer

Multipurpose Spectroradiometer

(3) NCAR and NOAA/ETL

Epply PSP Solar Radiation Sensor [visible]

Epply PYG Solar Radiation Sensor [IR.]

Microwave Radiometer

(4) BNL

Portable Radiation Package

Eppley Precision Spectral Pyranometer (PSP)

Eppley Precision Infrared Radiometer (PIR)

Fast Rotating Shadowband Radiometer (FRSR)

PNI flux-gate compass and pitch/roll sensor

Brookhaven National Laboratory data logger (DL99)

Microtops Handheld Sun Photometer

3.9 SSST Measurement

(1) RSMAS

Marine-Atmosphere Emitted Radiance Interferometer (M-AERI)

(2) Rutherford Appleton Laboratory

Scanning IR SST Radiometer (SISTeR)

(3) NCAR and NOAA/ETL

SST Sea Surface Temperature Probe

(4) BNL

Sea Snake (PRT temperature sensor with 4-20 mA interface)

3.10 CTD

(1) JAMSTEC

Sea-Bird CTD 9plus
Sea-Bird temperature sensor SBE3-04/F
Sea-Bird conductivity sensor SBE-4-04/0
Sea-Bird oxygen sensor 13-04-B
Sea-Bird deck unit SBE 11plus
Benthos altimeter 2110-2

3.11 Sea Surface Water Monitoring

(1) JAMSTEC

SEACAT Thermosalinograph SBE-21
Oubisufair Laboratories dissolved oxygen sensor
Turner Designs Fluorometer 10-AU-005
Nippon Kaiyo Particle Size Sensor P-05

3.12 Current Profiling

(1) JAMSTEC

RD Instrument broad-band ADCP VM-75

3.13 Miscellaneous

(1) JAMSTEC

Sena navigation system SAINS19
Nippon Hakuyo GMS receiving system
Terascan HRPT receiving system

(2) NCAR and NOAA/ETL

KVH Flux Gate Compass
Garman GPS Unit
Tilt & Accelerometer Sensors

(3) BNL

Scientific Computer System (SCS)

Micron Computer, NT OS
Digiport 16-com serial port

2.8 Data Policy

All data obtained during this cruise will be under the control of the Data Management Office (DMO) of JAMSTEC and follow the R/V MIRAI Data Policy (see Appendix).

Since this cruise is involved in the international field experiment Nauru99, all data also must follow the Nauru99 Data Protocol (see Appendix).

2.9 Overview

During the entire Intensive Observation Period (IOP : 17 June - 4 July), the R/V MIRAI had been located just in the convectively suppressed area/period, although the Sea Surface Temperature (SST) showed always around 29℃. This period is considered as corresponded to the end of La Nina-like phase just after the largest 1997/98 El Nino event in its history. From the TAO buoy data, it is evident that high SST (>29℃) existed west of 160E and easterlies were prevailed along the equator. From the satellite (GMS) cloud images, ITCZ could be found along 5N and was very active. Convectively very active (cloud clusters) area existed west of our observation area near the island of Nauru and apparently easterly wind blew into these clouds area. This area seemed to move eastward but did not reach us until we left there.

Because of this fine weather condition, we could obtain various data set related to solar radiation. Instead, unfortunately, we miss to conduct dual Doppler radar observation with NOAA's R/V Ronald H. Brown during the small triangle phase. For this reason, we changed the schedule a little bit and did an intercomparison of ship-to-ship measurement on 3 July.

2.10 Acknowledgment

This cruise is successfully accomplished with the skilful help of Captain Akamine and his crew. This Nauru99 cruise is carried out as collaborative work of DOE's ARM, NOAA, and JAMSTEC. Especially Nauru government is highly appreciated for their enormous help to conduct this campaign. To have Nauru officials as guests on board was a great honor for all of us.

As one sad accident Ms.Hanafin of Univ. of Miami broke her leg during the cruise from Majuro. We deeply express our sincere concern for her and do hope her quick recovery.

Finally, as a personal view of chief scientist of the cruise, I deeply thank to all on board scientists, engineers, and technical staff for their effort and smile. Of course, all kind of support from land was also inevitable. I could enjoy this cruise and definitely believe that fruitful results will be produced using the data obtained during this cruise.

4. Cruise Track and Log

4.1 Cruise Track

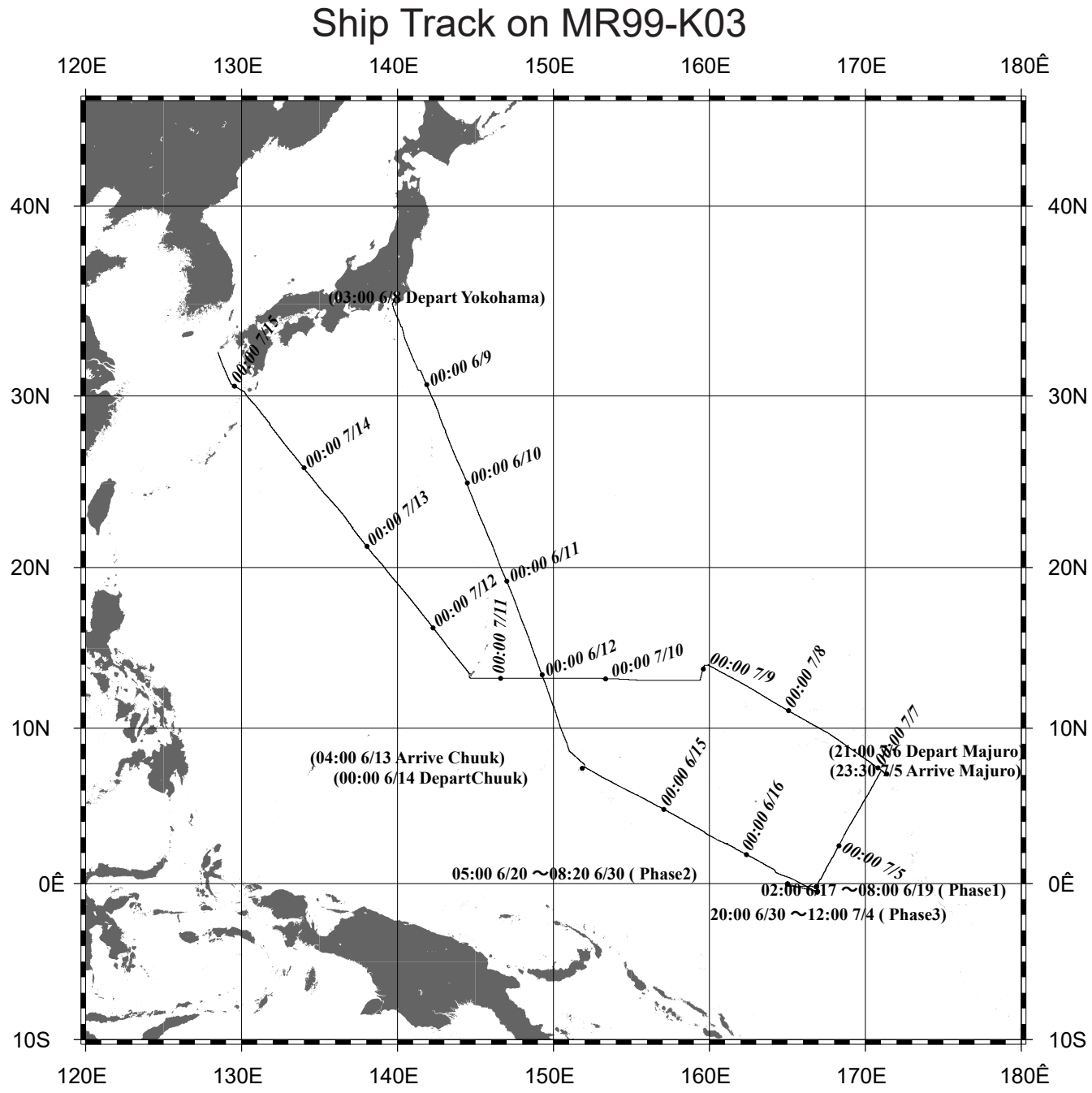

Fig. 4-1: Cruise track on MR99-K03.

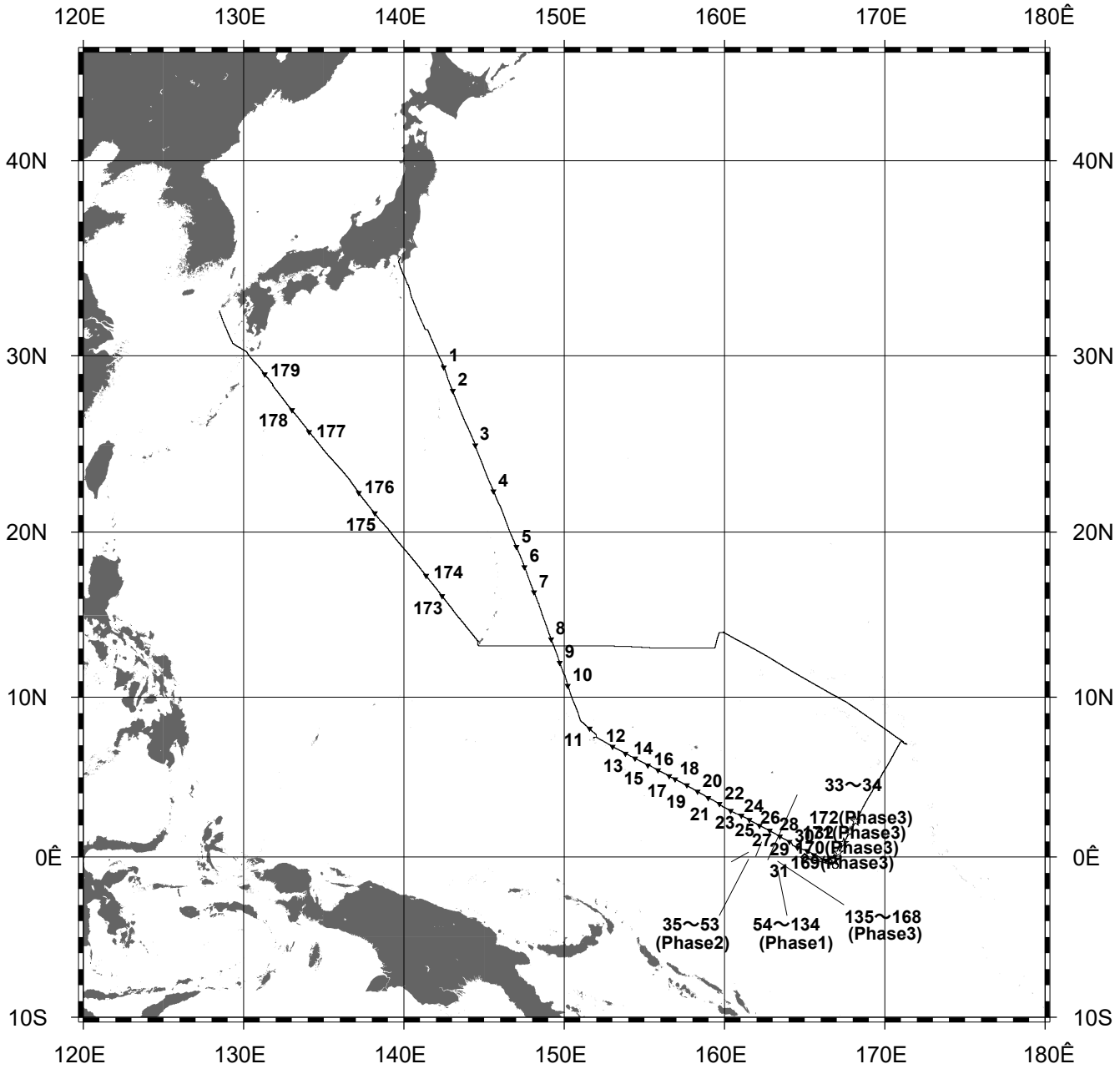

Fig. 4-2: Locations of radiosonde observation in MR99-K03. The number corresponds to the observation number in Cruise Log.

4.2 Cruise Log

Date	LST	UTC	Event	Lat.(deg.)	Lon. (deg.)
8-Jun			Fine		
	12:00	03:00	Depart Yokohama		
	15:00	06:00	Fire Drill		
	15:30	06:30	Briefing for safety instruction		
	19:30	10:30	Start oceanic environment monitoring system		
	23:15	14:15	Start Doppler radar observation		
9-Jun			Cloudy / Rainy		
	09:00	00:00	General meeting for observation / research		
	15:36	06:36	RS (Radiosonde Observation) - 001	29.30 N	142.53 E
	20:33	11:33	RS-002	28.02 N	143.06 E
10-Jun			Fine		
	09:34	00:34	RS-003	24.94 N	144.47 E
	20:31	11:31	RS-004	22.22 N	145.67 E
11-Jun			Fine		
	08:15	23:15	PI (Principle Investigtor) meeting		
	09:41	00:41	RS-005	19.00 N	147.06 E
	14:31	05:31	RS-006	17.85 N	147.56 E
	20:37	11:37	RS-007	16.35 N	137.56 E
12-Jun			Fine		
	08:15	23:15	PI meeting		
	08:39	23:39	RS-008	13.44 N	149.23 E
	14:31	05:31	RS-009	12.04 N	149.75 E
	20:24	11:24	RS-010	10.64 N	150.26 E
	22:00	12:00	Local Time Adjustment (LT = UT+10h)		
13-Jun			Rainy		
	08:15	22:15	PI meeting		
	09:30	23:30	RS-011	7.97 N	151.64 E
			Pause Doppler radar observation		
	14:00	04:00	Arrive Chuuk		
14-Jun			Fine		
	10:00	00:00	Depart Chuuk		
	13:00	03:00	PI meeting		
	13:15	03:15	Resume oceanic environment monitoring system		
			Resume Doppler radar observation		
	15:39	05:39	RS-012	6.89 N	153.09 E
	19:01	09:01	RS-013	6.47 N	153.89 E
	21:30	11:30	RS-014	6.16 N	154.49 E
	22:00	12:00	Local Time Adjustment (LT = UT+11h)		
15-Jun			Fine		
	01:53	14:53	RS-015	5.75 N	155.29 E
	04:30	17:30	RS-016	5.43 N	155.91 E
	07:36	20:36	RS-017	5.02 N	156.65 E
	08:32	21:32	Test of "Sea Snake" and Ocean Color Sensors		
	10:47	23:47	RS-018	4.84 N	157.03 E
	13:50	02:50	RS-019	4.44 N	157.76 E
	16:40	05:40	RS-020	4.03 N	158.47 E
	19:33	08:33	RS-021	3.68 N	159.10 E
	22:00	10:00	Local Time Adjustment (LT = UT+12h)		

	23:23	11:23	RS-022	3.25	N	159.74	E
16-Jun			Fine				
	02:31	14:31	RS-023	2.87	N	160.46	E
	05:38	17:38	RS-024	2.59	N	161.14	E
	08:15	20:15	PI meeting				
	08:24	20:24	RS-025	2.30	N	161.63	E
	11:28	23:28	RS-026	1.95	N	162.26	E
	14:27	02:27	RS-027	1.53	N	162.88	E
	17:39	05:39	RS-028	1.26	N	163.53	E
	20:32	08:32	RS-029	0.95	N	164.11	E
	23:24	11:24	RS-030	0.59	N	164.59	E
17-Jun			Fine				
	02:24	14:24	RS-031	0.37	N	165.21	E
	05:29	17:29	RS-032	0.05	N	165.82	E
	08:15	20:15	PI meeting				
	08:26	20:26	RS-033	0.27	S	166.40	E
	11:28	23:28	RS-034	0.49	S	166.89	E
	12:00	00:00	Arrive IOP Phase-1 observation point				
	14:00	02:00	Start IOP Phase-1 "Island-ship Intercomparison"				
	14:20	02:20	RS-035	0.52	S	166.91	E
	14:25	02:25	CTD-001 (200 m)	0.52	S	166.91	E
	15:07	03:07	Turbulent flux measurement				
	17:42	05:42	RS-036	0.52	S	166.91	E
	17:47	05:47	CTD-002 (200 m)	0.52	S	166.90	E
	18:22	06:22	Turbulent flux measurement				
	20:30	08:30	CTD-003 (200 m)	0.52	S	166.91	E
	20:45	08:45	RS-037	0.52	S	166.91	E
	21:04	09:04	Turbulent flux measurement				
	23:24	11:24	RS-038	0.52	S	166.91	E
	23:33	11:33	CTD-004 (200 m)	0.52	S	166.90	E
18-Jun			Fine				
	00:10	12:10	Turbulent flux measurement				
	02:25	14:25	CTD-005 (200 m)	0.52	S	166.91	E
	02:46	14:46	RS-039	0.52	S	166.91	E
	03:12	15:12	Turbulent flux measurement				
	05:23	17:23	RS-040	0.52	S	166.91	E
	05:25	17:25	CTD-006 (200 m)	0.52	S	166.91	E
	06:07	18:07	Turbulent flux measurement				
	08:00	20:00	PI meeting				
	08:11	20:11	RS-041	0.52	S	166.91	E
	08:11	20:11	CTD-007 (200 m)	0.52	S	166.91	E
	08:45	20:45	Turbulent flux measurement				
	10:40	22:40	Nauru Government Staff arrive				
	11:21	23:21	RS-042	0.52	S	166.90	E
	11:27	23:27	CTD-008 (200 m)	0.52	S	166.90	E
	11:58	23:58	Turbulent flux measurement				
	12:00	00:00	Nauru Government Staff leave / PI's depart for Nauru				
	14:23	02:23	RS-043	0.52	S	166.91	E
	14:31	02:31	CTD-009 (200 m)	0.52	S	166.90	E
	15:05	03:05	Turbulent flux measurement				
	16:35	04:35	PI's come back				
	17:15	05:15	CTD-010 (200 m)	0.52	S	166.91	E
	17:37	05:37	RS-044	0.52	S	166.90	E
	18:00	06:00	Turbulent flux measurement				
	20:20	08:20	CTD-011 (200 m)	0.52	S	166.91	E
	20:40	08:40	RS-045	0.52	S	166.91	E

	21:04	09:04	Turbulent flux measurement					
	23:23	11:23	CTD-012 (200 m)	0.52	S	166.91	E	
	23:39	11:39	RS-046	0.52	S	166.91	E	
19-Jun			Fine					
	00:03	12:03	Turbulent flux measurement					
	02:25	14:25	CTD-013 (200 m)	0.52	S	166.91	E	
	03:10	15:10	Turbulent flux measurement					
	05:29	17:29	RS-047	0.52	S	166.91	E	
	05:34	17:34	CTD-014 (200 m)	0.52	S	166.91	E	
	06:18	18:18	Turbulent flux measurement					
	08:00	20:00	PI meeting					
	08:24	20:24	CTD-015 (200 m)	0.52	S	166.91	E	
	09:00	21:00	Turbulent flux measurement					
	10:40	22:40	Nauru ARCS observation staff arrive					
	11:20	23:20	RS-048	0.52	S	166.90	E	
	11:25	23:25	CTD-016 (200 m)	0.52	S	166.90	E	
	12:40	00:40	Nauru ARCS observation staff leave					
	13:14	01:14	Turbulent flux measurement					
	14:24	02:24	CTD-017 (200 m)	0.52	S	166.91	E	
	14:30	02:30	Continuous RASS obs. Starts (to 17:30 LT)					
	15:00	03:00	Turbulent flux measurement					
	17:21	05:21	RS-049	0.52	S	166.90	E	
	17:30	05:30	CTD-018 (200 m)	0.52	S	166.90	E	
	20:00	08:00	Finish IOP Phase-1/ start moving to phase-2 station					
	23:29	11:29	RS-050	0.39	S	166.49	E	
20-Jun			Fine					
	05:27	17:27	RS-051	0.09	S	165.29	E	
	11:23	23:23	RS-052	0.01	S	164.99	E	
	13:00	01:00	ATLAS buoy repairing operation					
	14:26	02:26	RS-053	0.01	S	165.02	E	
	17:00	05:00	Start IOP Phase-2 "Large Triangle"					
	17:22	05:22	RS-054	0.02	N	164.99	E	
	17:27	05:27	CTD-019 (500 m)	0.02	N	164.99	E	
	17:58	05:58	Turbulent flux measurement					
	20:25	08:25	RS-055	0.02	S	164.99	E	
	20:26	08:26	CTD-020 (200 m)	0.02	S	164.99	E	
	20:43	08:43	Turbulent flux measurement					
	23:24	11:24	RS-056	0.02	S	164.99	E	
	23:27	11:27	CTD-021 (200 m)	0.02	S	164.99	E	
	23:50	11:50	Turbulent flux measurement					
21-Jun			Fine					
	02:23	14:23	RS-057	0.02	N	164.99	E	
	02:28	14:28	CTD-022 (200 m)	0.02	N	164.99	E	
	02:48	14:48	Turbulent flux measurement					
	05:24	17:24	RS-058	0.01	N	164.99	E	
	05:28	17:28	CTD-023 (200 m)	0.01	N	164.99	E	
	05:55	17:55	Turbulent flux measurement					
	08:00	20:00	PI meeting					
	08:20	20:20	RS-059	0.00	S	164.99	E	
	08:25	20:25	CTD-024 (200 m)	0.00	S	164.98	E	
	08:42	20:42	Turbulent flux measurement					
	11:21	23:21	RS-060	0.00	S	164.99	E	
	11:25	23:25	CTD-025 (1000 m)	0.00	S	164.99	E	
	12:20	00:20	Turbulent flux measurement					
	14:22	02:22	RS-061	0.00	N	164.99	E	
	14:25	02:25	CTD-026 (200 m)	0.00	N	164.99	E	

	14:44	02:44	Turbulent flux measurement					
	17:22	05:22	RS-062	0.00	N	164.99	E	
	17:26	05:26	CTD-027 (500 m)	0.00	N	164.99	E	
	18:15	06:15	Turbulent flux measurement					
	20:22	08:22	RS-063	0.01	S	164.99	E	
	20:24	08:24	CTD-028 (200 m)	0.01	S	164.99	E	
	20:39	08:39	Turbulent flux measurement					
	23:21	11:21	RS-064	0.01	S	165.00	E	
	23:24	11:24	CTD-029 (500 m)	0.01	S	165.00	E	
	23:48	11:48	Turbulent flux measurement					
22-Jun			Fine					
	02:19	14:19	RS-065	0.00	S	164.99	E	
	02:23	14:23	CTD-030 (200 m)	0.00	S	164.99	E	
	03:05	15:05	Turbulent flux measurement					
	05:21	17:21	RS-066	0.00	S	165.00	E	
	05:26	17:26	CTD-031 (500 m)	0.01	S	165.00	E	
	05:52	17:52	Turbulent flux measurement					
	08:00	20:00	PI meeting	0.01	S	165.00	E	
	08:21	20:21	RS-067	0.01	S	165.00	E	
	08:25	20:25	CTD-032 (200 m)	0.01	S	165.00	E	
	08:41	20:41	Turbulent flux measurement					
	11:20	23:20	RS-068	0.01	S	165.00	E	
	11:24	23:24	CTD-033 (1000 m)	0.01	S	165.01	E	
	12:14	00:14	Turbulent flux measurement					
	14:23	02:23	RS-069	0.02	S	165.00	E	
	14:27	02:27	CTD-034 (200 m)	0.02	S	165.00	E	
	14:58	02:58	Turbulent flux measurement					
	17:22	05:22	RS-070	0.00	S	164.99	E	
	17:26	05:26	CTD-035 (500 m)	0.00	S	164.99	E	
	17:54	05:54	Turbulent flux measurement					
	20:22	08:22	RS-071	0.01	S	164.99	E	
	20:24	08:24	CTD-036 (200 m)	0.01	S	164.99	E	
	20:42	08:42	Turbulent flux measurement					
	23:25	11:25	RS-072	0.00	S	164.99	E	
	23:26	11:26	CTD-037 (500 m)	0.00	S	164.99	E	
	23:51	11:51	Turbulent flux measurement					
23-Jun			Fine					
	02:25	14:25	RS-073	0.00	S	164.99	E	
	02:30	14:30	CTD-038 (200 m)	0.00	S	164.99	E	
	02:55	14:55	Turbulent flux measurement					
	05:24	17:24	RS-074	0.03	S	165.01	E	
	05:34	17:34	CTD-039 (500 m)	0.03	S	165.01	E	
	06:07	18:07	Turbulent flux measurement					
	08:00	20:00	PI meeting	0.01	S	164.99	E	
	08:24	20:24	RS-075	0.01	S	164.99	E	
	08:31	20:31	CTD-040 (200 m)	0.01	S	164.99	E	
	08:48	20:48	Turbulent flux measurement					
	11:21	23:21	RS-076	0.00	S	165.00	E	
	11:24	23:24	CTD-041(1000 m)	0.00	S	165.00	E	
	12:14	00:14	Turbulent flux measurement					
	14:23	02:23	RS-077	0.01	S	165.01	E	
	14:28	02:28	CTD-042 (200 m)	0.01	S	165.01	E	
	14:45	02:45	Turbulent flux measurement					
	17:21	05:21	RS-078	0.00	S	164.99	E	
	17:24	05:24	CTD-043 (500 m)	0.00	S	164.99	E	
	17:50	05:50	Turbulent flux measurement					
	20:22	08:22	RS-079	0.00	S	165.00	E	

	20:25	08:25	CTD-044 (200 m)	0.01	S	165.00	E
	20:40	08:40	Turbulent flux measurement				
	23:27	11:27	RS-080	0.01	S	165.00	E
	23:30	11:30	CTD-045 (500 m)	0.01	S	165.00	E
	23:55	11:55	Turbulent flux measurement				
24-Jun			Fine				
	02:23	14:23	RS-081	0.01	S	165.00	E
	02:28	14:28	CTD-046 (200 m)	0.01	S	165.00	E
	02:45	14:45	Turbulent flux measurement				
	05:26	17:26	RS-082	0.01	S	165.00	E
	05:30	17:30	CTD-047 (500 m)	0.02	S	165.00	E
	06:00	18:00	Turbulent flux measurement				
	08:00	20:00	PI meeting				
	08:21	20:21	RS-083	0.01	S	165.00	E
	08:24	20:24	CTD-048	0.01	S	164.99	E
	08:48	20:48	Turbulent flux measurement				
	10:30	22:30	Aircraft Observation (passing by)				
	11:24	23:24	RS-084	0.01	S	165.00	E
	11:26	23:26	CTD-049 (1000 m)	0.01	S	165.01	E
	12:20	00:20	Turbulent flux measurement				
	14:00	02:00	Aircraft Observation (passing by)				
	14:22	02:22	RS-085	0.01	S	165.01	E
	14:25	02:25	CTD-050 (200 m)	0.01	S	165.01	E
	14:50	02:50	Turbulent flux measurement				
	17:20	05:20	RS-086	0.00	S	165.00	E
	17:27	05:27	CTD-051 (500 m)	0.01	S	165.00	E
	17:58	05:58	Turbulent flux measurement				
	20:28	08:28	RS-087	0.01	S	164.99	E
	20:32	08:32	CTD-052 (200 m)	0.01	S	164.99	E
	20:49	08:49	Turbulent flux measurement				
	23:24	11:24	RS-088	0.01	S	164.99	E
	23:28	11:28	CTD-053 (500 m)	0.01	S	164.99	E
	23:55	11:55	Turbulent flux measurement				
25-Jun			Rainy / Fine				
	02:24	14:24	RS-089	0.00	S	165.00	E
	02:30	14:30	CTD-054 (200 m)	0.00	S	164.99	E
	02:50	14:50	Turbulent flux measurement				
	05:23	17:23	RS-090	0.01	S	165.00	E
	05:26	17:26	CTD-055 (500 m)	0.01	S	165.00	E
	05:52	17:52	Turbulent flux measurement				
	08:00	20:00	PI meeting				
	08:22	20:22	RS-091	0.01	S	165.00	E
	08:29	20:29	CTD-056 (200 m)	0.01	S	165.00	E
	08:47	20:47	Turbulent flux measurement				
	10:30	22:30	Tethered sonde observation				
	10:45	22:45	Aircraft Observation (passing by)				
	11:23	23:23	RS-092	0.00	S	165.00	E
	11:26	23:26	CTD-057 (1000 m)	0.00	S	165.00	E
	12:18	00:18	Turbulent flux measurement				
	13:46	01:46	Tethered sonde observation				
	14:20	02:20	Aircraft Observation (passing by)	0.01	S	165.00	E
	14:22	02:22	RS-093	0.01	S	165.00	E
	14:28	02:28	CTD-058 (200 m)	0.01	S	165.00	E
	14:44	02:44	Turbulent flux measurement				
	16:45	04:45	Tethered sonde observation				
	17:22	05:22	RS-094	0.01	S	164.99	E
	17:25	05:25	CTD-059 (500 m)	0.01	S	164.99	E

	17:50	05:50	Turbulent flux measurement					
	19:41	07:41	Tethered sonde observation					
	20:20	08:20	RS-095	0.01	S	164.99	E	
	20:24	08:24	CTD-060 (200 m)	0.01	S	164.99	E	
	20:40	08:40	Turbulent flux measurement					
	23:23	11:23	RS-096	0.01	S	165.00	E	
	23:27	11:27	CTD-061 (500 m)	0.01	S	165.00	E	
	23:59	11:59	Turbulent flux measurement					
26-Jun			Fine					
	02:23	14:23	RS-097	0.01	S	165.00	E	
	02:27	14:27	CTD-062 (200 m)	0.01	S	165.00	E	
	02:45	14:45	Turbulent flux measurement					
	05:23	17:23	RS-098	0.01	S	165.00	E	
	05:30	17:30	CTD-063 (500 m)	0.01	S	165.00	E	
	05:57	17:57	Turbulent flux measurement					
	08:00	20:00	PI meeting					
	08:20	20:20	RS-099	0.01	S	165.00	E	
	08:24	20:24	CTD-064 (200 m)	0.02	S	165.00	E	
	08:42	20:42	Turbulent flux measurement					
	11:22	23:22	RS-100	0.02	S	165.00	E	
	11:25	23:25	CTD-065 (1000 m)	0.02	S	165.01	E	
	12:13	00:13	Turbulent flux measurement					
	13:27	01:27	Tethered sonde observation					
	14:32	02:32	RS-101	0.04	S	165.00	E	
	15:05	03:05	CTD-066 (200 m)	0.01	S	165.00	E	
	15:21	03:21	Turbulent flux measurement					
	17:21	05:21	RS-102	0.01	S	164.99	E	
	17:24	05:24	CTD-067 (500 m)	0.01	S	165.00	E	
	17:48	05:48	Turbulent flux measurement					
	20:21	08:21	RS-103	0.01	S	165.00	E	
	20:25	08:25	CTD-068 (200 m)	0.01	S	165.00	E	
	20:41	08:41	Turbulent flux measurement					
	23:23	11:23	RS-104	0.01	S	165.00	E	
	23:29	11:29	CTD-069 (500 m)	0.01	S	165.00	E	
	23:54	11:54	Turbulent flux measurement					
27-Jun			Fine / Rainy					
	02:23	14:23	RS-105	0.01	S	165.00	E	
	02:27	14:27	CTD-070 (200 m)	0.01	S	165.00	E	
	02:50	14:50	Turbulent flux measurement					
	05:24	17:24	RS-106	0.01	S	165.00	E	
	05:28	17:28	CTD-071 (500 m)	0.01	S	165.00	E	
	05:54	17:54	Turbulent flux measurement					
	08:00	20:00	PI meeting					
	08:21	20:21	RS-107	0.01	S	165.00	E	
	08:27	20:27	CTD-072 (200 m)	0.01	S	165.00	E	
	08:43	20:43	Turbulent flux measurement					
	10:17	22:17	Aircraft Observation (passing by)					
	11:20	23:20	RS-108	0.01	S	165.00	E	
	11:24	23:24	CTD-073 (1000 m)	0.01	S	165.00	E	
	12:07	00:07	Turbulent flux measurement					
	13:35	01:35	Aircraft Observation (vertical profiling)					
	14:21	02:21	RS-109	0.01	S	165.00	E	
	14:25	02:25	CTD-074 (200 m)	0.01	S	165.00	E	
	14:44	02:44	Turbulent flux measurement					
	17:23	05:23	CTD-075 (500 m)	0.01	S	165.00	E	
	18:01	06:01	RS-110	0.01	S	165.00	E	
	18:03	06:03	Turbulent flux measurement					

	20:21	08:21	RS-111	0.01	S	164.99	E
	20:24	08:24	CTD-076 (200 m)	0.01	S	164.99	E
	20:42	08:42	Turbulent flux measurement				
	23:22	11:22	RS-112	0.01	S	164.99	E
	23:24	11:24	CTD-077 (500 m)	0.01	S	164.99	E
	23:52	11:52	Turbulent flux measurement				
28-Jun			Rainy / Cloudy / Fine				
	02:22	14:22	RS-113	0.01	S	165.00	E
	02:25	14:25	CTD-078 (200 m)	0.01	S	165.00	E
	02:43	14:43	Turbulent flux measurement				
	05:24	17:24	RS-114	0.01	S	165.00	E
	05:29	17:29	CTD-079 (500 m)	0.01	S	165.00	E
	05:56	17:56	Turbulent flux measurement				
	08:00	20:00	PI meeting	0.01	S	165.00	E
	08:22	20:22	RS-115	0.01	S	165.00	E
	08:26	20:26	CTD-080 (200 m)	0.01	S	165.00	E
	08:45	20:45	Turbulent flux measurement				
	10:20	22:20	Aircraft Observation (passing by + vertical profiling)				
	10:27	22:27	Drop ATLAS data cable from the aircraft				
	10:31	22:31	Scooping cable up				
	11:20	23:20	RS-116	0.01	S	165.00	E
	11:24	23:24	CTD-081 (1000 m)	0.01	S	165.00	E
	12:08	00:08	Turbulent flux measurement				
	14:23	02:23	RS-117	0.01	S	165.00	E
	14:28	02:28	CTD-082 (200 m)	0.01	S	165.00	E
	14:45	02:45	Turbulent flux measurement				
	17:20	05:20	RS-118	0.01	S	165.00	E
	17:24	05:24	CTD-083 (500 m)	0.01	S	165.00	E
	17:48	05:48	Turbulent flux measurement				
	20:21	08:21	RS-119	0.01	S	164.99	E
	20:24	08:24	CTD-084 (200 m)	0.01	S	164.99	E
	20:40	08:40	Turbulent flux measurement				
	23:24	11:24	RS-120	0.01	S	164.99	E
	23:28	11:28	CTD-085 (500 m)	0.01	S	164.99	E
	23:53	11:53	Turbulent flux measurement				
29-Jun			Fine				
	02:29	14:29	RS-121	0.01	S	164.98	E
	02:34	14:34	CTD-086 (200 m)	0.01	S	165.00	E
	02:51	14:51	Turbulent flux measurement				
	05:25	17:25	RS-122	0.01	S	165.00	E
	05:30	17:30	CTD-087 (500 m)	0.01	S	165.00	E
	05:56	17:56	Turbulent flux measurement				
	08:00	20:00	PI meeting				
	08:21	20:21	RS-123	0.01	S	165.00	E
	08:24	20:24	CTD-088 (200 m)	0.01	S	165.00	E
	08:41	20:41	Turbulent flux measurement				
	11:20	23:20	RS-124	0.01	S	165.00	E
	11:24	23:24	CTD-089 (1000 m)	0.01	S	165.00	E
	12:12	00:12	Turbulent flux measurement				
	14:27	02:27	RS-125 / Sphere calibration for Doppler radar	0.01	S	164.98	E
	14:44	02:44	CTD-090 (200 m)	0.00	S	165.00	E
	15:00	03:00	Turbulent flux measurement				
	17:21	05:21	RS-126	0.01	S	165.00	E
	17:24	05:24	CTD-091 (500 m)	0.01	S	165.00	E
	17:47	05:47	Turbulent flux measurement				
	20:21	08:21	RS-127	0.01	S	164.99	E
	20:24	08:24	CTD-092 (200 m)	0.01	S	164.99	E

	20:41	08:41	Turbulent flux measurement					
	23:19	11:19	RS-128	0.01	S	164.99	E	
	23:22	11:22	CTD-093 (1000 m)	0.01	S	164.99	E	
	23:46	11:46	Turbulent flux measurement					
30-Jun			Fine					
	02:21	14:21	RS-129	0.01	S	165.00	E	
	02:25	14:25	CTD-094 (200 m)	0.01	S	165.00	E	
	02:40	14:40	Turbulent flux measurement					
	05:24	17:24	RS-130	0.01	S	165.00	E	
	05:28	17:28	CTD-095 (500 m)	0.01	S	165.00	E	
	05:54	17:54	Turbulent flux measurement					
	08:00	20:00	PI meeting					
	08:22	20:22	RS-131	0.01	S	165.00	E	
	08:24	20:24	CTD-096 (200 m)	0.01	S	165.00	E	
	08:40	20:40	Turbulent flux measurement					
	10:47	22:47	Aircraft Observation (passing by + vertical profiling)					
	11:20	23:20	RS-132	0.01	S	164.99	E	
	11:24	23:24	CTD-097 (1000 m)	0.01	S	164.99	E	
	12:06	00:06	Turbulent flux measurement					
	14:25	02:25	CTD-098 (200 m)	0.01	S	165.00	E	
	14:43	02:43	RS-133	0.01	S	165.00	E	
	14:48	02:48	Turbulent flux measurement					
	17:20	05:20	RS-134	0.01	S	165.62	E	
	17:24	05:24	CTD-099 (500 m)	0.01	S	165.01	E	
	17:50	05:50	Turbulent flux measurement					
	20:00	08:00	RS-135 / Sphere calibration for Doppler radar	0.01	S	165.01	E	
	20:20	08:20	Finish IOP Phase-2 / start moving to phase-3 station					
	23:23	11:23	RS-136	0.18	S	165.42	E	
1-Jul			Fine					
	02:23	14:23	RS-137	0.16	S	165.89	E	
	05:26	17:26	RS-138	0.16	S	166.49	E	
	08:00	20:00	PI meeting					
	08:00	20:00	Start IOP Phase-3 "Small Triangle"					
	08:20	20:20	RS-139	0.18	S	166.85	E	
	08:24	20:24	CTD-100 (200 m)	0.18	S	166.85	E	
	09:19	21:19	Camera crew arrive					
	09:24	21:24	Turbulent flux measurement					
	11:20	23:20	RS-140	0.18	S	166.85	E	
	11:23	23:23	CTD-101 (1000 m)	0.18	S	166.85	E	
	12:12	00:12	Turbulent flux measurement					
	14:21	02:21	RS-141	0.18	S	166.84	E	
	14:30	02:30	CTD-102 (200 m)	0.18	S	166.85	E	
	14:45	02:45	Turbulent flux measurement					
	17:21	05:21	RS-142	0.19	S	166.84	E	
	17:26	05:26	CTD-103 (500 m)	0.19	S	166.84	E	
	18:05	06:05	Turbulent flux measurement					
	20:22	08:22	CTD-104 (200 m)	0.19	S	166.84	E	
	20:50	08:50	RS-143	0.18	S	166.84	E	
	20:55	08:55	Turbulent flux measurement					
	23:24	11:24	RS-144	0.17	S	166.83	E	
	23:26	11:26	CTD-105 (500 m)	0.19	S	166.83	E	
	23:50	11:50	Turbulent flux measurement					
2-Jul			Fine					
	02:20	14:20	RS-145	0.19	S	166.83	E	
	02:23	14:23	CTD-106 (200 m)	0.19	S	166.83	E	
	02:38	14:38	Turbulent flux measurement					

	05:24	17:24	RS-146	0.18	S	166.85	E
	05:27	17:27	CTD-107 (500 m)	0.20	S	166.85	E
	05:53	17:53	Turbulent flux measurement				
	08:00	20:00	PI meeting				
	08:24	20:24	CTD-108 (200 m)	0.18	S	166.85	E
	08:40	20:40	RS-147	0.18	S	166.85	E
	08:46	20:46	Turbulent flux measurement				
	09:30	21:30	Camera crew left				
	09:32	21:32	Aircraft Observation (passing by + vertical profiling)				
	11:20	23:20	RS-148	0.18	S	166.86	E
	11:24	23:24	CTD-109 (1000 m)	0.18	S	166.86	E
	12:13	00:13	Turbulent flux measurement				
	14:22	02:22	RS-149	0.18	S	166.85	E
	14:26	02:26	CTD-110 (200 m)	0.18	S	166.85	E
	14:47	02:47	Turbulent flux measurement				
	17:20	05:20	RS-150	0.18	S	166.85	E
	17:25	05:25	CTD-111 (500 m)	0.18	S	166.85	E
	17:48	05:48	Turbulent flux measurement				
	20:20	08:20	RS-151	0.18	S	166.85	E
	20:25	08:25	CTD-112 (200 m)	0.18	S	166.85	E
	20:40	08:40	Turbulent flux measurement				
	23:21	11:21	RS-152	0.18	S	166.85	E
	23:25	11:25	CTD-113 (500 m)	0.18	S	166.85	E
	23:50	11:50	Turbulent flux measurement				
3-Jul			Fine				
	02:22	14:22	RS-153	0.18	S	166.85	E
	02:25	14:25	CTD-114 (200 m)	0.18	S	166.85	E
	02:42	14:42	Turbulent flux measurement				
	05:29	17:29	CTD-115 (500 m)	0.18	S	166.85	E
	06:04	18:04	RS-154	0.18	S	166.86	E
	06:08	18:08	Turbulent flux measurement				
	08:00	20:00	PI meeting				
	08:20	20:20	RS-155	0.18	S	166.85	E
	08:23	20:23	CTD-116 (200 m)	0.18	S	166.85	E
	08:40	20:40	Turbulent flux measurement				
	11:30	23:30	RS-156	0.18	S	166.85	E
	11:33	23:33	CTD-117 (1000 m)	0.18	S	166.85	E
	12:18	00:18	Turbulent flux measurement (with Ronald H. Brown)				
	14:30	02:30	RS-157	0.21	S	166.89	E
	14:36	02:36	CTD-118 (200 m)	0.21	S	166.89	E
	15:18	03:18	RHB scientists + crew arrive / Mirai scientists depart for RHB				
	16:56	04:56	Mirai scientists come back / RHB scientist + crew left				
	17:31	05:31	RS-158	0.20	S	166.87	E
	17:34	05:34	CTD-119 (500 m)	0.20	S	166.87	E
	18:03	06:03	Turbulent flux measurement				
	20:20	08:20	RS-159	0.18	S	166.85	E
	20:23	08:23	CTD-120 (200 m)	0.18	S	166.85	E
	20:39	08:39	Turbulent flux measurement				
	23:21	11:21	RS-160	0.18	S	166.85	E
	23:25	11:25	CTD-121 (500 m)	0.18	S	166.85	E
4-Jul			Fine				
	02:21	14:21	RS-161	0.18	S	166.85	E
	02:24	14:24	CTD-122 (200 m)	0.18	S	166.85	E
	02:42	14:42	Turbulent flux measurement				
	05:21	17:21	RS-162	0.18	S	166.85	E
	05:25	17:25	CTD-123 (500 m)	0.18	S	166.85	E
	05:53	17:53	Turbulent flux measurement				

	08:00	20:00	PI meeting					
	08:20	20:20	RS-163	0.18	S	166.85	E	
	08:23	20:23	CTD-124 (200 m)	0.18	S	166.85	E	
	11:21	23:21	RS-164	0.18	S	166.85	E	
	11:24	23:24	CTD-125 (1000 m)	0.18	S	166.85	E	
	14:15	02:15	CTD-126 (200 m)	0.18	S	166.85	E	
	14:33	02:33	RS-165 / Sphere calibration for Doppler radar	0.18	S	166.85	E	
	17:20	05:20	RS-166	0.18	S	166.85	E	
	17:24	05:24	CTD-127 (500 m)	0.18	S	166.85	E	
	20:21	08:21	RS-167	0.18	S	166.85	E	
	20:24	08:24	CTD-128 (200 m)	0.18	S	166.85	E	
	23:25	11:25	RS-168	0.18	S	166.85	E	
	23:27	11:27	CTD-129 (500 m)	0.18	S	166.85	E	
5-Jul			Fine / Rainy					
	00:00	12:00	Finish Nauru99 IOP / start moving to Majuro					
	02:22	14:22	RS-169	0.29	N	167.12	E	
	05:26	17:26	RS-170	0.97	N	167.48	E	
	08:28	20:28	RS-171	1.65	N	167.86	E	
	11:22	23:22	RS-172	2.32	N	168.23	E	
6-Jul			Fine					
			Pause Doppler radar observation					
	11:30	23:30	Arrive Majuro					
7-Jul			Fine					
	09:00	21:00	Depart Majuro					
	22:00	11:00	Local time adjustment (LT = UT+11h)					
8-Jul			Rainy					
	22:00	12:00	Local time adjustment (LT = UT+10h)					
9-Jul			Cloudy / Rainy					
10-Jul			Cloudy / Fine					
11-Jul			Cloudy / Rainy					
	15:00	05:00	Pause Doppler radar observation					
	19:00	09:00	Arrive Guam					
	20:00	10:00	Depart Guam					
	22:00	13:00	Local time adjustment (LT = UT+9h)					
	22:00	13:00	Resume Doppler radar observation					
12-Jul			Cloudy / Rainy					
	08:30	23:30	RS-173	16.17	N	142.39	E	
	14:25	05:25	RS-174	17.41	N	141.38	E	
13-Jul			Rainy					
	08:30	23:30	RS-175	21.11	N	138.17	E	
	14:30	05:30	RS-176	22.28	N	137.18	E	
14-Jul			Cloudy / Fine					
	08:30	23:30	RS-177	25.79	N	134.08	E	
	12:00	03:00	Finish Doppler radar observation					
	14:30	05:30	RS-178	27.00	N	133.01	E	
	23:30	14:30	RS-179	28.98	N	131.31	E	
15-Jul			Cloudy / Fine					

16-Jul			Cloudy / Fine
17-Jul			Cloudy / Rainy
	08:30	23:30	Arrive Tsuruga

5. Participants List

5.1 On board Scientists / Engineers / Technical Staff

Name	Institute	On board
Kunio Yoneyama	JAMSTEC	Yokohama - Sekinehama
Masaki Katsumata	JAMSTEC	Yokohama - Sekinehama
R. Michael Reynolds	BNL	Yokohama - Sekinehama
Ray Edwards	BNL	Yokohama - Majuro
William Brown	NCAR	Yokohama - Majuro
Michael Susedik	NCAR	Yokohama - Nauru
Louis Verstraete	NCAR	Nauru - Majuro
Jennifer Hanafin	Univ. of Miami	Yokohama - Guam
Tim Nightingale	RAL	Yokohama - Tsuruga
Kenji Suzuki	Yamaguchi Univ.	Yokohama - Sekinehama
Hiroshi Ishida	MUK	Chuuk - Majuro
Mitsuru Hayashi	MUK	Yokohama - Majuro
Tomoko Iwamoto	MUK	Yokohama - Majuro
Masanao Kusakari	MUK	Yokohama - Majuro
Masayuki Sasaki	MRI/JMA	Yokohama - Majuro
Osamu Tsukamoto	Okayama Univ.	Yokohama - Chuuk
Toru Iwata	Okayama Univ.	Yokohama - Majuro
Takehiko Kono	Okayama Univ.	Yokohama - Majuro
Satoshi Takahashi	Okayama Univ.	Yokohama - Majuro
Eiji Yamashita	Okayama U.of Sci.	Yokohama - Majuro
Kunimitsu Ishida	Toba-CMT	Yokohama - Majuro
Ichiro Matsui	NIES	Yokohama - Sekinehama
Tetsuya Takemi	Osaka Univ.	Yokohama - Majuro
Kazuyoshi Kikuchi	Univ. of Tokyo	Yokohama - Majuro
Naoki Nakatani	Osaka Pref. Univ.	Yokohama - Majuro
Tomoki Ushiyama	FRSGC	Chuuk - Majuro
Saji N. Hameed	FRSGC	Chuuk - Majuro
Masaki Hanyu	GODI	Yokohama - Sekinehama
Fumitaka Yoshiura	GODI	Yokohama - Majuro
Satoshi Okumura	GODI	Yokohama - Majuro
Koyotake Kouzuma	GODI	Yokohama - Sekinehama
Satoshi Ozawa	MWJ	Yokohama - Majuro
Katsunori Sagishima	MWJ	Yokohama - Sekinehama
Ai Yasuda	MWJ	Yokohama - Majuro
Mikio Kitada	MWJ	Yokohama - Sekinehama
Mizue Hirano	MWJ	Yokohama - Majuro
Shinichiro Yokogawa	MWJ	Yokohama - Majuro
Keisuke Wataki	MWJ	Yokohama - Majuro
Masanori Satoh	MWJ	Yokohama - Majuro

Japan Marine Science and Technology Center (JAMSTEC)
2-15, Natsushima-cho, Yokosuka 237-0061, JAPAN
TEL : +81-468-66-3811
FAX : +81-468-65-3202

Brookhaven National Laboratory (BNL)
Bldg.490D, Upton, NY 11973, USA

National Center for Atmospheric Research (NCAR)
3450 Mitchell Lane, Boulder, CO 80303, USA

University of Miami / The Rosenstiel School of Marine and Atmospheric Science (RSMAS)
4600 Rickenbacker Causeway, Miami, FL 33149-1098, USA

Rutherford Appleton Laboratory (RAL)
Chilton, Didcot, OXON, OX11, OQX, England

Yamaguchi University
1677-1, Yoshida, Yamaguchi 753-8515, JAPAN

Maritime University of Kobe (MUK)
5-1-1, Fukae-minami, Higashi-Nada-ku, Kobe 658-0022, JAPAN

Meteorological Research Institute / Japan Meteorological Agency (MRI/JMA)
1-1, Nagamine, Tsukuba, Ibaraki 305-0052, JAPAN

Okayama University
3-1-1, Tsushimanaka, Okayama 700-8530, JAPAN

Okayama University of Science
1-1, Ridai-cho, Okayama 700-0005, JAPAN

Toba National College of Marine Technology (Toba-CMT)
1-1, Ikegami, Toba, Mie 517-8501, JAPAN

National Institute of Environmental Studies (NIES)
16-2, Onogawa, Tsukuba, Ibaraki 305-0053, JAPAN

Osaka University
2-1, Yamadaoka, Suita, Osaka 565-0871, JAPAN

Osaka Prefecture University
1-1, Gakuen-cho, Sakai, Osaka 599-8531, JAPAN

University of Tokyo / Center for Climate System Research
4-6-1, Komaba, Meguro-ku, Tokyo 153-8904, JAPAN

Frontier Research System for Global Change (FRSGC)
Seavans N-7, 1-2-1, Shibaura, Minato-ku, Tokyo 105-6791, JAPAN

Global Ocean Development Inc.
3-65, Oppamahigashi-cho, Yokosuka 237-0063, JAPAN

Marine Works Japan Ltd.
1-1-7, Mutsuura, Kanazawa-ku, Yokohama 236-0031, JAPAN

5.2 Ship Crew

Captain	Masaharu Akamine
Chief Officer	Takaaki Hashimoto
First Officer	Yuji Shibata
Second Officer	Hiroki Maruyama
Third Officer	Mitsunobu Asanuma
Chief Engineer	Toru Inoue
First Engineer	Minoru Ikeda
Second Engineer	Shinichiro Koga
Third Engineer	Koji Masuno
Chief Radio Officer	Shuji Nakabayashi
Second Radio Officer	Keiichiro Shishido
Boatswain	Tadao Suzuki
Able Seaman	Kenetsu Ishikawa
Able Seaman	Hisashi Naruo
Able Seaman	Hirokazu Kinoshita
Able Seaman	Isao Taguchi
Able Seaman	Kazunori Horita
Able Seaman	Akio Tasaki
Able Seaman	Kazuyoshi Kudo
Able Seaman	Tsuyoshi Sato
Able Seaman	Jo Tanimoto
Able Seaman	Tsuyoshi Monzawa
Able Seaman	Akito Oshige
No.1 Oiler	Sadanori Honda
Oiler	Shozo Abe
Oiler	Toshimi Yoshikawa
Oiler	Sunao Araki
Oiler	Takashi Miyazaki
Oiler	Toshio Matsuo
Chief Steward	Yasuaki Koga
Steward	Osamu Araki
Steward	Takayuki Akita
Steward	Tatsuya Hamabe
Steward	Kozo Uemura
Steward	Hiroyuki Yoshizawa

6. Meteorological Observations

6.1 General Meteorological Observation

(1) Personnel

Kunio Yoneyama (JAMSTEC) : Principal Investigator
Masaki Hanyu (GODI) : Operation Leader
Fumitaka Yoshiura (GODI)
Kiyotake Kouzuma (GODI)
Satoshi Okumura (GODI)
Kenji Suzuki (Yamaguchi Univ.)
Masaki Katsumata (JAMSTEC)

(2) Objectives

The surface meteorological parameters are observed as a basic dataset of the meteorology. These parameters brings us the information about temporal variation of the meteorological condition surrounding the ship.

(3) Measured Parameters

The surface meteorological parameters were observed throughout MR99-K03 cruise from the departure of Yokohama on 8 June 1999 to the arrive of Tsuruga on 17 July 1999.

Measured parameters are:

Name	Sampling Interval	Acronyms in Table 6.1-2
Wind direction	6 sec. / 10 min. averaged	WD
Wind speed	6 sec. / 10 min. averaged	WS
Weather	3 hourly	Weather
Pressure (adjusted to the sea surface level)		
	6 sec. / 10 min. averaged	P
Air temperature	6 sec. / 10 min. averaged	T
Dewpoint temperature	6 sec. / 10 min. averaged	DPT
Relative humidity	6 sec. / 10 min. averaged	RH
Sea surface temperature	6 sec. / 10 min. averaged	SST
Rainfall amount	3 hourly (accumulated)	Rain
Significant wave height	3 hourly (20 min. averaged)	Wv. Ht.
Significant wave period	3 hourly (20 min. averaged)	Wv. Pd.

(4) Methods

The R/V Mirai onboard meteorological sensors are listed in Table 6.1-1. Surface meteorological data were collected and processed by KOAC-7800 weather data processor and some sensors assembled by Koshin Denki, Japan.

Table 6.1-1: R/V Mirai onboard meteorological sensors.

Sensors	Type	Manufacturer	Location（Altitude from surface）
Anemometer	KE-500	Koshin Denki, Japan	Foremast (24 m)
Thermometer	FT	Koshin Denki, Japan	Compass deck (19 m)
Dew point meter	DW-1	Koshin Denki, Japan	Compass deck (19 m)
Barometer	F-451	Yokogawa, Japan	Weather observation room, Captain deck (13 m)
Raingauge	50202	Young, U.S.A.	Compass deck (19 m) *Navigational bridge deck (18m)
Optical raingauge	ORG-115DR	SCTI, U.S.A.	Compass deck (19m)
Radiometer	MS-801 (short wave)	Eiko Seiki, Japan	Radar mast (28 m)
Wave height meter	MW-2	Tsurumi-seiki, Japan	Bow

* Raingauge at the navigational bridge deck is installed temporally.

(5) Preliminary Results

Table 6.1-2 shows the part of the observation results for the permanent sensors. The result of the raingauge at the navigational bridge deck is shown in Fig. 6.1-1.

(6) Data Archive

The datasets with 6 seconds and 10 minutes interval are available in the 3.5” magnetic optical (MO) disk. The dataset will be submitted to the DMO (Data Management Office), JAMSTEC and will be under their control.

Table 6.1-2: Surface meteorological parameters obtained by permanent sensors. See article (?) for the acronyms on the header line. The symbols in "Weather" column is shown at the tail of this table.

Time				Position		Weather	WD	WS	P	T	DPT	RH	SST	Rain	Wv.Ht.	Wv.Pd.
UTC		Ship		Lat.	Lon.		(deg)	(m/s)	(hPa)	(deg.C)	(deg.C)	(%)	(deg.C)	(mm/3h)	(m)	(sec)
08-Jun	06:00	08-Jun	15:00	35 - 27 N	139 - 40 E	bc	14	5.6	1005.2	22.1	16.8	72	20.8	0.0	1.1	7
08	09:00	08	18:00	34 - 07 N	140 - 04 E	bc	23	4.3	1005.5	22.2	15.1	64	25.1	0.0	1.3	11
08	12:00	08	21:00	33 - 24 N	140 - 23 E	bc	22	4.5	1006.4	22.2	15.9	67	24.2	0.0	1.8	9
08	15:00	09	00:00	32 - 40 N	140 - 41 E	o	9	3.6	1005.2	19.8	18.2	91	23.9	0.0	2.1	12
08	18:00	09	03:00	31 - 55 N	141 - 03 E	r	23	14.3	1002.6	21.7	21.5	99	23.1	33.5	2.5	10
08	21:00	09	06:00	31 - 19 N	141 - 31 E	o	27	12.6	1005.3	21.6	21.7	100	23.8	32.0	3.0	12
09	00:00	09	09:00	30 - 37 N	141 - 51 E	o	27	12.8	1006.5	22.5	21.5	94	23.3	19.2	3.5	10
09	03:00	09	12:00	29 - 57 N	142 - 11 E	o	28	10.3	1007.7	21.7	20.9	95	23.4	0.4	2.5	9
09	06:00	09	15:00	29 - 19 N	142 - 30 E	o	30	8.3	1008.9	22.7	20.4	87	24.0	0.0	2.4	10
09	09:00	09	18:00	28 - 35 N	142 - 48 E	o	28	4.8	1010.5	21.9	19.4	86	24.6	1.6	1.8	10
09	12:00	09	21:00	27 - 54 N	143 - 05 E	o	24	4.4	1011.2	23.0	22.5	97	25.3	3.1	1.4	10
09	15:00	10	00:00	27 - 10 N	143 - 26 E	o	23	10.1	1010.4	25.3	23.3	89	26.4	0.1	1.2	9
09	18:00	10	03:00	26 - 26 N	143 - 46 E	o	23	9.6	1010.6	25.9	22.9	84	27.0	0.0	1.4	9
09	21:00	10	06:00	25 - 44 N	144 - 07 E	c	24	6.8	1012.3	26.0	22.5	81	27.1	0.0	1.1	11
10	00:00	10	09:00	25 - 44 N	144 - 07 E	bc	22	3.7	1012.7	27.7	22.0	71	27.9	0.0	1.0	13
10	03:00	10	12:00	24 - 21 N	144 - 43 E	bc	22	3.3	1011.9	28.7	22.5	69	28.9	0.0	0.9	11
10	06:00	10	15:00	23 - 35 N	145 - 02 E	c	22	2.7	1011.9	29.1	23.3	71	29.6	0.0	0.8	9
10	09:00	10	18:00	22 - 51 N	145 - 22 E	c	23	4.3	1012.8	28.2	23.5	76	29.2	0.0	0.8	6
10	12:00	10	21:00	22 - 05 N	145 - 42 E	bc	19	3.2	1014.7	28.2	23.4	75	29.3	0.0	0.9	9
10	15:00	11	00:00	21 - 22 N	146 - 04 E	bc	16	4.3	1013.7	27.9	23.6	78	29.3	0.6	0.9	8
10	18:00	11	03:00	20 - 38 N	146 - 21 E	bc	16	3.0	1013.4	28.0	23.3	76	29.4	0.0	0.8	7
10	21:00	11	06:00	19 - 53 N	146 - 39 E	bc	13	3.0	1014.9	27.3	23.2	78	29.5	0.0	0.9	7
11	00:00	11	09:00	19 - 10 N	146 - 59 E	bc	13	4.4	1015.0	28.8	22.5	69	29.5	0.2	0.8	8
11	03:00	11	12:00	18 - 27 N	147 - 18 E	bc	13	5.2	1012.6	28.9	23.0	70	29.8	0.0	0.8	6
11	06:00	11	15:00	17 - 43 N	147 - 36 E	bc	12	5.6	1011.3	28.6	22.9	71	29.8	0.0	0.9	5
11	09:00	11	18:00	16 - 58 N	147 - 52 E	bc	10	6.3	1012.2	28.1	22.6	72	29.7	0.0	1.0	6
11	12:00	11	21:00	16 - 15 N	148 - 10 E	bc	11	7.3	1014.0	27.9	22.7	74	29.3	0.2	1.0	6
11	15:00	12	00:00	15 - 32 N	148 - 27 E	bc	12	7.2	1012.9	27.2	23.2	79	29.2	0.2	1.1	7
11	18:00	12	03:00	14 - 48 N	148 - 43 E	bc	11	6.7	1011.7	27.4	23.3	78	29.2	0.0	1.1	6
11	21:00	12	06:00	14 - 04 N	148 - 59 E	bc	10	8.2	1012.7	28.1	23.0	74	29.2	0.0	1.1	6
12	00:00	12	09:00	13 - 22 N	149 - 15 E	bc	9	7.7	1012.9	28.6	23.2	73	29.3	0.0	1.3	7
12	03:00	12	12:00	12 - 39 N	149 - 32 E	bc	8	7.7	1011.2	28.5	23.8	76	29.3	0.0	1.3	7
12	06:00	12	15:00	11 - 55 N	149 - 47 E	bc	8	6.9	1009.7	28.5	23.4	74	29.5	1.0	1.3	7
12	09:00	12	18:00	11 - 13 N	150 - 04 E	bc	9	5.1	1010.9	27.1	22.8	78	29.3	0.5	1.4	7
12	12:00	12	21:00	10 - 29 N	150 - 18 E	bc	8	4.7	1011.9	27.1	23.5	81	29.1	0.0	1.2	8
12	15:00	13	01:00	09 - 46 N	150 - 33 E	bc	6	5.1	1009.6	27.0	23.7	83	29.1	0.0	1.1	8
12	18:00	13	04:00	09 - 02 N	150 - 51 E	bc	8	5.2	1009.1	27.0	23.6	82	29.1	0.1	1.2	9
12	21:00	13	07:00	08 - 22 N	151 - 12 E	o	8	6.5	1010.1	25.7	22.8	84	29.3	12.2	1.0	6
13	00:00	13	10:00	07 - 54 N	151 - 43 E	r	17	5.7	1011.0	24.7	22.7	89	29.0	15.6	1.0	5
14	00:00	14	10:00	07 - 26 N	151 - 50 E	bc	N/A	N/A	1010.1	28.4	22.6	71	29.1	0.0	0.1	6
14	03:00	14	13:00	07 - 15 N	152 - 26 E	bc	6	5.5	1009.4	27.9	22.0	70	29.4	0.0	0.1	6
14	06:00	14	16:00	06 - 50 N	153 - 10 E	bc	6	2.5	1008.3	28.1	21.2	66	29.4	0.0	0.1	6
14	09:00	14	19:00	06 - 28 N	153 - 52 E	bc	5	2.9	1010.1	27.3	20.9	68	29.1	0.0	0.9	7
14	12:00	14	23:00	06 - 05 N	154 - 36 E	bc	5	3.2	1011.8	27.3	21.5	71	29.0	0.0	0.9	7
14	15:00	15	02:00	05 - 45 N	155 - 18 E	bc	30	1.4	1010.1	27.0	23.6	82	29.0	6.0	0.9	6
14	18:00	15	05:00	05 - 22 N	156 - 01 E	bc	5	2.9	1009.4	26.8	22.1	75	29.0	0.0	0.8	6
14	21:00	15	08:00	04 - 58 N	156 - 43 E	c	8	4.4	1011.0	26.6	22.4	78	29.0	1.1	0.8	7
15	00:00	15	11:00	04 - 48 N	157 - 04 E	bc	8	5.2	1011.3	28.2	21.8	68	29.2	0.0	0.8	6
15	03:00	15	14:00	04 - 24 N	157 - 47 E	bc	11	3.2	1009.3	28.7	21.7	66	29.6	0.0	0.8	7
15	06:00	15	17:00	04 - 00 N	158 - 29 E	c	10	1.6	1008.3	27.5	21.8	71	29.4	0.0	0.9	5
15	09:00	15	20:00	03 - 37 N	159 - 12 E	bc	11	1.6	1009.6	27.4	22.3	74	29.6	0.0	1.0	5
15	12:00	16	00:00	03 - 11 N	159 - 52 E	bc	16	4.0	1010.5	26.1	23.8	87	29.1	1.6	1.0	5
15	15:00	16	03:00	02 - 48 N	160 - 34 E	p	11	5.8	1009.0	26.1	22.8	82	29.1	2.2	1.0	6
15	18:00	16	06:00	02 - 36 N	161 - 03 E	r	12	11.8	1010.1	22.9	20.6	87	29.0	55.4	2.0	18
15	21:00	16	09:00	02 - 14 N	161 - 42 E	o	8	1.1	1011.2	25.2	21.9	82	28.9	14.6	1.2	6
16	00:00	16	12:00	01 - 53 N	162 - 22 E	c	11	5.6	1010.7	28.9	21.7	65	28.8	0.6	1.4	5
16	03:00	16	15:00	01 - 33 N	162 - 59 E	c	12	6.3	1009.2	29.2	23.0	69	28.7	0.0	1.3	4
16	06:00	16	18:00	01 - 13 N	163 - 35 E	bc	14	5.5	1008.4	28.1	23.1	74	28.8	0.0	1.2	5
16	09:00	16	21:00	00 - 53 N	164 - 11 E	o	9	4.1	1010.1	24.8	21.7	83	28.7	7.7	1.2	6
16	12:00	17	00:00	00 - 32 N	164 - 42 E	c	9	4.5	1010.8	26.5	22.5	79	28.7	0.4	1.4	5
16	15:00	17	03:00	00 - 18 N	165 - 19 E	b	7	5.3	1009.2	26.6	22.1	76	28.6	0.0	1.4	5
16	18:00	17	06:00	00 - 00 N	165 - 55 E	bc	7	6.7	1009.0	26.3	21.9	77	28.4	3.1	1.2	5
16	21:00	17	09:00	00 - 19 S	166 - 29 E	bc	6	7.8	1010.5	27.7	21.9	71	28.2	0.0	1.4	6
17	00:00	17	12:00	00 - 30 S	166 - 54 E	bc	5	6.0	1011.5	28.4	23.4	75	28.2	0.0	1.2	8
17	03:00	17	15:00	00 - 29 S	166 - 55 E	bc	6	5.6	1009.2	29.3	21.7	64	28.4	0.0	0.9	7

17	06:00	17	18:00	00 - 31 S	166 - 54 E	bc	4	5.9	1008.8	28.1	23.4	76	28.2	0.0	0.9	8
17	09:00	17	21:00	00 - 29 S	166 - 54 E	bc	6	5.6	1010.6	27.4	23.6	80	28.3	0.0	0.8	7
17	12:00	18	00:00	00 - 29 S	166 - 55 E	bc	5	5.4	1011.0	27.3	23.2	78	28.3	0.0	0.9	8
17	15:00	18	03:00	00 - 30 S	166 - 55 E	bc	5	3.9	1009.7	27.0	23.3	80	28.2	0.0	0.8	7
17	18:00	18	06:00	00 - 28 S	166 - 55 E	bc	7	3.9	1009.2	26.6	21.7	74	28.3	0.0	0.9	7
17	21:00	18	09:00	00 - 29 S	166 - 55 E	bc	6	5.0	1010.7	28.0	23.1	75	28.2	0.0	1.1	7
18	00:00	18	12:00	00 - 29 S	166 - 55 E	bc	6	4.8	1009.9	28.3	23.4	75	28.3	0.1	0.8	7
18	03:00	18	15:00	00 - 29 S	166 - 54 E	bc	6	5.2	1008.2	28.4	22.9	72	28.5	0.0	0.8	7
18	06:00	18	18:00	00 - 29 S	166 - 55 E	bc	6	4.3	1008.3	28.2	21.7	68	28.5	0.0	0.8	7
18	09:00	18	21:00	00 - 29 S	166 - 55 E	bc	7	5.0	1010.1	27.3	21.7	72	28.4	0.0	0.7	7
18	12:00	19	00:00	00 - 29 S	166 - 55 E	bc	3	4.9	1010.3	26.5	22.3	78	28.3	0.0	0.6	7
18	15:00	19	03:00	00 - 28 S	166 - 55 E	bc	6	2.5	1009.5	27.0	23.4	81	28.3	0.0	0.7	6
18	18:00	19	06:00	00 - 30 S	166 - 54 E	bc	6	1.9	1009.3	26.4	23.5	84	28.2	0.0	0.6	7
18	21:00	19	09:00	00 - 29 S	166 - 55 E	bc	9	3.2	1010.9	27.7	23.1	76	28.2	0.1	0.7	6
19	00:00	19	12:00	00 - 31 S	166 - 53 E	bc	6	4.4	1010.0	27.5	23.1	77	28.3	0.0	0.7	8
19	03:00	19	15:00	00 - 29 S	166 - 55 E	bc	9	3.1	1007.5	28.7	22.9	71	28.8	0.0	0.8	7
19	06:00	19	18:00	00 - 31 S	166 - 54 E	bc	14	3.6	1007.9	28.3	22.8	72	28.3	0.0	0.7	8
19	09:00	19	21:00	00 - 30 S	166 - 59 E	bc	10	6.6	1009.8	26.1	23.3	85	28.7	0.1	1.0	7
19	12:00	20	00:00	00 - 22 S	166 - 22 E	bc	8	2.1	1010.3	26.7	23.6	83	28.5	0.3	1.2	13
19	15:00	20	03:00	00 - 13 S	165 - 46 E	bc	13	1.7	1009.2	26.7	21.9	75	28.5	0.0	1.4	13
19	18:00	20	06:00	00 - 03 S	165 - 11 E	bc	9	2.6	1009.2	26.9	23.0	79	28.6	0.0	1.3	13
19	21:00	20	09:00	00 - 00 N	165 - 00 E	bc	12	3.5	1010.0	27.4	23.3	78	28.6	0.0	1.2	8
20	00:00	20	12:00	00 - 00 N	164 - 59 E	bc	14	3.7	1009.1	28.0	22.5	72	28.6	0.0	1.0	8
20	03:00	20	15:00	00 - 00 N	165 - 01 E	bc	12	3.9	1007.3	28.6	23.2	72	28.8	0.0	1.1	8
20	06:00	20	18:00	00 - 01 N	164 - 59 E	bc	13	4.6	1007.6	28.5	21.5	66	28.8	0.0	1.0	8
20	09:00	20	21:00	00 - 00 N	164 - 59 E	bc	13	4.7	1009.3	27.3	21.5	71	28.7	0.0	1.0	7
20	12:00	21	00:00	00 - 00 N	165 - 00 E	bc	13	5.7	1009.7	27.0	21.8	73	28.6	0.0	1.0	7
20	15:00	21	03:00	00 - 00 N	164 - 59 E	bc	12	4.8	1008.5	26.9	23.1	80	28.5	0.0	1.1	8
20	18:00	21	06:00	00 - 00 N	164 - 59 E	bc	9	6.9	1008.6	27.3	22.5	75	28.5	0.0	1.0	7
20	21:00	21	09:00	00 - 00 N	165 - 00 E	bc	8	5.7	1010.5	28.1	21.5	68	28.5	0.0	1.1	7
21	00:00	21	12:00	00 - 00 N	164 - 59 E	bc	9	4.5	1010.4	29.2	21.8	65	28.6	0.0	1.1	8
21	03:00	21	15:00	00 - 00 N	164 - 59 E	bc	10	4.5	1008.0	29.8	21.4	60	28.9	0.0	1.2	8
21	06:00	21	18:00	00 - 00 N	164 - 59 E	bc	8	5.5	1008.5	28.7	20.5	61	28.8	0.0	1.1	8
21	09:00	21	21:00	00 - 00 N	164 - 59 E	bc	9	4.3	1010.7	27.4	20.6	67	28.6	0.0	1.1	7
21	12:00	22	00:00	00 - 00 N	165 - 00 E	bc	8	3.9	1011.0	27.3	21.8	72	28.5	0.0	1.0	7
21	15:00	22	03:00	00 - 00 N	164 - 59 E	bc	7	4.0	1009.7	26.7	20.1	67	28.5	0.0	1.0	8
21	18:00	22	06:00	00 - 00 N	165 - 00 E	b	7	2.5	1009.8	26.5	20.2	68	28.5	0.0	1.0	7
21	21:00	22	09:00	00 - 00 N	165 - 00 E	b	8	2.1	1011.5	27.8	21.8	70	28.5	0.0	1.2	8
22	00:00	22	12:00	00 - 00 N	165 - 00 E	b	10	2.1	1010.4	29.1	21.9	65	28.5	0.0	1.0	7
22	03:00	22	15:00	00 - 01 S	165 - 00 E	b	10	1.7	1008.8	29.8	21.6	62	29.0	0.0	1.0	7
22	06:00	22	18:00	00 - 00 N	164 - 59 E	b	10	1.6	1008.8	28.6	20.8	62	29.2	0.0	1.0	8
22	09:00	22	21:00	00 - 00 N	164 - 59 E	b	7	1.3	1010.7	27.3	21.4	70	29.1	0.0	1.0	7
22	12:00	23	00:00	00 - 00 N	164 - 59 E	bc	12	0.7	1011.2	27.0	21.3	71	28.8	0.0	1.0	8
22	15:00	23	03:00	00 - 00 N	164 - 59 E	bc	20	1.9	1009.8	26.5	21.5	74	28.7	0.0	1.0	8
22	18:00	23	06:00	00 - 02 N	165 - 00 E	bc	22	1.9	1009.3	26.2	20.3	70	28.6	0.0	0.9	8
22	21:00	23	09:00	00 - 00 N	165 - 00 E	bc	22	0.9	1010.9	27.7	21.3	68	28.6	0.0	1.1	8
23	00:00	23	12:00	00 - 00 N	165 - 00 E	bc	11	0.5	1010.3	28.4	21.5	67	28.6	0.0	1.0	8
23	03:00	23	15:00	00 - 00 N	165 - 01 E	bc	14	1.6	1008.4	29.0	20.5	60	29.2	0.0	0.9	8
23	06:00	23	18:00	00 - 00 N	165 - 00 E	bc	11	3.4	1008.5	28.7	20.4	61	29.3	0.0	1.0	7
23	09:00	23	21:00	00 - 00 N	165 - 00 E	bc	10	3.9	1010.4	27.5	21.4	70	29.0	0.0	1.0	7
23	12:00	24	00:00	00 - 00 N	165 - 00 E	bc	12	2.8	1010.3	27.4	20.6	67	28.7	0.0	1.1	7
23	15:00	24	03:00	00 - 01 S	165 - 00 E	bc	13	2.8	1008.6	26.8	19.9	66	28.6	0.0	1.1	7
23	18:00	24	06:00	00 - 01 S	165 - 00 E	bc	14	2.9	1009.0	27.1	21.4	71	28.6	0.0	0.9	8
23	21:00	24	09:00	00 - 01 S	164 - 59 E	bc	15	3.0	1010.8	27.8	20.9	66	28.6	0.0	1.0	8
24	00:00	24	12:00	00 - 00 N	165 - 00 E	bc	14	2.6	1010.6	28.8	22.0	67	28.7	0.0	1.1	8
24	03:00	24	15:00	00 - 01 S	165 - 00 E	bc	16	2.4	1008.5	29.9	21.9	62	29.2	0.0	1.2	7
24	06:00	24	18:00	00 - 00 N	164 - 59 E	bc	15	2.6	1008.7	28.6	20.1	60	29.1	0.0	1.1	8
24	09:00	24	21:00	00 - 00 N	164 - 59 E	bc	14	3.1	1010.5	27.5	20.5	66	28.9	0.0	1.2	8
24	12:00	25	00:00	00 - 00 N	164 - 59 E	bc	13	3.6	1011.1	27.3	20.9	68	28.7	0.0	1.3	7
24	15:00	25	03:00	00 - 00 N	165 - 00 E	bc	13	3.8	1009.6	27.4	22.0	72	28.7	0.0	1.0	7
24	18:00	25	06:00	00 - 00 N	165 - 00 E	bc	12	3.8	1009.8	27.3	21.9	73	28.6	0.0	1.0	7
24	21:00	25	09:00	00 - 01 S	165 - 00 E	bc	12	1.3	1011.1	26.0	20.7	73	28.6	0.3	1.0	7
25	00:00	25	12:00	00 - 00 N	165 - 00 E	bc	11	4.3	1010.5	28.6	22.4	69	28.7	0.0	1.0	7
25	03:00	25	15:00	00 - 00 N	165 - 00 E	bc	10	4.0	1009.1	29.6	21.0	60	29.0	0.0	1.1	8
25	06:00	25	18:00	00 - 00 N	164 - 59 E	bc	8	4.6	1008.5	28.6	22.0	68	29.0	0.0	1.0	8
25	09:00	25	21:00	00 - 00 N	165 - 00 E	bc	7	5.6	1009.7	27.6	21.4	69	28.8	0.0	1.0	8
25	12:00	26	00:00	00 - 00 N	165 - 00 E	bc	7	6.5	1010.1	27.6	22.0	72	28.7	0.0	1.0	7
25	15:00	26	03:00	00 - 00 N	165 - 00 E	bc	8	5.8	1009.0	27.4	22.1	73	28.6	0.0	1.0	7
25	18:00	26	06:00	00 - 00 N	165 - 00 E	bc	8	5.6	1009.3	27.3	21.4	70	28.6	0.0	0.9	8
25	21:00	26	09:00	00 - 01 S	165 - 00 E	bc	9	4.9	1011.1	28.1	22.1	70	28.6	0.0	1.1	7
26	00:00	26	12:00	00 - 00 N	165 - 00 E	bc	9	5.1	1010.7	28.7	22.5	69	28.7	0.0	1.0	7
26	03:00	26	15:00	00 - 00 N	164 - 59 E	bc	9	5.7	1008.7	28.9	22.6	69	28.9	0.0	1.0	7
26	06:00	26	18:00	00 - 00 N	165 - 00 E	bc	9	5.0	1008.6	28.4	22.4	70	28.9	0.0	1.0	7
26	09:00	26	21:00	00 - 00 N	165 - 00 E	bc	9	6.4	1010.5	27.4	21.5	70	28.8	0.0	1.0	7
26	12:00	27	00:00	00 - 00 N	165 - 00 E	bc	10	6.5	1010.8	27.3	21.6	71	28.7	0.0	0.9	7
26	15:00	27	03:00	00 - 00 N	165 - 00 E	bc	10	5.9	1009.4	27.2	20.7	68	28.7	0.0	1.0	7
26	18:00	27	06:00	00 - 00 N	165 - 00 E	bc	11	7.9	1009.1	27.4	21.6	71	28.7	0.0	1.0	7

26	21:00	27	09:00	00 - 00 N	165 - 00 E	bc	10	8.0	1010.6	28.1	21.1	66	28.6	0.0	1.0	6
27	00:00	27	12:00	00 - 00 N	165 - 00 E	bc	10	7.0	1010.3	28.7	22.6	69	28.7	0.0	1.1	6
27	03:00	27	15:00	00 - 00 N	165 - 00 E	bc	10	7.5	1008.4	29.2	22.6	68	28.8	0.0	1.2	6
27	06:00	27	18:00	00 - 00 N	164 - 59 E	bc	9	5.3	1008.0	28.6	22.4	69	29.0	0.0	1.0	6
27	09:00	27	21:00	00 - 00 N	164 - 59 E	bc	8	4.5	1010.4	25.8	22.8	84	28.9	6.3	1.2	6
27	12:00	28	00:00	00 - 00 N	164 - 59 E	bc	9	8.4	1010.4	27.9	21.6	69	28.9	0.0	1.2	6
27	15:00	28	03:00	00 - 01 S	165 - 00 E	bc	9	5.6	1009.5	27.5	21.0	68	28.8	0.0	1.2	6
27	18:00	28	06:00	00 - 00 N	165 - 00 E	bc	8	7.8	1009.6	27.6	21.4	69	28.8	0.0	1.1	6
27	21:00	28	09:00	00 - 00 N	165 - 00 E	bc	9	9.0	1011.9	28.6	22.7	70	28.8	0.0	1.2	6
28	00:00	28	12:00	00 - 00 N	164 - 59 E	bc	10	8.8	1011.3	28.9	22.6	69	28.8	0.0	1.4	6
28	03:00	28	15:00	00 - 00 N	165 - 00 E	bc	10	8.6	1009.6	29.4	21.1	61	28.9	0.0	1.5	6
28	06:00	28	18:00	00 - 01 S	165 - 00 E	bc	10	7.7	1009.3	28.5	21.3	65	28.9	0.0	1.4	6
28	09:00	28	21:00	00 - 01 S	165 - 00 E	bc	10	8.6	1010.4	28.1	21.7	68	28.8	0.0	1.3	6
28	12:00	29	00:00	00 - 01 S	164 - 59 E	bc	12	8.2	1011.0	27.9	20.6	65	28.8	0.0	1.5	6
28	15:00	29	03:00	00 - 00 N	165 - 00 E	bc	11	7.4	1010.0	27.7	21.1	67	28.8	0.0	1.5	6
28	18:00	29	06:00	00 - 00 N	165 - 00 E	bc	12	7.8	1009.9	27.7	21.7	70	28.8	0.0	1.5	6
28	21:00	29	09:00	00 - 00 N	165 - 00 E	bc	11	6.9	1011.5	28.2	20.6	64	28.8	0.0	1.5	6
29	00:00	29	12:00	00 - 00 N	164 - 59 E	bc	11	5.5	1011.1	28.9	22.0	67	28.8	0.0	1.5	6
29	03:00	29	15:00	00 - 00 N	165 - 00 E	bc	11	5.4	1009.5	29.4	21.3	62	28.9	0.0	1.5	7
29	06:00	29	18:00	00 - 00 N	165 - 00 E	bc	9	5.2	1008.9	28.7	21.6	66	28.9	0.0	1.5	6
29	09:00	29	21:00	00 - 00 N	164 - 59 E	bc	10	5.3	1010.7	27.8	20.8	66	28.8	0.0	1.3	7
29	12:00	30	00:00	00 - 00 N	165 - 00 E	bc	10	5.3	1011.1	27.8	22.1	71	28.8	0.0	1.3	7
29	15:00	30	03:00	00 - 00 N	165 - 00 E	bc	10	5.5	1009.6	27.6	22.3	73	28.8	0.0	1.3	6
29	18:00	30	06:00	00 - 00 N	165 - 00 E	bc	9	6.2	1009.2	27.3	21.4	70	28.8	0.0	1.1	6
29	21:00	30	09:00	00 - 00 N	165 - 00 E	bc	9	5.3	1010.6	28.2	21.3	66	28.8	0.0	1.1	6
30	00:00	30	12:00	00 - 00 N	164 - 59 E	bc	10	5.5	1010.3	29.0	22.3	67	28.8	0.0	1.1	6
30	03:00	30	15:00	00 - 00 N	165 - 00 E	bc	11	6.4	1008.7	29.6	22.1	64	29.0	0.0	1.1	6
30	06:00	30	18:00	00 - 00 N	165 - 00 E	bc	10	5.1	1008.3	28.4	21.8	67	28.9	0.0	1.0	6
30	09:00	30	21:00	00 - 05 S	165 - 03 E	bc	9	5.5	1009.4	27.4	21.6	71	28.9	0.0	0.9	6
30	12:00	01-Jul	00:00	00 - 10 S	165 - 31 E	bc	9	6.3	1010.4	27.8	22.6	74	28.8	0.0	1.0	6
30	15:00	01	03:00	00 - 08 S	165 - 59 E	bc	8	7.1	1008.5	27.3	21.2	69	28.7	0.0	1.0	7
30	18:00	01	06:00	00 - 10 S	166 - 34 E	bc	8	7.7	1008.5	27.4	22.0	73	28.7	0.0	0.9	6
30	21:00	01	09:00	00 - 11 S	166 - 51 E	bc	8	7.5	1010.1	28.1	22.2	70	28.5	0.0	1.0	7
01-Jul	00:00	01	12:00	00 - 10 S	166 - 50 E	bc	8	6.4	1010.1	29.2	22.4	67	28.5	0.0	1.2	7
01	03:00	01	15:00	00 - 10 S	166 - 51 E	bc	7	5.3	1008.2	28.9	22.4	68	28.7	0.0	1.1	7
01	06:00	01	18:00	00 - 11 S	166 - 50 E	bc	8	6.6	1007.7	28.7	20.9	63	28.7	0.0	1.2	7
01	09:00	01	21:00	00 - 10 S	166 - 50 E	bc	7	6.9	1009.4	27.7	22.3	73	28.6	0.0	1.2	7
01	12:00	02	00:00	00 - 11 S	166 - 50 E	bc	8	6.7	1010.1	27.4	21.1	69	28.5	0.0	1.2	7
01	15:00	02	03:00	00 - 11 S	166 - 50 E	bc	7	6.5	1009.1	27.2	21.0	69	28.5	0.0	1.4	7
01	18:00	02	06:00	00 - 10 S	166 - 51 E	bc	7	7.9	1009.0	27.3	20.6	67	28.6	0.0	1.4	7
01	21:00	02	09:00	00 - 10 S	166 - 51 E	bc	7	8.1	1010.5	28.2	22.3	70	28.7	0.0	1.6	7
02	00:00	02	12:00	00 - 10 S	166 - 51 E	bc	9	7.4	1010.8	28.7	22.5	69	28.7	0.0	1.6	7
02	03:00	02	15:00	00 - 11 S	166 - 51 E	bc	9	7.7	1008.8	29.4	22.2	65	28.8	0.0	1.5	7
02	06:00	02	18:00	00 - 11 S	166 - 51 E	bc	9	8.0	1008.7	28.5	21.7	67	28.7	0.0	1.6	7
02	09:00	02	21:00	00 - 10 S	166 - 51 E	bc	8	7.0	1010.3	27.8	22.1	71	28.7	0.0	1.6	7
02	12:00	03	00:00	00 - 11 S	166 - 51 E	bc	9	7.3	1011.0	27.5	20.8	67	28.7	0.0	1.4	7
02	15:00	03	03:00	00 - 11 S	166 - 51 E	o	10	6.9	1009.8	27.6	22.5	74	28.7	0.0	1.3	7
02	18:00	03	06:00	00 - 10 S	166 - 51 E	bc	10	7.5	1009.4	27.7	22.6	74	28.7	0.0	1.4	7
02	21:00	03	09:00	00 - 11 S	166 - 51 E	bc	11	7.0	1010.4	28.2	22.6	72	28.6	0.0	1.4	7
03	00:00	03	12:00	00 - 11 S	166 - 51 E	bc	11	7.2	1010.1	28.8	22.3	68	28.7	0.0	1.2	7
03	03:00	03	15:00	00 - 12 S	166 - 53 E	bc	11	7.2	1008.3	28.1	22.2	70	28.8	0.0	1.3	7
03	06:00	03	18:00	00 - 11 S	166 - 52 E	bc	11	7.1	1008.2	28.7	20.8	62	28.7	0.0	1.3	7
03	09:00	03	21:00	00 - 11 S	166 - 51 E	bc	11	5.9	1009.8	27.7	22.9	75	28.7	0.0	1.4	7
03	12:00	04	00:00	00 - 11 S	166 - 51 E	bc	12	7.0	1010.2	27.6	22.7	75	28.6	0.0	1.4	8
03	15:00	04	03:00	00 - 11 S	166 - 51 E	bc	13	8.0	1008.7	27.5	22.2	73	28.6	0.0	1.4	8
03	18:00	04	06:00	00 - 10 S	166 - 51 E	bc	12	8.4	1008.4	27.3	19.8	64	28.6	0.0	1.4	7
03	21:00	04	09:00	00 - 10 S	166 - 51 E	bc	12	8.7	1009.6	28.1	22.5	72	28.5	0.0	1.4	8
04	00:00	04	12:00	00 - 10 S	165 - 51 E	bc	12	8.8	1009.0	28.6	21.8	67	28.6	0.0	1.3	7
04	03:00	04	15:00	00 - 10 S	166 - 50 E	bc	10	7.4	1007.2	29.1	21.4	63	28.7	0.0	1.4	7
04	06:00	04	18:00	00 - 10 S	166 - 51 E	bc	10	7.4	1007.0	28.4	22.5	70	28.7	0.0	1.4	8
04	09:00	04	21:00	00 - 10 S	166 - 51 E	bc	9	6.7	1009.2	27.7	22.9	75	28.6	0.0	1.4	7
04	12:00	05	00:00	00 - 10 S	166 - 51 E	bc	9	6.0	1009.4	27.6	23.1	77	28.6	0.0	1.4	7
04	15:00	05	03:00	00 - 24 N	167 - 11 E	bc	9	7.0	1008.3	27.4	23.0	77	28.7	0.0	1.6	11
04	18:00	05	06:00	01 - 04 N	167 - 31 E	bc	9	7.0	1008.6	27.7	22.6	74	28.8	0.0	1.7	10
04	21:00	05	09:00	01 - 46 N	167 - 55 E	bc	9	8.1	1009.6	28.1	22.3	71	28.6	0.0	1.7	11
05	00:00	05	12:00	02 - 26 N	168 - 18 E	bc	9	6.9	1009.0	28.8	22.8	70	28.9	0.5	1.7	11
05	03:00	05	15:00	03 - 10 N	168 - 39 E	bc	7	7.3	1007.4	28.8	22.0	67	29.0	0.0	1.7	12
05	06:00	05	18:00	03 - 52 N	169 - 03 E	bc	8	7.0	1007.7	28.3	22.5	71	28.8	0.0	1.3	9
05	09:00	05	21:00	04 - 34 N	169 - 28 E	bc	8	7.5	1009.1	28.2	22.0	69	28.7	0.0	1.3	8
05	12:00	06	00:00	05 - 17 N	169 - 53 E	bc	9	7.2	1009.2	27.7	22.9	75	28.6	0.0	1.5	11
05	15:00	06	03:00	06 - 00 N	170 - 18 E	bc	7	5.3	1008.2	27.6	22.4	73	28.5	0.0	1.3	10
05	18:00	06	06:00	06 - 43 N	170 - 42 E	bc	7	5.8	1008.9	27.2	23.1	78	28.5	1.8	1.0	10
05	21:00	06	09:00	07 - 14 N	171 - 02 E	bc	4	5.2	1010.6	26.5	21.5	74	29.1	0.0	1.1	6
06	00:00	06	12:00	07 - 05 N	171 - 21 E	bc	N/A	N/A	1010.1	29.4	23.1	69	29.2	0.0	0.2	8

07	00:00	07	12:00	07 - 28 N	170 - 47 E	bc	6	3.9	1010.3	28.2	22.3	70	29.4	0.0	1.5	13
07	03:00	07	15:00	07 - 57 N	170 - 06 E	bc	7	7.4	1008.8	28.7	23.7	74	28.7	0.0	1.1	14
07	06:00	07	18:00	08 - 27 N	169 - 23 E	bc	8	5.5	1008.8	27.8	23.5	78	28.6	0.0	1.2	14
07	09:00	07	21:00	08 - 56 N	168 - 42 E	bc	7	7.6	1010.5	27.6	23.8	80	28.4	0.0	1.2	14
07	12:00	07	23:00	09 - 25 N	168 - 00 E	bc	7	6.4	1010.9	27.3	23.5	80	28.3	0.0	1.2	13
07	15:00	08	02:00	09 - 52 N	167 - 16 E	bc	7	7.5	1009.8	27.2	23.5	80	28.3	1.2	1.2	13
07	18:00	08	05:00	10 - 16 N	166 - 31 E	bc	7	7.4	1009.3	27.2	23.6	81	28.2	0.0	1.3	13
07	21:00	08	08:00	10 - 41 N	165 . 47 E	bc	7	7.8	1010.8	28.9	23.7	73	28.2	0.0	1.4	17
08	00:00	08	11:00	11 - 06 N	165 - 03 E	bc	8	8.1	1010.4	29.1	23.8	73	28.4	0.0	1.4	15
08	03:00	08	14:00	11 - 31 N	164 - 19 E	bc	9	5.8	1009.0	29.2	23.6	72	28.7	0.0	1.6	17
08	06:00	08	17:00	11 - 57 N	163 - 35 E	bc	8	6.9	1008.8	28.5	24.0	77	28.7	0.0	1.6	17
08	09:00	08	20:00	12 - 23 N	162 - 52 E	bc	8	7.9	1010.4	27.9	23.8	79	28.7	0.0	1.6	17
08	12:00	08	22:00	12 - 47 N	162 - 09 E	bc	8	7.7	1011.1	27.8	23.9	79	28.7	0.0	1.5	17
08	15:00	09	01:00	13 - 11 N	161 - 25 E	bc	8	8.2	1009.3	27.7	23.9	80	28.8	0.0	1.6	19
08	18:00	09	04:00	13 - 34 N	160 - 40 E	bc	8	8.9	1009.3	27.2	22.6	76	28.7	0.0	1.8	20
08	21:00	09	07:00	13 - 58 N	159 - 56 E	q	22	5.4	1012.4	25.2	22.7	86	28.8	2.5	1.6	21
09	00:00	09	10:00	13 - 43 N	159 - 35 E	q	1	11.6	1013.3	24.4	21.8	86	28.6	33.4	1.8	16
09	03:00	09	13:00	13 - 01 N	159 - 17 E	c	6	11.9	1009.2	25.9	22.8	83	28.7	0.3	2.3	22
09	06:00	09	16:00	13 - 00 N	158 - 26 E	bc	9	7.9	1008.2	28.6	21.9	67	28.8	0.0	2.5	25
09	09:00	09	19:00	13 - 00 N	157 - 34 E	bc	13	6.2	1009.8	27.0	22.3	76	28.9	0.0	2.5	25
09	12:00	09	22:00	13 - 00 N	156 - 43 E	bc	13	2.5	1010.7	27.2	22.4	75	29.1	0.0	1.8	23
09	15:00	10	01:00	13 - 01 N	155 - 52 E	bc	9	5.9	1008.7	27.1	22.9	78	29.2	0.0	1.8	25
09	18:00	10	04:00	13 - 03 N	155 - 01 E	bc	15	3.2	1008.2	26.6	23.2	82	29.3	0.0	1.7	23
09	21:00	10	07:00	13 - 06 N	154 - 10 E	bc	11	4.6	1009.3	27.4	23.1	77	29.3	0.0	1.5	20
10	00:00	10	10:00	13 - 07 N	153 - 19 E	bc	11	5.5	1010.3	29.2	21.6	64	29.5	0.0	1.4	19
10	03:00	10	13:00	13 - 08 N	152 - 28 E	bc	12	4.2	1008.9	29.4	21.5	62	29.5	0.0	1.3	18
10	06:00	10	16:00	13 - 08 N	151 - 37 E	bc	9	2.3	1008.3	30.1	23.2	67	29.8	0.1	1.1	18
10	09:00	10	19:00	13 - 08 N	150 - 46 E	bc	8	1.7	1009.7	28.6	22.8	71	29.8	0.0	0.9	16
10	12:00	10	22:00	13 - 08 N	149 - 55 E	bc	15	3.0	1010.6	28.3	22.0	69	29.7	0.0	0.8	15
10	15:00	11	01:00	13 - 08 N	149 - 05 E	bc	17	5.3	1008.2	28.0	22.1	71	29.5	0.0	1.0	17
10	18:00	11	04:00	13 - 08 N	148 - 14 E	bc	19	3.7	1007.7	27.9	22.0	70	29.5	0.0	0.9	15
10	21:00	11	07:00	13 - 08 N	147 - 24 E	bc	27	5.0	1009.8	27.2	23.6	81	29.4	0.5	1.1	13
11	00:00	11	10:00	13 - 08 N	146 - 35 E	bc	27	1.5	1010.3	26.9	21.1	71	29.5	0.0	1.0	12
11	03:00	11	13:00	13 - 08 N	145 - 46 E	bc	19	4.0	1008.7	27.9	20.8	66	29.5	0.0	1.0	13
11	06:00	11	16:00	13 - 09 N	144 - 57 E	bc	17	4.0	1007.7	28.4	21.6	67	29.6	0.0	1.0	16
11	12:00	11	21:00	13 - 43 N	144 - 22 E	bc	16	4.0	1010.6	27.9	22.3	72	29.8	0.0	0.7	9
11	15:00	12	00:00	14 - 22 N	143 - 50 E	bc	17	5.5	1009.8	28.0	22.2	71	29.7	0.0	0.7	10
11	18:00	12	03:00	15 - 00 N	143 - 18 E	bc	18	5.6	1008.4	27.6	22.0	71	29.7	0.0	0.9	13
11	21:00	12	06:00	15 - 39 N	142 - 47 E	bc	18	5.9	1009.6	28.2	22.3	70	29.9	0.0	0.9	9
12	00:00	12	09:00	16 - 18 N	142 - 16 E	bc	18	6.6	1010.3	29.1	22.5	68	30.1	0.0	1.1	10
12	03:00	12	12:00	16 - 56 N	141 - 45 E	q	15	8.2	1009.4	27.1	23.2	79	30.1	0.4	1.1	10
12	06:00	12	15:00	17 - 33 N	141 - 15 E	o	18	8.8	1007.9	29.4	22.2	65	30.3	0.0	1.3	10
12	09:00	12	18:00	18 - 09 N	140 - 45 E	o	19	8.6	1007.9	28.3	22.6	71	30.2	0.0	1.3	10
12	12:00	12	21:00	18 - 46 N	140 - 13 E	o	24	5.3	1009.1	28.8	23.0	71	30.1	0.0	1.1	9
12	15:00	13	00:00	19 - 22 N	139 - 40 E	o	5	0.7	1008.2	27.5	23.5	79	30.4	0.0	1.1	8
12	18:00	13	03:00	20 - 00 N	139 - 08 E	bc	21	5.4	1007.5	27.6	23.7	80	30.2	0.0	1.1	7
12	21:00	13	06:00	20 - 39 N	138 - 34 E	c	21	8.1	1006.9	28.4	23.2	73	30.0	0.0	1.2	8
13	00:00	13	09:00	21 - 16 N	138 - 01 E	q	20	10.3	1007.2	29.4	23.9	72	30.0	0.0	1.6	8
13	03:00	13	12:00	21 - 52 N	137 - 30 E	c	26	13.6	1005.7	26.2	22.7	81	29.7	2.5	2.1	8
13	06:00	13	15:00	22 - 27 N	137 - 03 E	r	24	16.8	1005.4	23.8	22.5	93	29.5	37.7	2.8	9
13	09:00	13	18:00	23 - 02 N	136 - 36 E	o	23	10.8	1005.0	27.5	22.7	75	29.0	16.4	2.7	8
13	12:00	13	21:00	23 - 35 N	136 - 07 E	o	22	11.3	1004.8	27.1	24.2	84	27.9	10.6	2.9	8
13	15:00	14	00:00	24 - 08 N	135 - 35 E	r	23	12.3	1003.7	26.3	24.9	92	27.5	7.7	2.9	10
13	18:00	14	03:00	24 - 42 N	135 - 02 E	o	25	12.0	1002.0	26.7	24.8	89	27.6	4.3	2.3	8
13	21:00	14	06:00	25 - 18 N	134 - 30 E	o	26	9.1	1002.7	27.3	25.0	87	28.4	0.0	2.3	8
14	00:00	14	09:00	25 - 54 N	133 - 59 E	c	32	7.0	1003.5	25.7	23.8	89	28.4	4.2	2.0	9
14	03:00	14	12:00	26 - 31 N	133 - 27 E	bc	24	5.9	1002.7	27.7	25.0	85	28.6	0.7	1.5	8

* Symbols in "Weather" column mean:

- b: Blue sky (Cloud 0-2)
- bc: Fine but Cloudy (Cloud 3-7)
- c: Cloudy (Cloud 8-10)
- d: Drizzling rain
- f: Fog
- g: Gloom
- h: Hail
- l: Lightning
- m: Mist
- o: Overcast (Cloud 10)
- p: Passing showers
- q: Squalls
- r: Rain
- s: Snow
- t: Thunder
- u: Ugly threatening wr
- v: Visibility
- w: Dew
- z: Haze

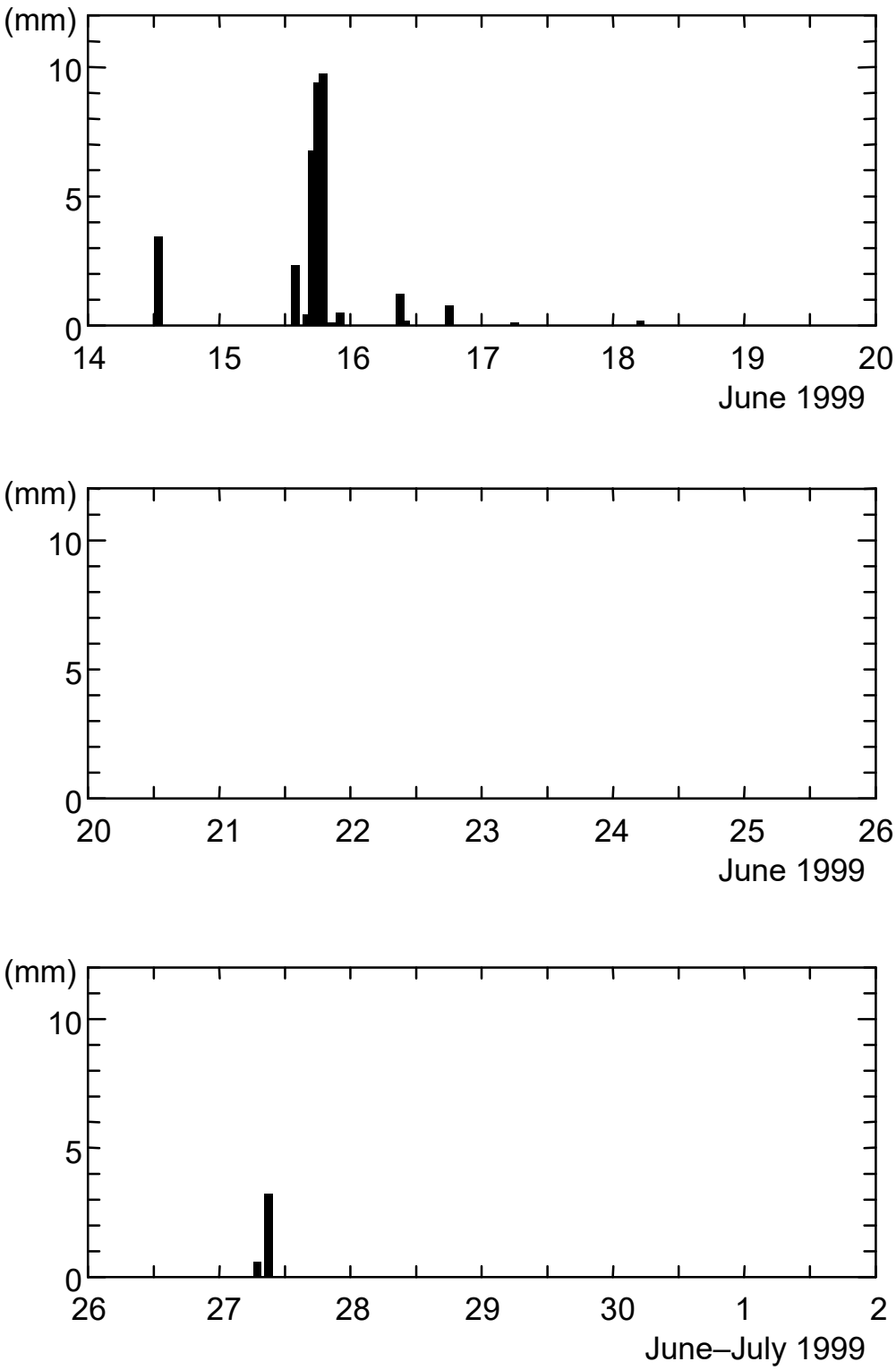

Fig. 6.1-1: Time series of hourly rainfall amount, measured by raingauge on the navigational bridge deck.

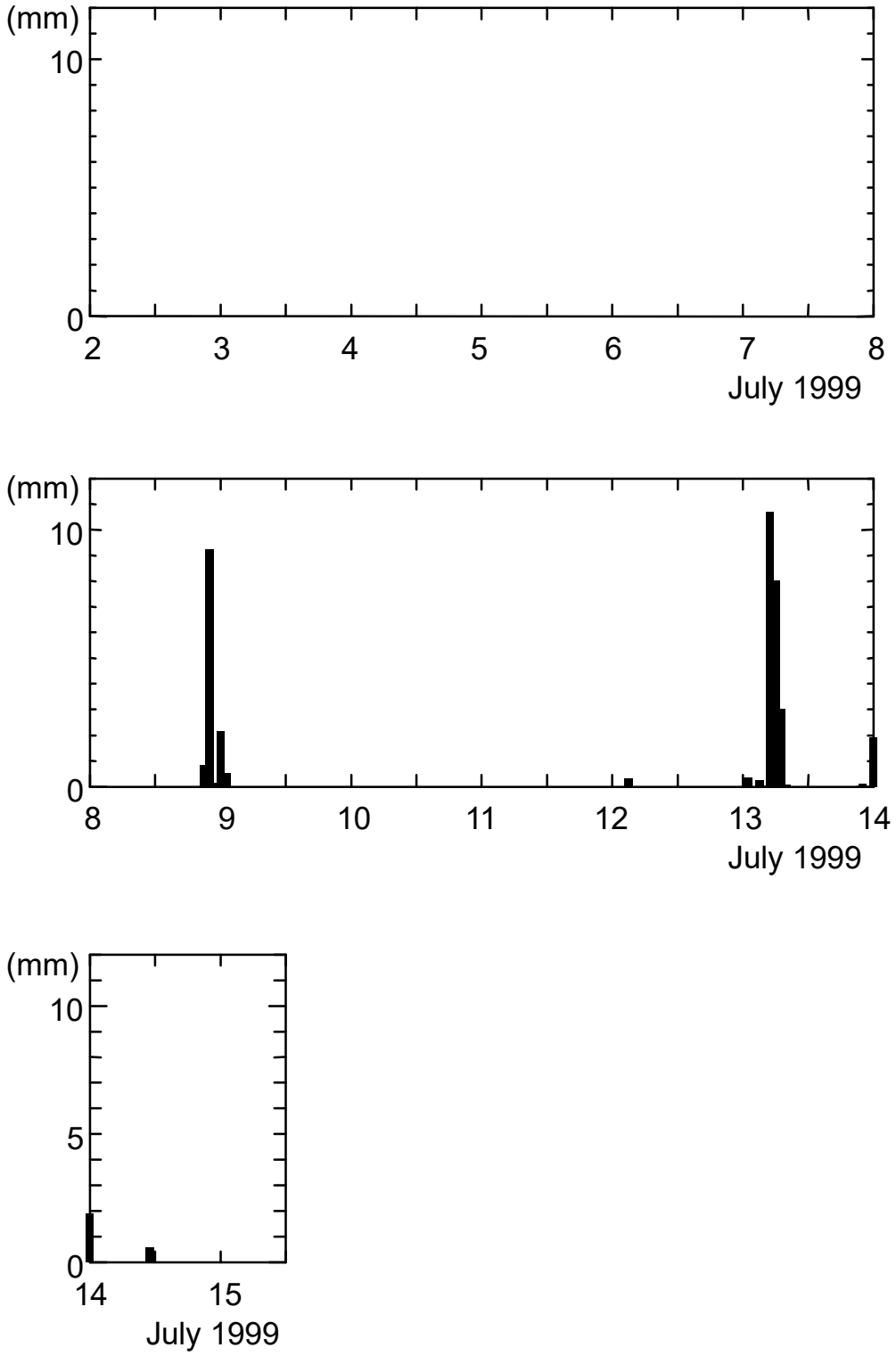

Fig. 6.1-1 (continued)

6.2 Radiosonde Observation

(1) Personnel

Kunio Yoneyama (JAMSTEC): Principal Investigator
Fumitaka Yoshiura (GODI): Operation Leader
Kiyotake Kouzuma (GODI)
Satoshi Okumura (GODI)
Kenji Suzuki (Yamaguchi Univ.)
Tomoki Ushiyama (FRSGC)
Saji N. Hameed (FRSGC)
Kazuyoshi Kikuchi (Univ. of Tokyo)
Masaki Katsumata (JAMSTEC)

(2) Objectives

Atmospheric soundings are measured using radiosonde. Especially the diurnal cycle of atmospheric stability is aimed by dense observation (eight times per day) through the IOP.

(3) Measured Parameters

Pressure
Temperature
Relative humidity
Wind speed / direction

(4) Methods

Atmospheric sounding by launching radiosonde was carried out every three hours (00, 03, 06, 09, 12, 15, 18, 21 UTC) during the IOP, and twice a day and occasionally in other periods (see Table 6.2-1). The system mainly consists of Main processor (Vaisala DigiCORA MW11), Balloon Launcher (Vaisala ASAP), GPS antenna (GA20), UHF telemetry antenna (RB21), PC (Toshiba Dynabook 430CDT), and H-type Humicap GPS sonde (RS80-15GH).

Before launching, temperature and humidity were calibrated by Humidity calibrator (Digilog Instruments VAPORPAK H-31). The balloon launcher was ventilated well to reduce the influence of a) sensor arm heating, and b) launch from air-conditioned container. Nevertheless, we found surface 30-m data were affected by the warming of ship body, probably due to the fact that we conducted stationary observation and were in the condition of light wind during the IOP. So we conducted tetherd sonde measurement for the surface 100-m layer and confirmed that these data can be corrected enough by linear outerpolation (not shown here).

During this cruise, data are obtained as RESEARCH mode (1.5 sec. interval non-edited data) for both wind and temperature/humidity. After the operation, data are converted to the 2 sec. interval edited data by using software SIMUL.

(5) Preliminary Results

Profiles of temperature and dew point temperature are plotted on the thermodynamic chart (EMAGRAM) and shown in the Appendix. Wind profile is also shown there.

Easterlies were dominant in the entire troposphere in the beginning of IOP (17 - 20 June). Westerlies can be found near the tropopause on 21 June and then gradually prevailed downward. As a result, easterlies were dominant in the lower and middle troposphere (surface - 400 hPa) with maximum speed

of 15 m/sec at 600-500 hPa layer, and westerlies were dominant in the higher troposphere (400 - 100 hPa) with maximum speed of 20 m/sec at 200 hPa during the latter half period of IOP.

During the IOP, basically almost all sounding showed relatively dry conditions. Very strong dry layer near the melting (0 ℃) layer can be often found in the latter half period of large triangle phase (25 - 30 June). These wind and humidity profiles corresponds to the fact that we were just in the convectively suppressed area/period, as we can also confirm from satellite images and we had no significant precipitation during the IOP. Only from the night of 27 June to the morning of 28 June in local time, there was a rainfall. In spite of this, it remained dry except only lower troposphere and quickly recovered dry enough.

(6) Data Archive

All sounding data have been sent to the world through GTS by Japan Meteorological Agency. Non-edited are stored as Binary and edited are stored as ASCII format, respectively. All data will be archived and available from Kunio Yoneyama of JASMTEC. All data will be corrected and 5-hPa interval data set will be made and available.

Table 6.2-1: List of radiosonde observations.

No.	Time (UTC) YYMMDD HH	Position Lat.	Lon.	Surface State P (hPa)	T (deg. C)	RH (%)	WD (deg)	WS (m/s)	Max Altitude (hPa)	(m)	Cloud Amount	Cloud Type
1	99 06 09 06	29.38N	142.49E	1007.2	24.6	80	303	7.4	49.1	20907	10	Cb,Cu,Nb
2	99 06 09 12	28.07N	143.06E	1009.4	24.3	91	240	4.5	402.6	7503	10	Nb,Cu
3	99 06 10 00	25.01N	144.45E	1011.1	28.1	73	244	3.7	28.4	24336	6	Cu,Ac
4	99 06 10 12	22.39N	145.59E	1012.4	27.3	80	210	2.5	48.5	20903	5	Cu,Ac,As
5	99 06 11 00	19.11N	147.02E	1013.1	29.5	61	110	4.0	40.1	22106	4	Ac,Cu,Cb
6	99 06 11 06	17.93N	147.53E	1009.7	29.0	73	120	5.8	38.7	22271	3	Cu,Ci
7	99 06 11 12	16.41N	148.12E	1012.0	28.7	72	108	8.3	25.0	25107	3	Cu,Ac
8	99 06 12 00	13.56N	149.18E	1011.1	29.4	75	90	7.6	36.8	22604	2	Cu
9	99 06 12 06	12.12N	149.72E	1008.0	28.9	73	89	7.4	25.0	25107	1 +	Cu,Ci
10	99 06 12 12	10.72N	150.23E	1010.3	28.2	76	84	5.8	62.6	19288	4	Ac,Cu
11	99 06 13 00	08.05N	151.58E	1009.1	26.9	82	132	7.1	59.6	19707	10	Ns,Cu
12	99 06 14 06	06.93N	153.02E	1006.5	28.4	75	40	1.0	32.4	23343	5	Ci,Cb,Sc
13	99 06 14 09	06.50N	153.83E	1008.3	27.8	76	57	2.6	83.6	17549	1	Sc
14	99 06 14 12	06.20N	154.42E	1009.1	27.7	79	40	2.7	47.0	20999	2	Sc,Ac,Ci
15	99 06 14 15	05.77N	155.23E	1008.4	27.0	83	291	1.5	46.8	21012	1	Cu,Sc
16	99 06 14 18	05.47N	155.84E	1007.9	27.3	79	55	2.9	43.3	21505	1	Si,Cu
17	99 06 14 21	05.08N	156.55E	1008.6	26.9	87	38	5.4	41.6	21812	8	Cu,As,Cs,Cc
18	99 06 15 00	04.90N	156.91E	1009.8	28.4	75	80	5.3	53.8	20213	6	Cu,Sc,Ci
19	99 06 15 03	04.51N	157.64E	1007.7	28.5	80	93	3.5	42.5	21659	6	Cu,Cb,Cc
20	99 06 15 06	04.12N	158.32E	1006.5	28.3	77	77	0.8	41.0	21897	9	Cu,Cb,Sc
21	99 06 15 09	03.73N	159.00E	1007.8	27.8	81	72	2.2	34.0	23022	2	Cu
22	99 06 15 12	03.34N	159.69E	1008.8	27.7	81	76	3.7	52.4	20334	10	Cu,Cb,Ac
23	99 06 15 15	02.92N	160.38E	1007.6	27.0	85	119	2.6	N/A	N/A	7	Cu,Cb,Ac
24	99 06 15 18	02.60N	161.06E	1007.9	24.8	91	121	12.1	578.9	4655	10	Cb
25	99 06 15 21	02.36N	161.55E	1009.0	25.4	86	124	1.0	38.3	22384	10	Ac,As,Cu
26	99 06 16 00	01.99N	162.20E	1009.5	28.8	72	116	6.9	32.3	23445	8	Cu,Cc,Cs,As
27	99 06 16 03	01.66N	162.83E	1008.2	28.5	73	119	6.1	75.4	18215	8	Cu,Ci,Cs
28	99 06 16 06	01.31N	163.44E	1006.3	28.5	72	137	6.4	45.6	21231	9	Cu,Ci
29	99 06 16 09	00.98N	164.04E	1008.0	26.3	86	103	5.6	51.7	20429	10	Cb
30	99 06 16 12	00.61N	164.54E	1008.9	26.8	85	81	5.7	57.6	19794	10	Ax,SC,Cu,Cb
31	99 06 16 15	00.39N	165.16E	1007.7	27.4	81	74	5.5	46.7	21037	2	Cu,Ac
32	99 06 16 18	00.12N	165.59E	1007.1	26.1	86	52	6.8	62.0	19327	9	Cu,Cb
33	99 06 16 21	00.22S	166.31E	1008.8	28.2	79	46	7.2	31.5	23596	3	Ci,Cu,Sc
34	99 06 17 00	00.47S	166.82E	1009.8	28.5	76	50	6.8	36.4	22649	6	Cs,Ci,Cu
35	99 06 17 03	00.52S	166.91E	1008.2	28.5	74	57	6.3	45.4	21298	5	Cu,Ci
36	99 06 17 06	00.52S	166.91E	1007.0	28.8	75	33	4.4	45.2	21254	10	Cu,Cb,Ac,Ci
37	99 06 17 09	00.52S	166.91E	1008.4	27.7	80	53	6.2	53.3	20252	2	Cu,Ci
38	99 06 17 12	00.52S	166.90E	1009.1	27.1	83	57	5.4	48.7	20832	2	Cu,Ci
39	99 06 17 15	00.52S	166.91E	1008.0	27.1	84	47	3.4	49.0	20744	1	Cu
40	99 06 17 18	00.52S	166.91E	1007.4	26.9	85	79	3.3	47.5	20932	1	Cu
41	99 06 17 21	00.50S	166.91E	1008.4	27.5	82	57	3.7	32.0	23489	3	Cu,Ci
42	99 06 18 00	00.52S	166.90E	1008.6	28.2	75	53	5.6	36.0	22728	2	Cu,Ci,Cs
43	99 06 18 03	00.52S	166.91E	1007.0	29.7	74	43	4.8	34.3	23047	3	Cu,Ci
44	99 06 18 06	00.52S	166.91E	1006.6	29.1	72	38	3.9	30.0	23843	3	Cu,Ci
45	99 06 18 09	00.52S	166.91E	1008.2	27.7	78	60	5.6	43.3	21525	2	Ci,Cu
46	99 06 18 12	00.52S	161.91E	1008.5	27.0	85	22	6.5	34.6	22965	1	Cu
47	99 06 18 18	00.52S	166.91E	1007.2	26.2	85	77	1.9	36.4	22635	1	Cu
48	99 06 19 00	00.52S	166.90E	1008.8	28.4	73	14	4.2	30.6	23787	3	Cu,Ci
49	99 06 19 06	00.52S	166.90E	1005.7	29.3	68	101	4.3	32.0	23465	4	Cu,Ci
50	99 06 19 12	00.40S	166.54E	1008.4	27.1	85	103	1.9	36.8	22580	4	Cu,Ci
51	99 06 19 18	00.11S	165.36E	1007.4	26.5	84	87	2.1	43.3	21525	3	Cu,Ci
52	99 06 20 00	00.01S	164.99E	1007.9	28.1	76	125	4.1	33.0	23301	5	Ci,Cs,Cu
53	99 06 20 03	00.00N	165.02E	1005.8	28.8	70	143	4.0	40.2	22032	4	Cu,Ci,Cs
54	99 06 20 06	00.03N	164.99E	1005.6	28.4	73	106	5.0	33.2	23470	2	Cu,Cs,Ci
55	99 06 20 09	00.02N	164.99E	1007.3	27.6	78	115	5.0	35.7	22743	1	Cu,Ci
56	99 06 20 12	00.02N	164.99E	1008.1	27.3	76	122	4.8	38.3	22301	1	Cu,Ci
57	99 06 20 15	00.02N	164.99E	1007.1	26.7	86	106	4.2	36.4	22606	1	Cu
58	99 06 20 18	00.02N	164.99E	1006.4	27.2	79	90	7.7	40.3	21974	2	Ci
59	99 06 20 21	00.00N	164.98E	1008.4	27.4	76	79	6.8	35.2	22915	1 +	Cu
60	99 06 21 00	00.00N	164.99E	1008.5	28.5	69	94	5.4	33.2	23274	0 +	Cu
61	99 06 21 03	00.00N	164.99E	1006.7	28.7	70	88	3.9	48.1	20946	1	Cu,Ci

62	99	06	21	06	00.01N	164.99E	1006.3	28.7	69	85	5.9	27.3	24648	1		Cu,Cs,Ci
63	99	06	21	09	00.00N	164.99E	1008.2	27.8	72	92	4.2	56.7	19686	0	+	Cu
64	99	06	21	12	00.01S	164.99E	1009.3	27.4	73	76	4.4	45.9	21207	3		Cu
65	99	06	21	15	00.01S	164.99E	1008.2	26.9	75	85	4.5	41.7	21778	1		Cu
66	99	06	21	18	00.01S	165.00E	1008.0	27.0	74	78	2.9	40.3	21981	1		Cu
67	99	06	21	21	00.01S	165.00E	1008.9	27.4	73	77	2.1	31.8	23564	0	+	Cu
68	99	06	22	00	00.01S	165.00E	1009.0	28.6	68	80	2.3	35.9	22779	3		Cu
69	99	06	22	03	00.01S	165.00E	1007.3	29.8	66	119	1.1	33.9	23121	2		Cu
70	99	06	22	06	00.00N	164.99E	1006.6	28.9	68	147	1.2	40.9	21941	2		Cu
71	99	06	22	09	00.00N	164.99E	1008.7	27.5	73	50	1.6	42.3	21704	0	+	Cu
72	99	06	22	12	00.00N	164.99E	1009.5	26.8	74	130	0.7	40.9	21902	1		Cu
73	99	06	22	15	00.00N	164.99E	1008.2	26.3	75	198	1.3	51.0	20513	0	+	Cu
74	99	06	22	18	00.03N	165.01E	1007.5	26.1	79	235	2.0	49.8	20676	1		Cu
75	99	06	22	21	00.01S	164.99E	1008.8	26.7	72	240	0.7	32.5	23391	3		Cu,Ac
76	99	06	23	00	00.00N	165.00E	1009.0	28.6	63	227	0.1	46.4	21164	0	+	Ci,Cu
77	99	06	23	03	00.01S	165.00E	1007.2	29.8	61	143	0.7	28.7	24150	1		Cu,Ci
78	99	06	23	06	00.01S	164.99E	1006.1	29.2	65	107	2.1	40.6	21934	2		Cu,Ci,Cs
79	99	06	23	09	00.00N	165.00E	1008.1	27.6	72	109	4.7	34.1	23052	1		Cu
80	99	06	23	12	00.01S	165.00E	1008.7	27.3	70	106	2.7	37.7	22394	2		Cu
81	99	06	23	15	00.01S	165.00E	1006.9	26.9	72	111	3.1	39.3	22136	0	+	Cu
82	99	06	23	18	00.01S	165.00E	1006.9	26.7	75	124	3.1	40.5	21915	2		Cu
83	99	06	23	21	00.02S	165.00E	1008.5	27.4	73	143	1.6	40.9	21933	1	+	Cu
84	99	06	24	00	00.01S	165.00E	1009.0	29.3	67	141	2.8	39.7	22119	1	+	Cu,Cb
85	99	06	24	03	00.02S	165.02E	1007.1	30.4	61	161	1.9	40.7	21937	2		Cu,Ci
86	99	06	24	06	00.00N	165.00E	1006.6	30.1	63	141	1.8	31.8	23486	0	+	Cu
87	99	06	24	09	00.01S	164.99E	1008.2	28.2	70	150	3.6	64.7	19075	1		Cu
88	99	06	24	12	00.01S	164.99E	1009.5	27.4	75	142	3.8	36.7	22566	3		Ac,Cu
89	99	06	24	15	00.01S	165.00E	1008.1	27.2	76	119	3.4	37.8	22356	1	+	Cu
90	99	06	24	18	00.00N	164.99E	1007.5	27.4	75	114	4.8	37.2	22449	3		Cu
91	99	06	24	21	00.01S	165.00E	1008.9	27.6	78	89	4.5	25.4	24938	5		Cu
92	99	06	25	00	00.00N	165.00E	1009.1	28.8	71	113	3.8	30.2	23851	3		Cu
93	99	06	25	03	00.01S	165.00E	1007.7	29.5	65	98	3.5	76.4	18116	1		Cu,Cb
94	99	06	25	06	00.01S	164.99E	1006.6	29.5	67	73	4.6	65.8	18990	2		Cu
95	99	06	25	09	00.01S	164.99E	1007.4	27.6	76	69	5.0	38.6	22240	1		Cu
96	99	06	25	12	00.01S	165.00E	1008.2	27.5	77	74	4.6	45.4	21231	3		Cu
97	99	06	25	15	00.01S	165.00E	1007.5	27.4	72	76	6.8	37.2	22451	1	+	Cu
98	99	06	25	18	00.01S	164.99E	1007.2	27.4	72	85	5.4	50.1	20615	2		Cu
99	99	06	25	21	00.01S	165.00E	1009.0	27.8	72	84	5.3	36.4	22677	1		Cu
100	99	06	26	00	00.01S	165.00E	1009.4	28.9	69	91	6.0	39.3	22191	1	-	Cu
101	99	06	26	03	00.05S	165.00E	1007.1	29.3	69	87	5.3	35.8	22737	1		Cu
102	99	06	26	06	00.01S	165.00E	1006.4	28.4	73	83	5.3	37.7	22446	1		Cu,Ci,Cs
103	99	06	26	09	00.01S	164.99E	1008.0	27.8	75	98	6.5	41.0	21857	0	+	Cu
104	99	06	26	12	00.01S	165.00E	1009.0	27.5	77	105	6.4	38.8	22220	1	+	Cu
105	99	06	26	15	00.01S	165.00E	1007.9	27.4	75	102	6.2	37.5	22426	2		Cu
106	99	06	26	18	00.01S	164.99E	1007.2	27.3	77	117	5.7	49.6	20681	2		Cu
107	99	06	26	21	00.01S	164.99E	1008.4	27.9	71	97	8.1	34.4	23051	1	+	Cu
108	99	06	27	00	00.01S	165.00E	1008.9	28.9	72	97	8.1	35.1	22911	2	+	Cu
109	99	06	27	03	00.01S	165.00E	1007.0	28.7	73	91	8.1	35.9	22749	3		Cu
110	99	06	27	06	00.01S	165.00E	1006.2	28.5	77	99	5.2	40.5	21971	6		Cb,Cu
111	99	06	27	09	00.01S	164.99E	1008.0	27.1	89	90	12.3	79.4	17849	10	-	Cb,Cu,Ac
112	99	06	27	12	00.01S	164.99E	1008.8	27.5	73	92	8.8	44.1	21434	2	+	Cu,Ac
113	99	06	27	15	00.01S	165.00E	1008.0	27.7	76	90	5.0	41.7	21758	2		Cu
114	99	06	27	18	00.01S	165.00E	1007.7	27.6	75	83	6.0	46.1	21147	5		Cu
115	99	06	27	21	00.01S	165.00E	1009.3	28.2	75	85	8.6	30.7	23750	7		Cu,Cs
116	99	06	28	00	00.01S	164.99E	1010.0	28.9	69	108	10.0	46.5	21152	2		Cu,Ci
117	99	06	28	03	00.01S	165.00E	1008.2	28.8	64	92	7.7	30.2	23876	6		Cs,Ci,Cu
118	99	06	28	06	00.01S	164.99E	1007.1	28.7	67	103	7.4	50.5	20598	6		Cs,Ci,Cu
119	99	06	28	09	00.01S	164.99E	1008.3	27.9	74	104	8.0	54.0	20163	7		Cs,Cu
120	99	06	28	12	00.01S	164.99E	1009.4	28.1	72	100	7.0	52.1	20394	4		Cu,Ac,Ci
121	99	06	28	15	00.01S	165.00E	1008.4	27.8	72	111	7.4	39.3	22134	3		Cu,Ci
122	99	06	28	18	00.01S	165.00E	1007.6	27.3	75	107	8.0	41.3	21834	3		Cu
123	99	06	28	21	00.01S	165.00E	1009.4	28.1	71	111	7.5	34.1	23107	2		Cu
124	99	06	29	00	00.01S	165.00E	1009.7	28.5	67	115	6.4	32.1	23511	1	+	Cu
125	99	06	29	03	00.01S	165.00E	1008.1	29.2	69	101	5.7	46.9	21083	1		Cu
126	99	06	29	06	00.00N	164.99E	1007.0	29.3	69	101	4.0	40.3	22019	1		Cu
127	99	06	29	09	00.01S	164.99E	1008.5	27.9	73	101	5.9	33.6	23158	3		Cu,Cb
128	99	06	29	12	00.01S	164.99E	1009.2	27.8	74	105	6.1	36.4	22652	3		Cu

129	99	06	29	15	00.01S	165.00E	1008.2	27.6	73	89	6.1	35.7	22748	4		Cu
130	99	06	29	18	0.001S	164.99E	1007.3	27.2	76	100	5.8	36.7	22587	3	+	Cu
131	99	06	29	21	00.01S	165.00E	1008.5	27.6	75	88	5.2	33.2	23269	3		Cu
132	99	06	30	00	00.01S	164.99E	1008.8	28.6	71	99	5.7	28.6	24194	2		Cu
133	99	06	30	03	00.01S	165.00E	1006.8	28.7	74	100	6.5	49.7	20733	1		Cu,Cb
134	99	06	30	06	00.01S	165.00E	1006.5	28.4	67	93	6.1	34.5	23055	1		Cu,Cb
135	99	06	30	09	00.00N	165.00E	1007.3	27.6	74	79	5.0	42.7	21628	0	+	Cu
136	99	06	30	12	00.17S	165.38E	1008.4	27.8	74	91	6.2	50.4	20607	3		Cu,Cb
137	99	06	30	15	00.16S	165.84E	1007.1	27.6	76	79	6.3	37.4	22457	7		Cu,Ac
138	99	06	30	18	00.15S	166.41E	1006.2	27.6	74	89	7.0	37.7	22396	4		Cu
139	99	06	30	21	00.18S	166.85E	1007.8	27.7	73	76	8.3	57.2	19860	1		Cu
140	99	07	01	00	00.18S	166.84E	1008.6	28.7	68	80	5.8	40.2	22060	2		Cu
141	99	07	01	03	00.18S	166.84E	1006.6	28.7	72	80	6.4	28.6	24192	2		Cu
142	99	07	01	06	00.19S	166.83E	1005.8	28.8	69	81	7.5	35.7	22779	1		Cu,Ci
143	99	07	01	09	00.19S	166.84E	1007.5	28.0	71	77	7.1	91.1	17048	1		Cu
144	99	07	01	12	00.19S	166.83E	1008.5	27.7	74	73	7.9	29.6	23916	2	+	Cu
145	99	07	01	15	00.19S	166.82E	1007.7	27.5	74	80	7.9	35.5	22766	1	+	Cu
146	99	07	01	18	00.18S	166.85E	1006.8	27.4	77	63	8.8	37.8	22364	2		Cu
147	99	07	01	21	00.18S	166.85E	1008.5	28.2	72	65	8.9	42.7	21680	3		Cu
148	99	07	02	00	00.18S	166.85E	1009.2	28.9	69	80	8.8	46.7	21134	0	+	Cu
149	99	07	02	03	00.18S	166.85E	1007.3	28.6	69	83	7.1	37.8	22412	1		Cu
150	99	07	02	06	00.18S	166.85E	1006.6	28.3	70	94	8.1	45.3	21277	1		Cu
151	99	07	02	09	00.18S	166.85E	1008.2	27.7	73	92	7.6	36.3	22630	0	+	Cu
152	99	07	02	12	00.18S	166.85E	1009.3	27.7	76	95	6.8	35.3	22851	2		Cu,Sc
153	99	07	02	15	00.18S	166.85E	1008.2	27.6	76	83	8.7	45.1	21266	8		Ac,Cu
154	99	07	02	18	00.18S	166.85E	1007.6	27.6	75	103	8.1	68.8	17203	5		Cu,Ac
155	99	07	02	21	00.18S	166.85E	1008.1	27.8	76	109	6.9	45.9	21237	3		Cu
156	99	07	03	00	00.18S	166.85E	1008.1	27.8	76	109	6.9	42.4	21719	3		Cu
157	99	07	03	03	00.20S	166.88E	1006.8	28.7	72	94	7.2	32.1	23458	1		Cu,Ci
158	99	07	03	06	00.20S	166.87E	1006.3	28.7	71	112	6.3	37.9	22375	3		Cu
159	99	07	03	09	00.18S	166.85E	1007.7	27.7	74	110	6.6	29.0	24084	0	+	Cu
160	99	07	03	12	00.18S	166.85E	1008.3	27.6	76	127	6.7	44.0	21428	2		Cu
161	99	07	03	15	00.18S	166.85E	1007.7	27.6	76	121	7.9	41.1	21873	1	+	Cu
162	99	07	03	18	00.18S	166.85E	1006.2	27.4	74	130	9.0	46.2	21127	2		Cu
163	99	07	03	21	00.18S	166.85E	1007.9	27.8	72	118	8.3	31.7	23572	0	+	Cu
164	99	07	04	00	00.18S	166.85E	1007.5	28.5	69	119	8.2	33.7	23191	1		Cu
165	99	07	04	03	00.18S	166.85E	1005.7	29.5	69	110	8.1	61.8	19410	1		Cu
166	99	07	04	06	00.18S	166.85E	1004.8	28.4	75	109	6.7	30.1	23880	1		Cu
167	99	07	04	09	00.18S	166.85E	1006.7	27.9	79	102	7.3	53.9	20182	1		Cu
168	99	07	04	12	00.18S	166.85E	1007.5	27.5	81	94	5.4	43.8	21464	1		Cu
169	99	07	04	15	00.29N	167.09E	1006.6	27.8	77	86	9.0	30.5	23720	3	+	Cu
170	99	07	04	18	00.90N	167.45E	1006.3	27.5	79	101	7.2	41.5	21816	2		Cu
171	99	07	04	21	01.60N	167.82E	1007.6	28.1	75	94	8.6	27.8	24409	8		Cu,Ac,As,Cb
172	99	07	05	00	02.26N	168.18E	1007.8	28.6	74	97	7.0	28.2	24334	2		Cu
173	99	07	12	00	16.17N	142.39E	1008.3	30.0	69	187	7.7	49.5	20815	9		Cu,Cb,Ac
174	99	07	12	06	17.41N	141.38E	1006.3	30.0	65	177	7.1	38.0	22485	10	-	Sc,Ac,Cu
175	99	07	13	00	21.11N	138.17E	1005.5	30.0	73	205	8.6	47.8	21091	4		Ci,As,Cu,Cb
176	99	07	13	06	22.28N	137.18E	1003.2	26.8	87	237	10.7	562.3	4848	10		-
177	99	07	14	00	25.79N	134.08E	1001.3	27.3	84	280	5.5	235.9	11332	10		Cu,Sc
178	99	07	14	06	27.00N	133.01E	1000.3	29.3	79	253	6.0	47.7	21126	2		Sc,Cu
179	99	07	14	15	28.98N	131.31E	1000.5	27.4	74	275	10.2	43.3	21726	0		-

6.3 Doppler Radar Observation

(1) Personnel

Masaki Katsumata (JAMSTEC): Principle Investigator
Masaki Hanyu (GODI): Operation Leader
Kunio Yoneyama (JAMSTEC)
Fumitaka Yoshiura (GODI)
Satoshi Okumura (GODI)
Kiyotake Kouzuma (GODI)
Kenji Suzuki (Yamaguchi Univ.)
Kazuyoshi Kikuchi (Univ. of Tokyo)
Tetsuya Takemi (Osaka Univ.)
Tomoki Ushiyama (Frontier Research System for Global Change)
Saji N. Hameed (Frontier Research System for Global Change)

(2) Objectives

The Doppler radar is operated to obtain spatial and temporal distribution of rainfall amount, and structure of precipitating cloud systems.

(3) Parameters

Spatial and temporal distribution of two parameters, radar reflectivity and Doppler velocity, are obtained for 100 km radius and 7.5 minutes intervals by 17-elevations volume scan. The horizontal radar reflectivity fields are also obtained for 200 km radius and 7.5 minute intervals by one elevation (0.7 degrees) PPI (Plan Position Indicator) scan.

(4) Methods

The hardware specifications of this shipborne Doppler radar (RC-52B, made by Mitsubishi Electric Co. Ltd., Japan) are

Frequency:	5290 MHz
Beam Width:	better than 1.5 degrees
Output Power:	250 kW (PEP)
Signal Processor:	RVP-6 (Sigmet Inc., U.S.A.)
Inertial Navigation Unit:	DRUH (Honeywell Inc., U.S.A.)
Application Software:	IRIS / Open (Sigmet Inc., U.S.A.).

The hardware is calibrated by checking (1) frequency, (2) mean power output, (3) transmitting pulse width, (4) pulse repetition frequencies, and (5) receiver linearity for once par a day, at least.

On the operation, on the other hand, the programmed “tasks” are repeated every 7.5 minutes. One cycle consists of one volume scan (consists of PPIs for 17 elevations) with Doppler-mode (100-km range for reflectivity, Doppler velocity), one-elevation PPI with Intensity-mode (200-km range for reflectivity), and one RHI (Range Height Indicator) scan with Doppler-mode, if needs.

The parameters for the above three are shown in Table 6.3-1.

Table 6.3-1: Parameters for each tasks.

	Intensity-mode PPI	Volume Scan	RHI
Pulse Width	2 [μs]	0.5 [μs]	
Scan Speed	18 [deg./sec.]		automatically determined
PRF	260 [Hz]	900 / 720 [Hz]	
Sweep Integration	32 samples		
Ray Spacing	about 1.0 [deg.]		0.2 [deg.]
Bin Spacing	250 [m]	125 [m]	
Elevations	0.7	0.7, 1.4, 2.1, 3.0, 4.0, 5.0, 6.0, 7.1, 8.2, 9.5, 11.0, 12.5, 14.5, 17.0, 20.0, 24.0, 30.0	0.0 to 85.0
Azimuths	Full Circle		Optional
Filters	Speckle filter	Speckle filter / Dual-PRF velocity unfolding	
Gain Control	Fixed		

(5) Results

An example of observed precipitating system, on 27 July, are shown in Fig. 6.3-1. In the event, a band-shaped, northeast-southwest oriented precipitating system moves westward in the south of R/V Mirai. The reflectivity field (a, b) shows that the strongest reflectivity is over 40 dBZ (corresponds 10 mm / hr precipitation). From the Doppler velocity fields (c), the wind in the lower layer in the system had the easterly component, against to the westerly component in the upper layer (both wind is shown by arrows in (c)). In general, such “vertical wind shear” supposed to be important to maintain precipitating system for long period. The further analyses are in future work.

(6) Data Archives

The inventory information of the Doppler radar data obtained in this cruise will be submitted to the DMO (Data Management Office) of JAMSTEC. The original data will be archived at Ocean Research Department of JAMSTEC (Contact Masaki Katsumata [e-mail:])

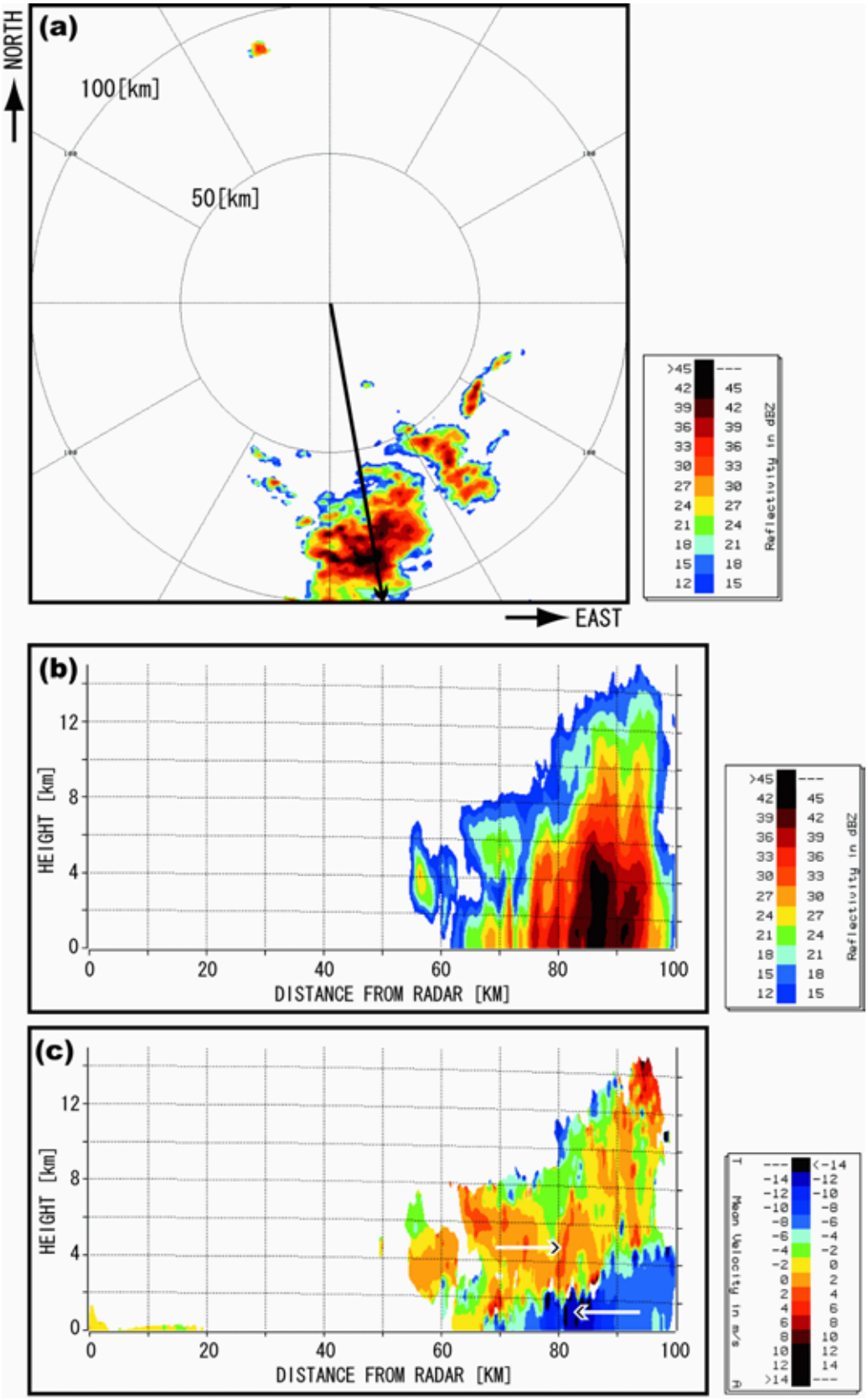

Fig. 6.3-1: An example of Doppler radar image at 1645 UTC on 27 July 1999, at (0, 165E). (a) is an horizontal distribution of reflectivity at 2-km height (CAPPI image). (b) and (c) are vertical cross sections (RHI) of reflectivity and Doppler velocity (radial velocity), respectively, on the line in top panel. See article for the arrows in (c).

6.4 Disdrometer

(1) Personnel

Kenji Suzuki (Yamaguchi Univ.)

(2) Objectives

The torrential rainfalls occur all over the world and kill a lot of irreplaceable lives. In the developed cumulonimbus clouds, which cause the torrential rainfall, there are two precipitation processes, the warm rain process and the cool rain process. For the understanding of the torrential rainfall, it is important to know how efficiently the precipitation processes work and the water is concentrated in cloud.

According to the results of TOGA-COARE, the warm rain process is dominant in the tropical maritime cloud. Thus we can investigate only the warm rain process in the tropics. And these data would be compared with the shallow snow cloud in winter, which the cool rain process is dominant. In this cruise, for the understanding of the warm rain process in the tropical maritime cloud, the raindrop size distribution was investigated by a disdrometer.

(3) Parameters

Raindrop size distribution

(4) Methods

This portable disdrometer consists of a CCD camera, an IR sensor, a strobe and a signal control unit. When a raindrop > 0.1 mm in diameter interrupts the IR sensor beam, the strobe flashes and the image of the raindrop is recorded in a VTR tape. We can get the raindrop size distribution by this portable disdrometer after some data processing.

The disdrometer was set up on the navigational bridge deck. In this cruise, the rainfall detector was out of use because of some trouble. So, the recording was started judging from the Doppler radar echoes and GMS images,

(5) Results

Unfortunately, total rainfall amount during Nauru99 IOP was approximately 3mm. However, on the way back to Japan, we encountered two tropical depressions (July 8 and July 13). The raindrop size distribution will be calculated after this cruise. Table 6.4.1 shows the operation time.

Table 6.4.1 : Operation time.

Date	Obs. Start (UTC)	Obs. Stop (UTC)	Remarks
8-Jun	13:49	19:50	Intermittent rain
24-Jun	20:30	21:06	Shower
25-Jun	14:07	19:58	no rain
27-Jun	7:30	12:30	Shower
30-Jun	2:23	7:10	no rain
4-Jul	10:45	16:49	no rain
5-Jul	14:08	19:28	Shower
5-Jul	19:30	1:34	no rain
7-Jul	0:45	6:49	no rain
7-Jul	6:53	10:59	no rain
7-Jul	11:01	17:05	Shower
8-Jul	14:24	20:23	Shower
8-Jul	20:25	2:25	rain from outerband of subtropical depression
9-Jul	2:50	8:53	no rain
9-Jul	12:25	18:28	Shower
9-Jul	20:20	2:24	no rain
10-Jul	3:16	9:20	Shower
10-Jul	15:08	21:12	Shower
10-Jul	21:30	3:33	no rain
11-Jul	16:30	22:33	no rain
12-Jul	1:00	7:03	no rain
12-Jul	9:33	15:37	no rain
12-Jul	17:15	23:18	no rain
13-Jul	0:05	5:46	heavy rain from TD with strong wind
13-Jul	5:47	11:50	heavy rain from TD with strong wind
13-Jul	12:03	18:06	heavy rain from TD with strong wind
13-Jul	19:05	1:08	heavy rain from TD with strong wind
14-Jul	1:38	7:41	no rain

(6) Data Archive

The data of raindrop size distribution were recorded in VTR tapes. The processed data will be archived in Yamaguchi University (Contact Kenji Suzuki) and open to public after the data processing and quality check.

6.5 Vertical Profilers

(1) Personnel (* indicates on board personnel, + set-up only personnel at Yokohama)

William Brown* (NCAR/ATD) : On-board Principle Investigator
Dave Parsons (NCAR/ATD) : Principle Investigator
Mike Susedik* (NCAR/ATD)
Lou Verstraete* (NCAR/ATD)
Charlie Martin +(NCAR/ATD)
Steve Semmer +(NCAR/ATD)
Dave Costa +(NOAA/ETL)
Jesse Leach +(NOAA/ETL)

NCAR/ATD = National Center for Atmospheric Research / Atmospheric Technology Division, Boulder, Colorado, USA

NOAA/ETL = National Oceanic and Atmospheric Administration / Environmental Technology Laboratory, Boulder, Colorado, USA

(2) Objectives

Three vertically pointing radars are deployed to observe precipitation and air motion (both general background flow and smaller scale motion such as convection and turbulence) throughout the atmospheric boundary layer and into the free atmosphere. One of the radars, MAPR (see below), is a new type of wind profiler radar, that can make much faster measurements than regular wind profiler radars, and one objective has been to investigate the performance of this type of radar at sea. Surface meteorological sensors were deployed to provide background information. Sea surface temperature was also measured to provide background meteorological information, and also to be used in bulk flux calculations. Navigational sensors were deployed to provide necessary adjustments to wind and other measured quantities.

(3) Measured Parameters

Wind profile throughout the boundary layer using DBS and MAPR (see below)
Boundary Layer Height from profiler radar echo power
Temperature profile using RASS (see below)
Cloud height and thickness using an S-Band radar
Rainfall using profiler radar echo power as a function of vertical Doppler velocity
Vertical air motion using Doppler velocity
Precipitable and Liquid Water Vapor using a microwave radiometer
Surface meteorology (pressure, temperature, humidity, solar radiation, wind).
Sea surface temperature
Navigational data using GPS receiver and compass

(4) Methods

(4.1) DBS Wind Profiler Radar

915 MHz (33 cm) vertical pointing, and near vertical pointing radar using the Doppler Beam Swinging (DBS) technique to measure the wind profile (i.e., wind as a function of height) of the atmospheric boundary layer and the lower part of the free atmosphere. This radar can measure the wind profile every 15 – 30 minutes. This system can also measure the fall speed of rain, and thus provide raindrop distribution information. The DBS profiler was located on the stern deck.

(4.2) MAPR (Multiple Antenna Profiler Radar)

This is an experimental 915 MHz vertically pointing radar that uses a new technique for measuring the wind profile of the boundary layer known as the spaced antenna technique. This technique can measure the wind profile every minute and can also measure the fall speed of rain. This cruise was the first time this type of radar has been operated at sea. MAPR was located on the stern deck.

(4.3) RASS (Radio Acoustic Sounding System)

This is an accompiant to the profiler radar and is used to measure the temperature profile of the boundary layer. Loudspeakers emit sound that travels upwards and the radar tracks the sound waves; the speed of sound is related to temperature so the system is used to measure temperature as a function of height. The RASS speakers were located around the DBS profiler on the stern deck.

(4.4) S-Band Radar

This is 3 GHz (10 cm) vertically pointing radar that can detect cloud droplets and rain. It is used to study boundary layer clouds, and precipitating clouds, and can also measure the fall speed of rain and boundary layer depth. The S-Band radar was located on the stern deck. This radar is owned by NOAA / ETL (contact Jim Jordan) and was operated on the cruise by NCAR / ATD.

(4.5) Microwave Radiometer.

This instrument measures the precipitable and liquid water vapor of the atmosphere using microwave emittance. The instrument is owned by Radiometrics Corporation (contact Fred Solheim) and control and analysis software was supplied by Jim Liljegren of Ames Laboratory. This instrument was located on the stabilizer deck.

(4.6) Surface meteorology

Surface meteorology instruments included sensors for pressure, temperature, relative humidity, broadband visible and infrared solar radiation, wind speed and direction. The measurements were made every 5 seconds. These instruments were located on a mast above the bridge.

(4.7) Sea Surface Temperature

The sea surface temperature was made by a thermistor encased in a brass rod on the end of a plastic hose (known as the “sea snake”) lowered from the bow boom. The independent sample time for this measurement is approximately one minute.

(4.8) Navigation Instruments

Navigational information was required for making continuous adjustments to measurements made by the wind profilers and surface wind sensor. A GPS receiver (located on the stern deck) was used for

location and course, and a flux gate magnetometer compass (located above the Rear Bridge) was used for heading. These measurements were made every 5 seconds. Pitch, roll, and acceleration were measured every second using sensors on the stern deck.

(5) Preliminary Results

All instruments performed very well and produced interesting observations.

The wind profiler radars recorded the general flow and state of the atmosphere up to about 4 km. For much of the IOP periods the general flow was light to moderate easterly winds, with only very occasional squalls.

This was the first use of MAPR at sea and it was very successful. Fine scale measurements were made of motion around squalls (Fig. 6.5-1), and of boundary layer convective cells. Experiments were also conducted into using MAPR with RASS, which were intended to show that the radar can measure winds and simultaneously measure temperature (which cannot be done with conventional profilers). Initial analysis suggests the experiments were successful. Also comparisons between larger scale flow measured by MAPR and the conventional DBS system showed that MAPR performed very well.

RASS also produced very interesting results. An example is shown in Fig 6.5-2.

This is air temperature between 100 and 500 metres altitude as measured by RASS on a 3 hour cruise near the island of Nauru. Initially the Mirai was directly downwind of the island (the flow was easterly and the Mirai was 500 metres west of the ARM ARK site), then over the next 30 minutes moved north to become clear of downwind island flow), and then for the last hour gradually returned to downwind of the island. The air temperature dropped as we left the downwind flow, then later rose again as we returned to downwind flow, suggesting an island heating effect up into the boundary layer.

The surface and navigational sensors performed well, as did the sea surface temperature sensor (the “sea snake”), which compared well to similar sensors deployed by other groups. The microwave radiometer detected very low levels of atmospheric water vapor on several days, suggesting dry air was be advected over the Mirai. Comparisons with radiosonde total water vapor as calculated by JAMSTEC staff indicated the measurements were accurate.

(6) Data Archive

All data will be archived at NCAR / ATD (contact William Brown)

Requests for S-Band radar data should be directed to NOAA / ETL (contact Jim Jordan).

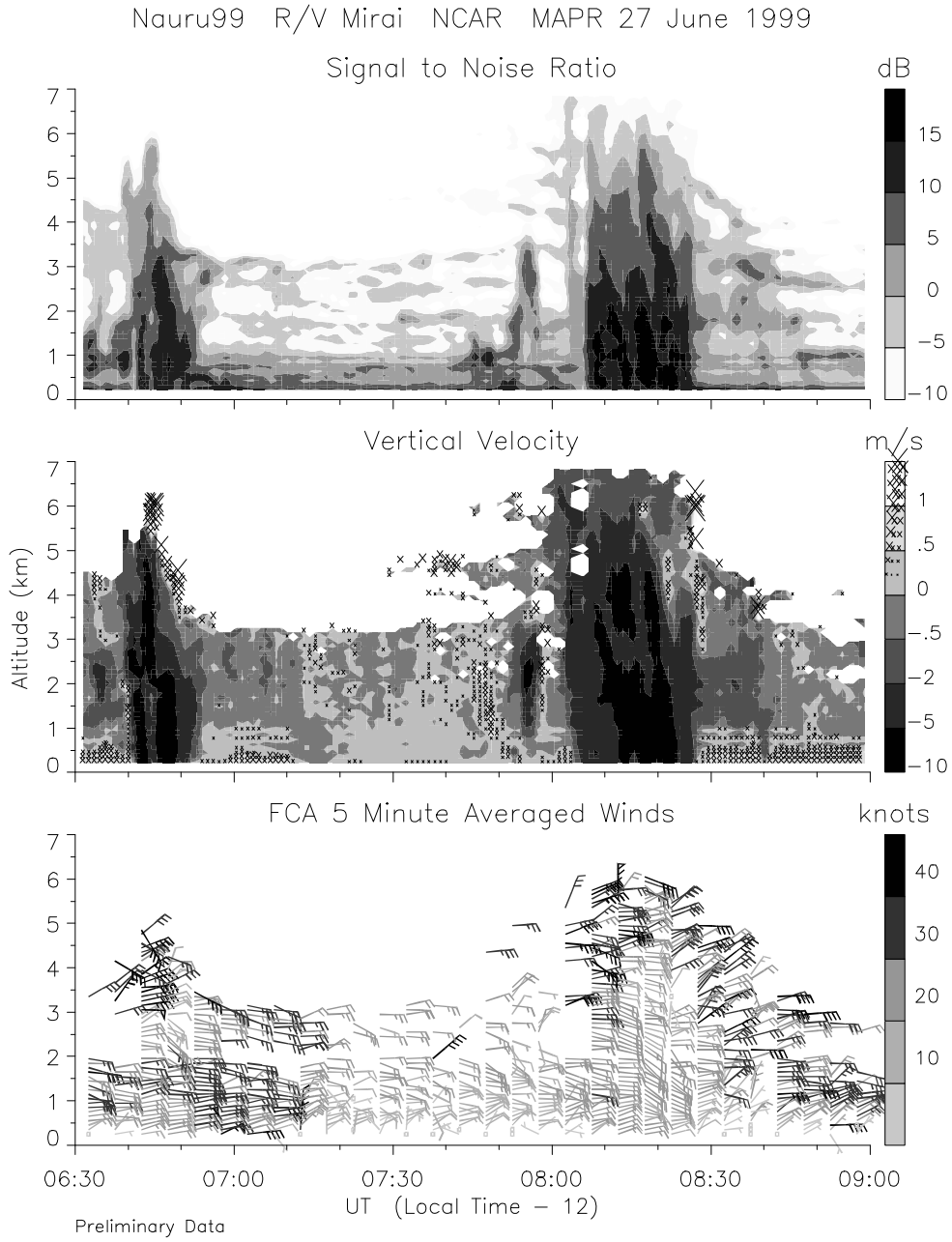

Fig. 6.5-1: Observations of two squalls made using MAPR (Multiple Antenna Profiler Radar). The top panel indicates echo power, the middle vertical motion (with upward motion indicated by "x"), and the bottom panel shows wind barbs. Note the upward motion around the two squalls in the middle panel (the dark areas indicate falling rain), and the rapidly changing winds in the bottom panel. Such detail of motion is only possible using MAPR.

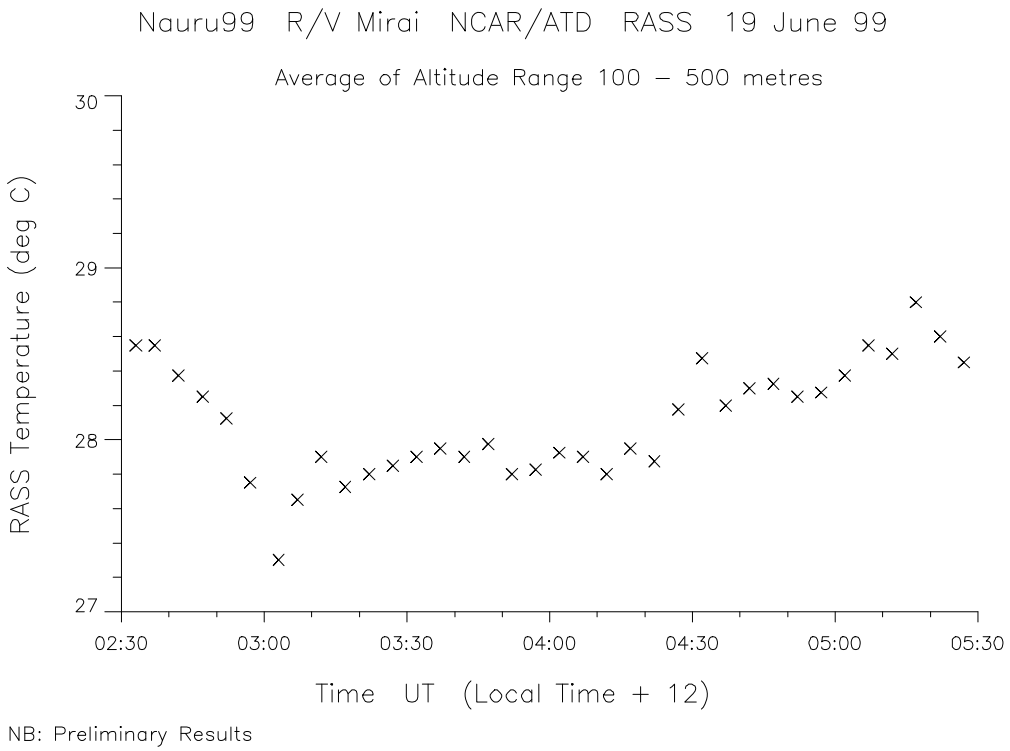

Fig.6.5-2: RASS (Radio Acoustic Sounding System) temperature as averaged over altitude levels from 100 to 500 metres. The Mirai was within about one kilometre downwind of the island of Nauru for approximately the first 15 minutes and last 30 minutes of this period.

6.6 Lidar Observation

6.6.1 NIES / TIT Lidar

(1) Personnel

Ichiro Matsui (NIES)*
Nobuo Sugimoto (NIES)
Isao Tamamushi (TIT)
Kazuhiro Asai (TIT)

(2) Objectives

Shipborne Mie scattering lidar observation of aerosols and clouds have been started this year using R/V Mirai. The purposes of the observation are to obtain global distribution and optical characteristics of aerosols and clouds which are used in the climatological study and in the study on the data reduction algorithms and data methods for space borne lidars.

(3) Measured Parameters

Aerosols:	Density distribution, Backscatter coefficient, Depolarization, Optical depth.
Clouds:	Height of cloud bottom, Backscatter coefficient, Depolarization, Optical depth.

(4) Methods

The lidar employs a compact flashlamp pumped second-harmonics Nd:YAG laser. Mie scattering at 1064 nm and 532 nm, and depolarization ratio at 532 nm were recorded. System parameters are as follows;

Laser: Big Sky Laser CFR-200
Output power: 532 nm 50 mJ/Pulse, 1064 nm 100 mJ/pulse
Repetition rate: 10 Hz Beam div.: 0.5 mrad
Receiver: Schmidt cassegrainian
Diameter: 280 mm Field of view: 1 mrad
Detector: PMT(532 nm) , APD(1064nm)
Data collection: LeCroy LC574AL
Measurement range: 0-24 km Range resolution: 6 m
Sampling rate: 10 sec

(5) Results

Figure 6.6.1-1 shows a temporal variation of vertical profile. The range-corrected lidar signal at 532 nm is indicated with a gray scale. Diurnal variation of boundary layer is not significant as seen in Fig.6.6.1-1. Low clouds are frequently observed at the top of the planetary boundary layer. Cirrus clouds are also frequently observed in an altitude range of 10 to 15 km.

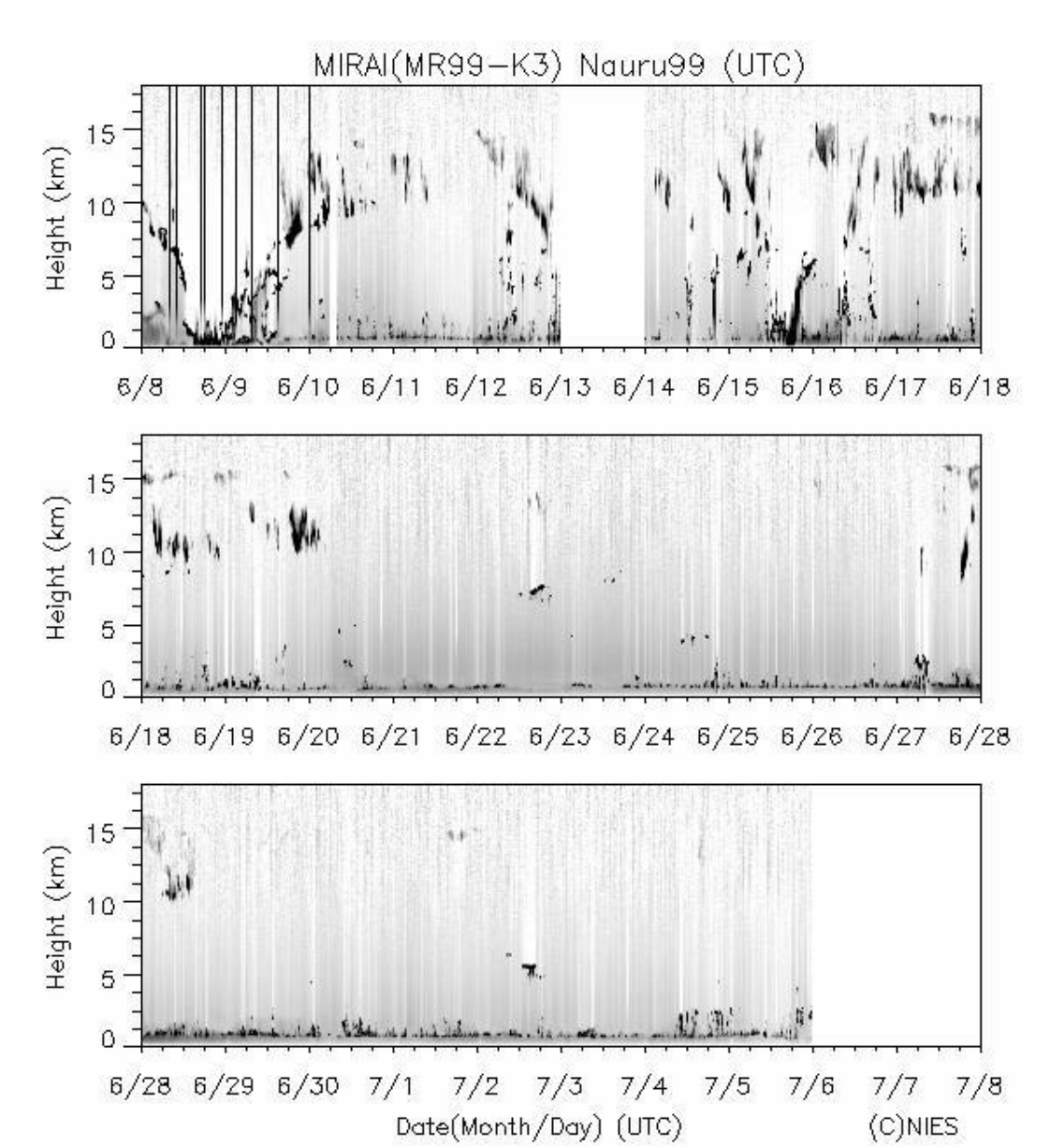

Fig.6.6.1-1: Temporal variation of range-corrected lidar signal at 532 nm.

(6) Data archive

All data will be archived at NIES and TIT. The data is also submitted to and archived at JAMSTEC DMO.

6.6.2 Ceilometer Observation

(1) Personnel

Masaki Hanyu (GODI) : Operation Leader
Fumitaka Yoshiura (GODI)
Kiyotake Kouzuma (GODI)
Satoshi Okumura (GODI)

(2) Objectives

The information around cloud base, cloud base height and the liquid water amount around cloud base, is important to understand where and how much the water vapor condensate to liquid water. As few method to measure them, the ceilometer observation was carried out.

(3) Measured Parameters

Cloud base height [m]
Backscatter profile, sensitivity and range normalized at 30 m resolution

(4) Methods

We measured cloud base height and backscatter profiles using CT-25K (Vaisala, Finland) ceilometer throughout MR99-K03 cruise from the departure of Yokohama on 8 June 1999, to the arrival of Tsuruga, on 17 July 1999 via Chuuk, Majuro, Guam.

Major parameters for the measurement configuration are as follows;

Laser source :	Indium Gallium Arsenide (InGaAs) Diode
Transmitting wave length :	905 +-5 nm at 25 deg-C
Transmitting average power :	8.9 mW
Repetition rate :	5.57 kHz
Detector :	Silicon avalanche photodiode (APD)
	Responsibility at 905 nm : 65 A/W
Measurement range :	0-7.5 km
Resolution :	50 ft in full range
Sampling rate :	60 sec.

(5) Preliminary results

Examples of lidar echo image is shown in Fig. 6.6.2-1. The cloud base height was about 500 m before 2:45 UTC. The echo after that moment became strong and reached ground: it means rainfall.

The data will be analyzed in detail with radiosonde data, Doppler radar data, etc.

(6) Data archives

Ceilometer data obtained during this cruise will be submitted to the DMO (Data Management Office), JAMSTEC and will be under their control.

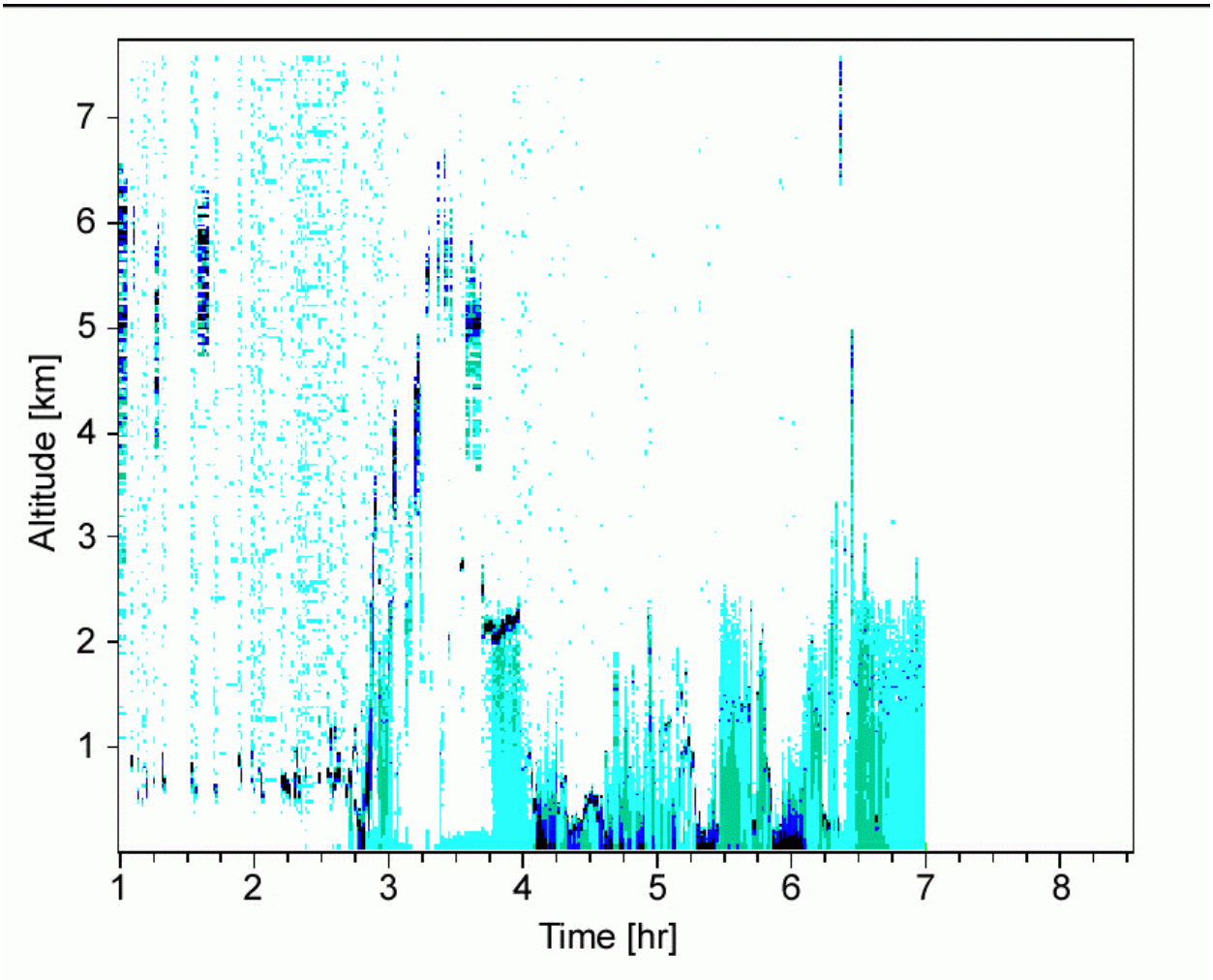

Fig. 6.6.2-1: An example of the ceilometer data plot, for 13 July 1999.

6.7 Radiation Fluxes and Surface Meteorology

(1) Personnel

R. Michael Reynolds (BNL): Principal Investigator
Ray Edwards (BNL): Electronic Engineer

(2) Objectives

The Brookhaven National Laboratory through funding from the U.S. Department of Energy's Atmospheric Radiation Measurement (ARM) Program, and in collaboration with the Japan Marine Science and Technology Center (JAMSTEC), provided instrumentation sufficient to acquire a complete set of measurements sufficient to completely define the energy and water flux budget across the air-sea interface by bulk transfer methods. These estimates will be compared to the turbulent flux measurement by Tsukamoto/Ishida with the goal of deriving the optimum set of bulk transfer algorithms that will be used in an on-going program of continuous mean measurements.

Identical radiation instrumentation was installed on Nauru island, on the R/V RON BROWN, and on the R/V MIRAI so there would be a calibrated standard by which all radiation measurements could be gauged.

The Radiation Package measured shortwave and longwave downwelling irradiance using Eppley radiometers, but also used a novel Fast Rotating Shadowband Radiometer (FRSR) to reduce the solar irradiance into its diffuse and direct beam components. These measurements are used to estimate aerosol optical depth and cloud forcing. The Microtops hand-held sun photometer was used as a check on the FRSR estimates. The instrumentation was installed on the MIRAI in Yokohama and was operated nearly continuously across the Pacific, during Nauru99, and during the return voyage.

(3) Measured Parameters

Brookhaven National Laboratory provided three sets of instrumentation (Figs 6.7.1-1 and 6.7.1-2),

1. Portable Radiation Package (PRP) – short and long wave downwelling radiation
2. Zeno meteorological system – named after the Zeno data logger that is central to the design.
3. Scientific Computer System (SCS) – centralized data acquisition and logging of all data sets.

Other instrumentation that supported the above systems are: Microtops hand-held sun photometer, Assman psychrometer (loan from NCAR), Calibrated temperature bath (courtesy of Rutherford Appelton Laboratory)

Table 6.7-1: Parameters in the BNL data set. The following list is a summary of all measurements that are available from the bnl data set. These time series are saved in 2-minute and one-hour averaged sets. They are cleaned and edited of all spurious spikes or obvious problems.

Var	Source	Description	units	
1:lat	GPS	Latitude in degrees	f.p. degrees	
2:lon	GPS	Longitude in degrees	f.p. degrees	
3:sog	GPS	Speed over ground	m/s	
4:cse	GPS	ship course	degT	
5:hdg	MIRAI	heading	degT	
6:var	GPS	magnetic variation	deg	
7:dep	MIRAI	depth	m	
8:sal	MIRAI	salinity	psu	
9:tair	Zeno	air temperature	degC	
10:rh	Zeno	relative humidity	%RH	
11:sst	Zeno	sea surface temperature (1cm)	degC	
12:ssst	M-AERI	sea surface skin temperature	degC	
13:pspu	PRP	Precision Spectral Pyranometer	W/m^2	(a)
14:pir	PRP	Precision Infrared Radiometer	W/m^2	(b)
15:piru	PRP	Uncorrected PIR	W/m^2	
16:case	PRP	PIR case temperature	degC	
17:dome	PRP	PIR dome temperature	degC	
18:bp	Zeno	Barometric pressure	hPa	(c)
19:wsr	Zeno	Relative wind speed	m/s	
20:wdr	Zeno	Relative wind direction	deg	
21:wst	Zeno/GPS	True wind speed	m/s	
22:wdt	Zeno/GPS	True wiind direction	degT	
23:sst5	MIRAI	sea temperature (-5 m)	degC	
24:ssthat	M-AERI	sea temperature (-10 cm)	degC	
25:pitch	PRP	mean pitch (bow up)	deg	
26:roll	PRP	mean roll (port up)	deg	
27:comp	PRP	uncorrected mag heading	degM	
28:org	Zeno	rain rate	mm/hr	
29:org_max	Zeno	max rain in 2-min period	mm/hr	
30:ppt(RMY)	Zeno	rain rate from R.M. Young	mm/hr	
31:pspu	PRP	PIR thermopile	W/m^2	
32:pitch_std	PRP	2min RMS pitch	deg	
33:roll_std	PRP	2min RMS roll	deg	
34:comp_std	PRP	2min RMS heading	deg	
40:psp	PRP	PSP corrected for tilt	W/m^2	(d)
41-47:d_1..d_7	PRP	Diffuse irradiation	W/m^2	
48-54:n_1..n_7	PRP	Direct normal irrad.	W/m^2	(e)
55-61:g_1..g_7	PRP	Computed global irrad.	W/m^2	(f)

(a) PSP uncorrected for platform tilt.
(b) computed using Eppley standard equation with Tcase and Tdome.
(c) uncorrected gauge pressure.
(d) PSP corrected for platform tilt
(e) These are corrected for platform tilt.
(f) Sum of diffuse and direct irradiances onto a horizontal plane.

(4) Methods

The various instruments were located in exposed positions around the ship (see Figure 6.7-1) at heights above the sea level as described in Table 6.7-2 below. Measurements were digitized at measurement locations and returned to the research room behind the bridge via RS422 serial connections. For our data analysis and for quality assurance we made use of other measurements from different groups. These are listed in the table also.

Table 6.7-4. INSTRUMENT INSTALLATION LOCATIONS

Instrument/measurement	Location	ht (m)	Comments
BNL Instruments			
Portable Radiation	Foremast top	24.2 m	Excellent view
SST, sea snake	Bow, 3 m extension	-1cm	0-12 kts okay
Winds	Foremast top	24	excellent exposure
T/RH	Foremast top	24	ditto
ORG	Foremast top	24	high wind error possible
Rain gauge	Foremast top	24	ditto
Barometer	Foremast top	24	gill port after 6/14
Total Sky Imager (TSI)	Top deck midship	17	radar dome and main mast in view
MIRAI Instruments			
Wind	Foremast top	24	
Air temp/RH	Bridge deck	20	port and stbd measurements
Barometer	Bridge deck	20	add 1.4 mb for sl reading
SW down radiation	Main mast	29	
LW down radiation	Main mast	29	
SW up radiation	Bow boom	8.9	
LW upradiation	Bow boom	8.9	
Optical rain gauge (ORG)			
Rain gauge (PPT)			
NCAR Instruments			
Wind	Port bridge deck	20 m	All the NCAR maesuarments are
T/RH	ditto	20	susceptable to periods when the
Barometer	ditto	20	relative winds crossed the ship
SW down radiation	ditto	20	from the starboard.
LW down radiation	ditto	20	
SST (Sea snake)	bow boom	-5cm	
RSMAS Instruments			
M-AERI	Foremast, lower	14 m	View off port bow
Hardhat SST	Port side midship	-10 cm	Occasionally in the ship wake.
RAL Instrument			
SISTeR SSST	Foremast lower	14 m	View off stbd bow.

(4-1) Portable Radiation Package

The ship-board shortwave radiation instrument is called the Portable Radiation Package (PRP). The PRP is composed of a broadband Precision Spectral Pyranometer (PSP) made by Eppley Laboratory, Inc., a fast-rotating shadowband (FRSR) spectral radiometer, which is the subject of this paper, attitude sensors for the measurement of platform pitch, roll, and azimuth, and a special microprocessor for data collection and instrument control.

The FRSR spectral radiometer is designed to provide quality estimates of direct and diffuse shortwave irradiance from a moving platform without need of special gyro-stabilized tables. It is small, environmentally robust, low power, and is well suited for research ships, for ice floes, or for larger buoys in all but the higher Beaufort conditions.

The arm rotational speed is 7.0 sec per revolution, meaning the arm moves across the upper hemisphere, relative to the sensor, in 3.5 sec. The hemispherical shape of the arm ensures that the sensor will see a shadow, regardless of its azimuth heading. The arm moves across the face of the sun in a few tenths of a second and the head is in full shadow for about one tenth of a second.

Spectral irradiance measurements are made with a modified spectral radiometer head (Yankee Environmental Systems, Inc.). The head has seven detectors (channels), a broadband channel and six 10 nm bandpass measurements at 415, 500, 610, 655, 860, and 960 nm. It can be accurately calibrated and has an excellent zenith angle response. The head construction, adeptly described by Harrison et al.(1994), is environmentally sound and the package is weatherproof, robust, and suitable for use in a marine environment.

The PRP was installed on the top of the foremast on the rear railing. It was leveled as well as possible. The RS422 serial output from the PRP computer was routed back to the science room behind the bridge via a sky cable from the foremast to the flying bridge deck.

The PRP is automatic and begins collecting solar radiation when the global irradiance exceeds 10 W/m^2. For each sweep of the shadowband, two measurements of the PSP, PIR, tilt, and compass sensors are read and transmitted to the data collection PC in the science room. Each evening, the days solar data were retrieved from the data collection PC and analyzed.

Daily service to the PRP was minimal and consisted of cleaning the domes of the three optical instruments with wet and soft dry lintless paper towels. This service was done each day at dawn.

(4-2) Zeno Meteorological System

The Zeno meteorological system, named after the Zeno data logger, was located on the top of the foremast at the front rail just port side of the flux system (Figure 6.7-3). The following instruments were monitored by the Zeno data logger:

Wind monitor	R.M. Young	Relative wind speed and direction
T/RH sensor	Vaisala	Temperature and relative humidity, active aspiration
mini-ORG	STI	optical rain gauge, instantaneous rain rate to 500 mm/hr
Rain Gauge	R.M. Young	Accumulation rain gauge, 2min rain rate estimates.
Pressure	R.M. Young	Analog barometer
SST	BNL	Sea snake, measures at about 1-2 cm

The Zeno data logger is packaged with backup battery, voltage regulators, and RS232-to-RS422 converter into a waterproof canister with wet-pluggable oceanographic connectors. The data logger makes all measurements at a 1-sec rate and transmits these to the SCS computer via the RS422 serial cable. The platinum resistance thermometer measurement is converted directly to temperature in the data logger.

All scaling and calibration factors are programmed into the Zeno so it will transmit actual physical units. This makes it easier to monitor the current information using the SCS (below).

Each morning during the intensive operations, a psychrometer reading was made next to the T/RH sensor as a cross check on its accuracy. These reading agreed with the Zeno system usually to within 0.1 C in temperature and with 1 % RH.

(4-3) Total Sky Imager

The Total Sky Imager (Figure 6.7-4) provides a means of having automated sky photography and cloud fraction analysis. The TSI (developed jointly by Penn State University, Brookhaven National Laboratory, and Yankee Environmental Systems, Inc. and manufactured by YES Inc.) Incorporates three main sub-components: (a) The ethernet-ready IP camera, the motorized mirrored dome that maintains an occluding black band over the reflection of the solar disk in the mirror and prevents overload to the camera, and (c) the image processing PC that captures images at set time intervals and performs a cloud analysis to determine cloud fraction. During intensive operations images were taken each minute and during the transit legs each five minutes. Images and analyses are saved as JPEG images.

The dome alignment motor is controlled by a small microprocessor located in the TSI junction box. For operation on land the dome control computer needs the latitude and longitude. It has a good real-time clock so that can be set once and routinely re-checked. The image processing software also needs to know the geographic position of the instrument. On a ship, the instantaneous latitude, longitude, and heading, which change as the ship moves, must be regularly updated in both computers. During the first part of the cruise, these data were provided by the SCS (below) but later we were able to develop software code that would access the MIRAI SOJ data file independently from SCS and thus make the TSI completely independent from SCS.

The TSI was installed on the upper deck behind the science room. This location provided about as clear a view of the whole sky as possible on the ship. However, as Fig 6.7-4 shows, there are many ship objects, the radar dome, main mast, etc., that will need to be masked out of the analysis during the post-processing period.

(4-4) Micro Tops

The MicroTops handheld sun photometer has five 10-nm filter bands (440, 500, 675, 870, 936) and uses these to estimate aerosol optical thickness (AOT) at all bands plus it uses the 936 nm band to estimate integrated water vapor. MicroTops measurements were made during periods when the cirrus shield and other clouds were absent and a clear solar beam could be measured. MicroTops measurements were made to substantiate the continuous measurements from the PRP.

(4-5) Scientific Computer System

The Scientific Computer System (SCS) operated in a Micron NT computer with 128 MB of RAM and 9GB hard disk. A digiport interface provided 16 RS232 ports more than the basic two ports that come with the computer. The SCS was programmed to accept the following data:
(1) MIRAI "soj" data file at a 2-sec input rate. (2) Zeno data logger output at a 1-Hz rate. (3) Trimble GPS receiver at a 1-Hz update rate. (4) the PRP averaged data at a 1-minute rate.

The SCS was quite useful in that it logged all data on a common time base. The computer internal clock was set daily and never drifted by more than 1-2 seconds from UTC. The GPS time was logged and compared to the SCS computer clock.

(4-6) Data Processing

All SCS data streams were collected and analyzed on a daily basis. The raw ascii data files from all sources were first averaged and converted to a basic 2-min data set with standard time blocks. Care was taken to ensure that the time of the samples corresponded to the beginning of the 2-min time period. For example, the data for time 0000 was averaged from 000000 to 000159, and the data for 2358 was averaged from 235800 to 235959.

The 2min data files were edited with a special editing program (All data processing was done using Matlab 5.2 on an iMac computer). Redundant measurements from other investigators were used for comparison. The cleaned and edited time series were stored in individual files indicated by table 6.7-5 below.

PRP measurements of AOT require a post calibration. PRP units on Nauru, the MIRAI, and the RON BROWN are all being shipped to Mauna Loa Hawaii for full post calibration exercise.

(4-7) Cruise Legs and Positions

The entire cruise of 39 days can be segmented into five distinct period as shown below. Periods II, III, and IV occurred during the Nauru99 campaign while periods I and V are transects across the western Pacific Ocean. All of these periods are of interest.

Table 6.7-3: LEG TIMES: For the purposes of our data analysis we define the following times for each component of the voyage. The times are selected so as to have the most days with total solar coverage and are not precisely those used by the MIRAI to define intensive CTD or radiosonde operations.

Description		Start	End
Leg I	Yokohama to Nauru Island	99-6-8 (159) 0500Z	99-6-16 (167) 1800Z
Leg II	Nauru Intercomparison	99-6-16 (167) 1100Z	99-6-19 (170) 0800Z
Leg III	TAO Intercomparison	99-6-19 (170) 1800Z	99-6-30 (181) 0800Z
	a Large Triangle	99-6-24 (181) 0200Z	99-7-30 (181) 0800Z
Leg IV	Small Triangle	99-6-30 (181) 1800Z	99-7-4 (185) 1200Z
	a Ship comparison	99-7-3 (184) 1200Z	99-7-3 (184) 1800Z
Leg V	Nauru to Tsuruga	99-7-4 (185) 1200Z	99-7-15 (196) 2359Z
	a Nauru to Majuro	99-7-4 (185) 1200Z	99-7-5 (186) 2340Z
	b Majuro to Guam	99-7-6 (187) 2100Z	99-7-11 (192) 0900Z
	c Guam to Tsuruga	99-7-11 (192) 1000Z~	99-7-16 (197) 2200Z

Table 6.7-3: KEY GEOGRAPHIC LOCATIONS

Chuuk Dock	+7.4457 (N)	+151.8393 (E)
Nauru ARCS Site	-0.5206	+166.9159
Nauru MIRAI offshore site	-0.521	+166.903
TAO Intercomparison (Lg Tri.)	-0.010	+164.992 (a)
Small Triangle	-0.183	+166.853
Majuro Dock	+7.0860	+171.3658
Guam Dock	+13.460	+144.667
TAO Buoy Exact Locations		
Equator	+0.004	+164.998 (b)
2S	-1.930	+164.390

(a) The ship held position away from the buoy but made flux runs upwind each three hours. The holding position was near the buoy but depended on wind direction. The position here is approximate for the holding position.
(b) Ship position during the buoy maintenance operation on J171.

(5) Results

In this section we present a brief review of some of the earliest findings. These are presented solely to indicate the sort of features we see in the first look at the data.

During the Nauru intercomparison (Figure 6.7-5) the ship occupied a position west of the island just offshore from the ARCS site. Figure 6.7-8 is a comparison of measurements from the two units. The data are quite close to each with some notable differences. The longwave fluxes on Nauru are much lower on Nauru then from the ship. Importantly, the island site shows considerably more cloud than the ship even though the ship was very close by. Diffuse fluxes are greater over the island which is indicative of added cloud reflections. We can make the above statements more assuredly after the Mauna Loa calibration.

One goal of the large triangle period was to provide a calibration for the radiation sensors on the TAO buoys at 165E-Eq and 165E-2S. Another goal was to assess any differences between the ship measurements of insolation and the island. Figure 6.7-7 shows some results of data from the ARCS site, the RON BROWN and the MIRAI. We compared total solar insolation for the buoys, ships, and the island. The total insolation for the solar day is shown to the left of each solar curve. We see that while the comparison between the two ships is comparable, the MIRAI had 3.4% more insolation than the RON BROWN., the ARCS site on Nauru Island had a reduced amount, 9.5% less than the MIRAI. For the TAO buoy at the equator, comparisons to the MIRAI were excellent with an overall the MIRAI being 1.4% less than the buoy. The comparisons between the RON BROWN and the buoy at 2S were not good and indicate that the calibration or the instrument in the 2S buoy are in error.

The small triangle period was just 3.5 days and included an intercomparison between the two ship on J184. A summary plot is shown in Figure 6.7-9 for days j182-185. The radiation data show the presence of the cirrus shield by the reduced insolation at noon on each day. The following features are typical for the entire Nauru99 IOP. (a) Longwave downwelling radiation is nearly constant at 400 W/m^2 but shows evidence of cloud activity and the daily air temperature cycle. (b) Air temperature cycles by about 0.4 C over each 24-hour period while specific humidity varies around 18 g/kg with amplitude 0.5. (c) Winds were easterly and fairly strong. (d) The barometric pressure showed the typical semi-diurnal 2mb oscillation common to the tropics.

Table 6.7-6: MICROTOPS DATA FOR THE MIRAI AND RON BROWN

MIRAI MicroTops

DATE	*UTC*	*LAT*	*LON*	*440*	*500*	*675*	*870*	*936*	*WV*
10-Jun-1999	20:59:00	19.9000	146.6500	0.601	0.417	0.181	0.121	0.110	11.32
10-Jun-1999	22:28:00	19.5500	146.8170	0.057	0.056	0.035	0.042	0.038	3.75
11-Jun-1999	02:26:00	18.5830	147.2330	0.096	0.090	0.064	0.066	0.060	3.58
12-Jun-1999	00:14:00	13.3000	149.2670	0.100	0.088	0.066	0.071	0.065	3.85
12-Jun-1999	02:22:00	12.8000	149.4670	0.116	0.100	0.079	0.085	0.078	4.06
12-Jun-1999	02:59:00	12.6330	149.5330	0.161	0.138	0.111	0.117	0.106	4.28
14-Jun-1999	00:21:00	7.4830	151.8330	0.069	0.050	0.024	0.030	0.028	4.17
14-Jun-1999	01:14:00	7.4830	152.0500	0.070	0.051	0.023	0.030	0.027	4.29
20-Jun-1999	21:26:00	0.0000	165.0000	0.042	0.044	0.032	0.029	0.026	2.92
20-Jun-1999	22:36:00	0.0000	165.0000	0.048	0.046	0.031	0.031	0.028	2.88
21-Jun-1999	00:53:00	0.0000	165.0000	0.051	0.049	0.030	0.034	0.031	2.92
21-Jun-1999	01:46:00	0.0000	165.0000	0.056	0.054	0.035	0.035	0.032	2.85
21-Jun-1999	20:23:00	0.0000	165.0000	0.040	0.043	0.033	0.026	0.024	2.81
22-Jun-1999	01:15:00	0.0000	165.0000	0.068	0.063	0.044	0.044	0.041	3.13
22-Jun-1999	04:37:00	0.0000	165.0000	0.048	0.048	0.035	0.029	0.026	3.05
22-Jun-1999	21:47:00	0.0000	165.0000	0.047	0.047	0.033	0.030	0.028	3.26
22-Jun-1999	22:39:00	0.0000	165.0000	0.046	0.047	0.029	0.028	0.026	3.28
22-Jun-1999	22:59:00	0.0000	165.0000	0.049	0.047	0.030	0.029	0.026	3.34
24-Jun-1999	00:46:00	0.0000	165.0000	0.062	0.056	0.035	0.034	0.031	3.79
24-Jun-1999	03:36:00	0.0000	165.0000	0.059	0.055	0.036	0.033	0.030	3.86
24-Jun-1999	23:43:00	0.0000	165.0000	0.059	0.052	0.031	0.033	0.030	3.70
25-Jun-1999	02:07:00	0.0000	165.0000	0.060	0.053	0.033	0.034	0.031	3.55
25-Jun-1999	04:23:00	0.0000	165.0000	0.050	0.049	0.031	0.027	0.025	3.46
26-Jun-1999	01:01:00	0.0000	165.0000	0.070	0.063	0.046	0.049	0.045	3.07
26-Jun-1999	04:51:00	0.0000	165.0000	0.038	0.039	0.026	0.023	0.021	2.80
28-Jun-1999	00:57:00	0.0000	165.0000	0.140	0.133	0.120	0.127	0.116	2.83
28-Jun-1999	03:06:00	0.0000	165.0000	0.112	0.107	0.095	0.101	0.092	2.48

Table 6.7-6 (continued)

RON BROWN MICROTOP DATA

DATE	*UTC*	*LAT*	*LON*	*380*	*500*	*675*	*870*	*1020*
15-Jun-1999	02:32:00	-12.0830	130.9500	0.259	0.136	0.055	0.040	0.063
15-Jun-1999	04:37:00	-11.9830	131.2830	0.285	0.154	0.065	0.042	0.035
21-Jun-1999	22:31:00	-4.7500	158.7500	0.180	0.083	0.032	0.020	0.036
22-Jun-1999	00:02:00	-4.5670	159.0000	0.191	0.104	0.037	0.029	0.035
22-Jun-1999	02:24:00	-4.3170	159.4330	0.187	0.100	0.031	0.024	0.037
22-Jun-1999	04:16:00	-4.1670	159.7500	0.184	0.103	0.035	0.024	0.032
22-Jun-1999	21:31:00	-2.5500	163.0670	0.189	0.094	0.042	0.025	0.035
22-Jun-1999	22:35:00	-2.4500	163.2830	0.187	0.104	0.039	0.021	0.027
22-Jun-1999	23:37:00	-2.3670	163.4500	0.181	0.106	0.035	0.017	0.023
23-Jun-1999	00:19:00	-2.3000	163.6000	0.188	0.121	0.036	0.019	0.018
23-Jun-1999	01:39:00	-2.1830	163.8170	0.184	0.113	0.036	0.021	0.021
23-Jun-1999	02:57:00	-2.1000	164.0170	0.183	0.107	0.036	0.021	0.026
23-Jun-1999	04:17:00	-1.9830	164.2500	0.178	0.099	0.036	0.021	0.027
23-Jun-1999	05:22:00	-1.9330	164.3830	0.170	0.088	0.035	0.019	0.025
23-Jun-1999	06:38:00	-1.9170	164.3830	0.162	0.077	0.037	0.020	0.025
23-Jun-1999	21:02:00	-1.9170	164.3830	0.209	0.110	0.053	0.037	0.053
23-Jun-1999	22:51:00	-1.9170	164.4000	0.183	0.093	0.035	0.025	0.041
24-Jun-1999	00:04:00	-1.9170	164.3830	0.188	0.107	0.036	0.027	0.040
24-Jun-1999	01:02:00	-1.9170	164.4000	0.193	0.115	0.038	0.028	0.035
24-Jun-1999	02:03:00	-1.9170	164.4000	0.198	0.123	0.038	0.027	0.032
24-Jun-1999	03:33:00	-1.9170	164.3830	0.185	0.108	0.037	0.025	0.034
24-Jun-1999	04:59:00	-1.9170	164.4000	0.181	0.096	0.038	0.023	0.034
25-Jun-1999	21:16:00	-1.9170	164.3830	0.194	0.103	0.043	0.023	0.026
25-Jun-1999	23:51:00	-1.9170	164.3830	0.202	0.129	0.046	0.024	0.016
26-Jun-1999	00:01:00	-1.9170	164.3830	0.197	0.134	0.041	0.017	0.001
26-Jun-1999	01:04:00	-1.9170	164.3830	0.194	0.136	0.039	0.015	-0.002
26-Jun-1999	03:03:00	-1.9170	164.3830	0.190	0.127	0.039	0.016	0.003
26-Jun-1999	04:18:00	-1.9170	164.3830	0.181	0.113	0.038	0.017	0.010
26-Jun-1999	05:32:00	-1.9170	164.3830	0.173	0.093	0.038	0.018	0.018
26-Jun-1999	23:44:00	-1.9170	164.3830	0.195	0.111	0.040	0.022	0.017
27-Jun-1999	00:53:00	-1.9170	164.3830	0.201	0.132	0.044	0.021	0.009
27-Jun-1999	02:45:00	-1.9170	164.3830	0.211	0.140	0.050	0.027	0.014
27-Jun-1999	04:00:00	-1.9170	164.3830	0.202	0.127	0.050	0.028	0.020

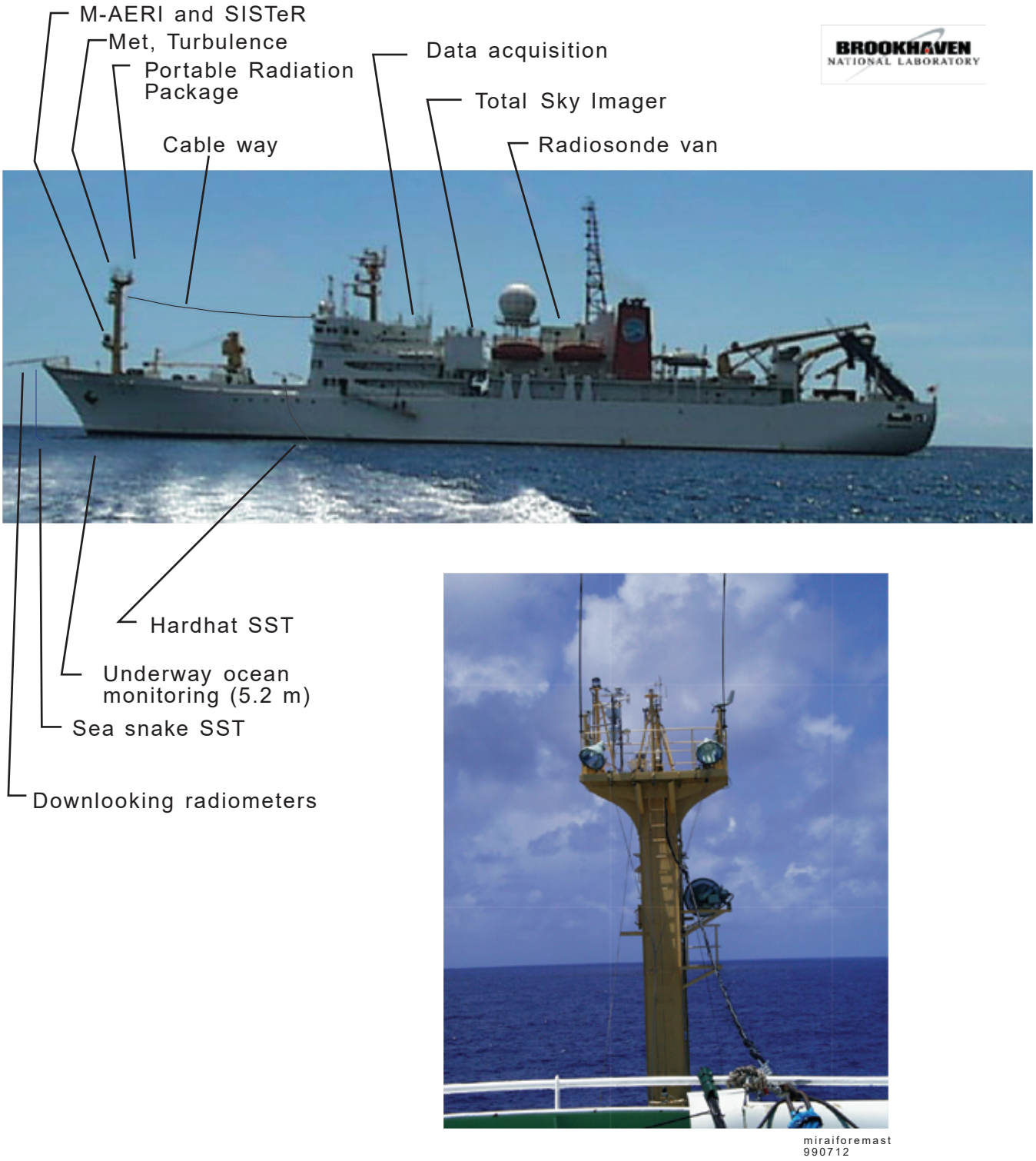

Figure 6.7-1. The location of the various instrumentation on the MIRAI during the Nauru99 intensive operation.

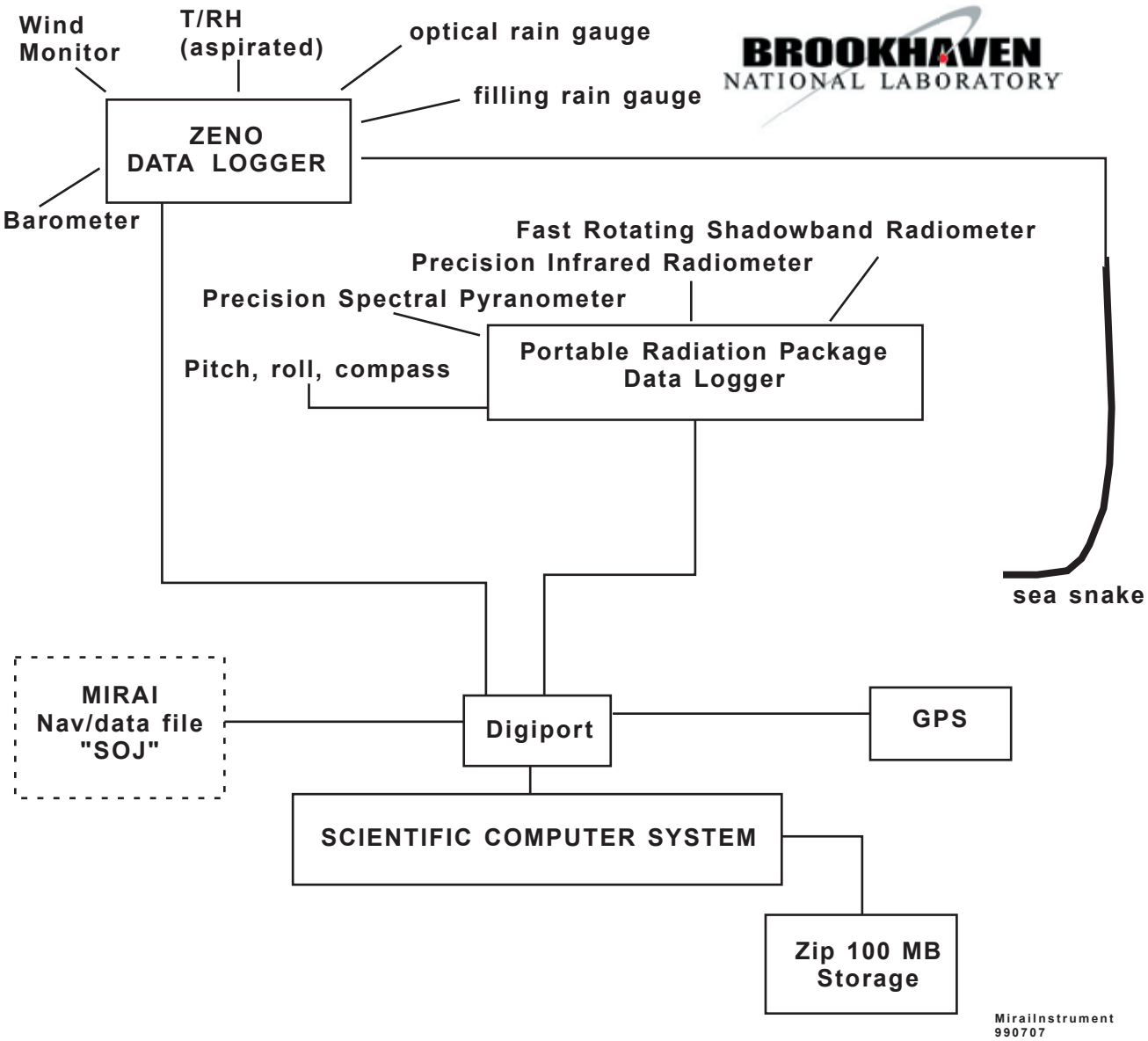

Figure 6.7-2 BNL instruments came in three main components: (a) the Zeno data logger measures all meteorological variables and transmits a data line each second, (b) the Portable Radiation Package makes high-quality measurements of global long and short wave total down irradiances, solar direct normal and hemispheric diffuse components, and platform pitch, roll and azimuth, (c) the Scientific Computer System (SCS) provides a single platform for gathering all measurements with a common timebase.

Figure 6.7-3. The Zeno meteorological observing system is shown to the left of the turbulence flux system. Shown are the wind monitor, rain gauge, aspirated T/RH and, just at the bottom of the figure, the Zeno data logger in its water proof canister. Out of view are the barometer pressure port, the optical rain gauge (ORG) and the sea snake at the bottom of the mast.

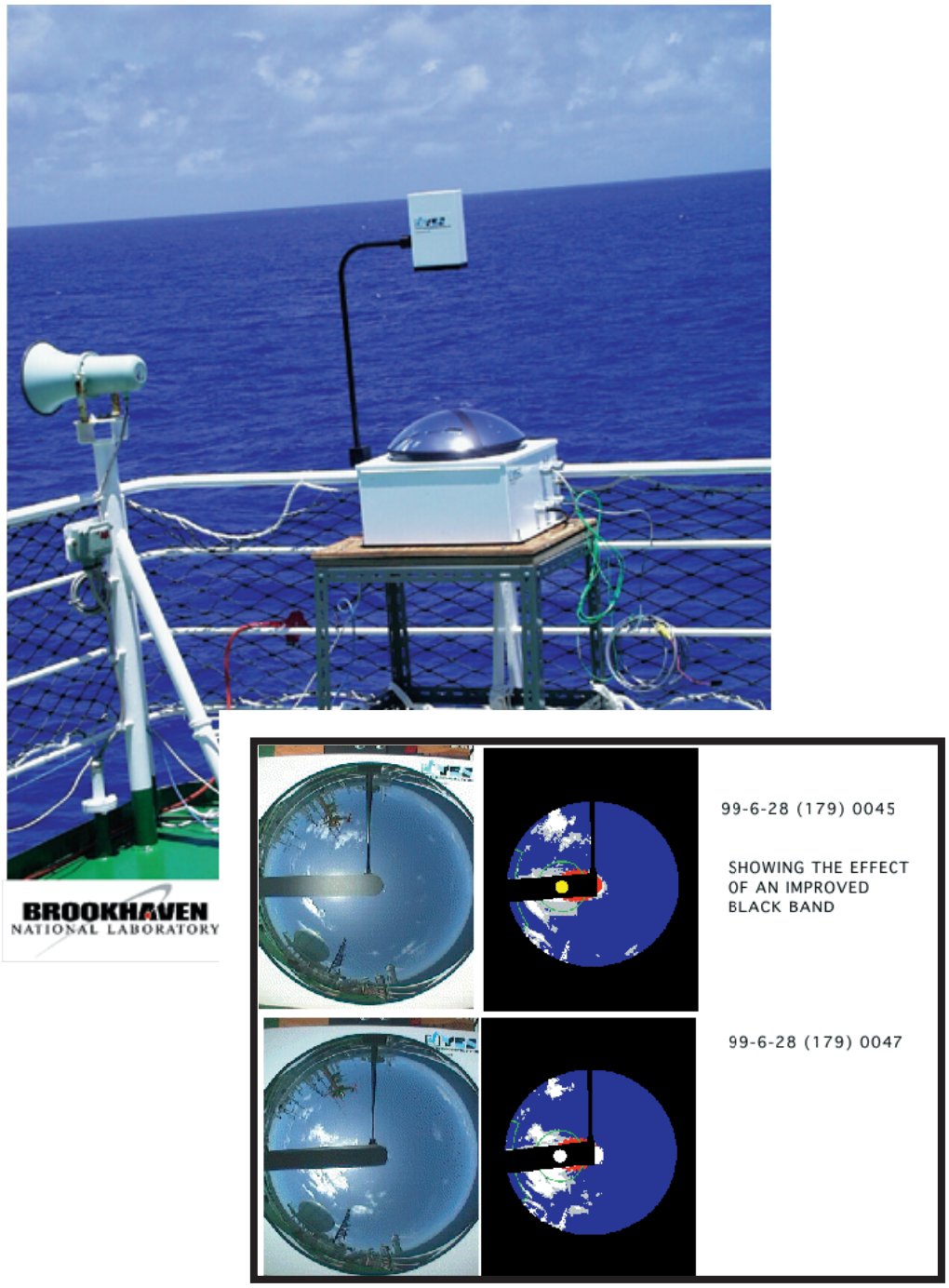

Figure 6.7-4. the Total Sky Imager (TSI) mounted on the upper deck of the MIRAI with the camera arm facing forward. Eaxmples of the images are shwon for two different times on J179. these examples demonstrate the improved performance from a no-glare occulting band.

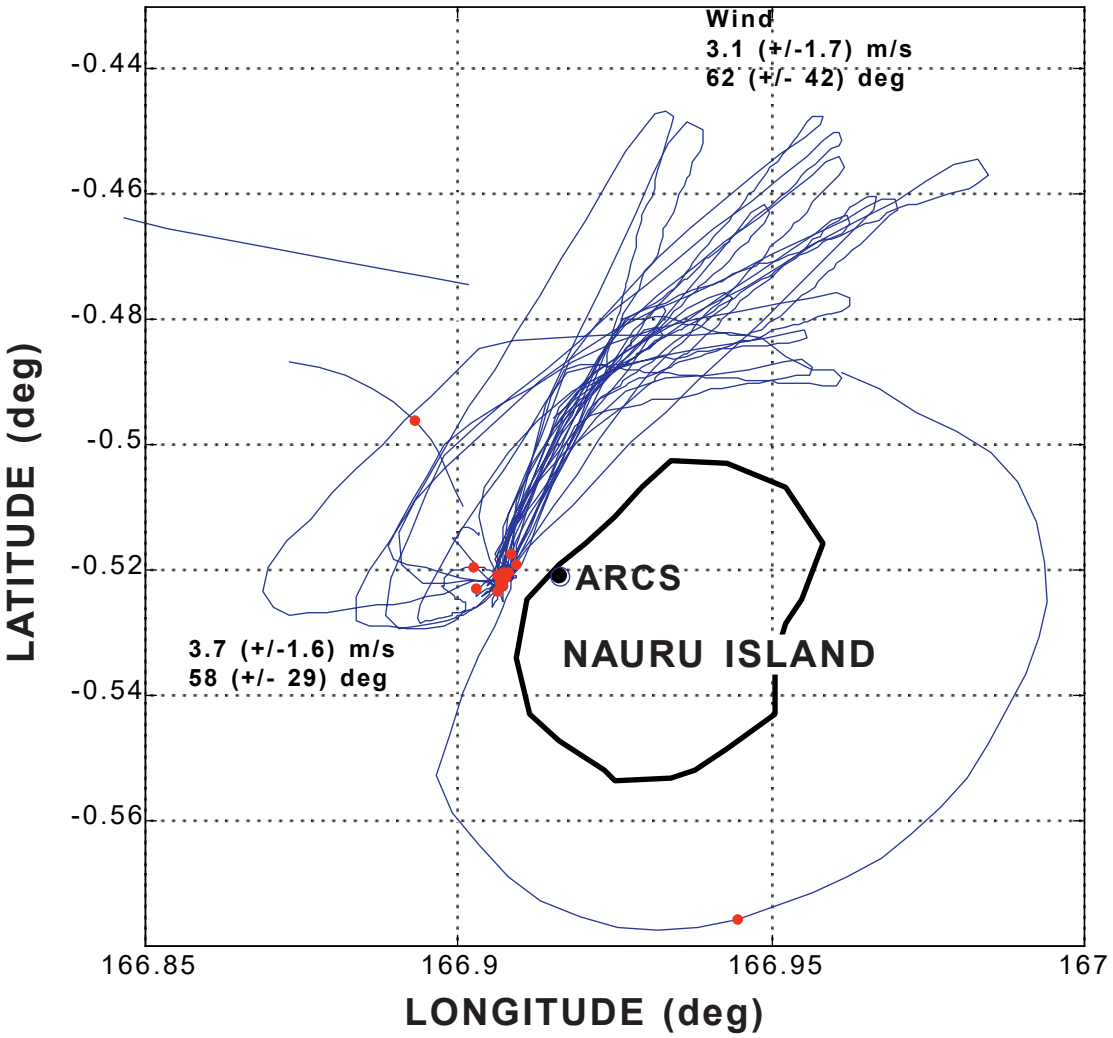

Figure 6.7-5. The mirai position during its island intercomparison period, 167-11Z to 179-08Z. The red dots on the trackline are the locations of the ship at balloon launch times 0530, 1130, 1730, and 2330. The mean wind speed and direction while the ship was in open water and while behind the island are shown.

Figure 6.7-6. The TAO buoy at 165E, EQ with the MIRAI in the background. The newly designed radiation sensor in the next-generation Atlas meteorological package was compared to radiation measurements on the MIRAI during the 11-day buoy inter-comparison period.

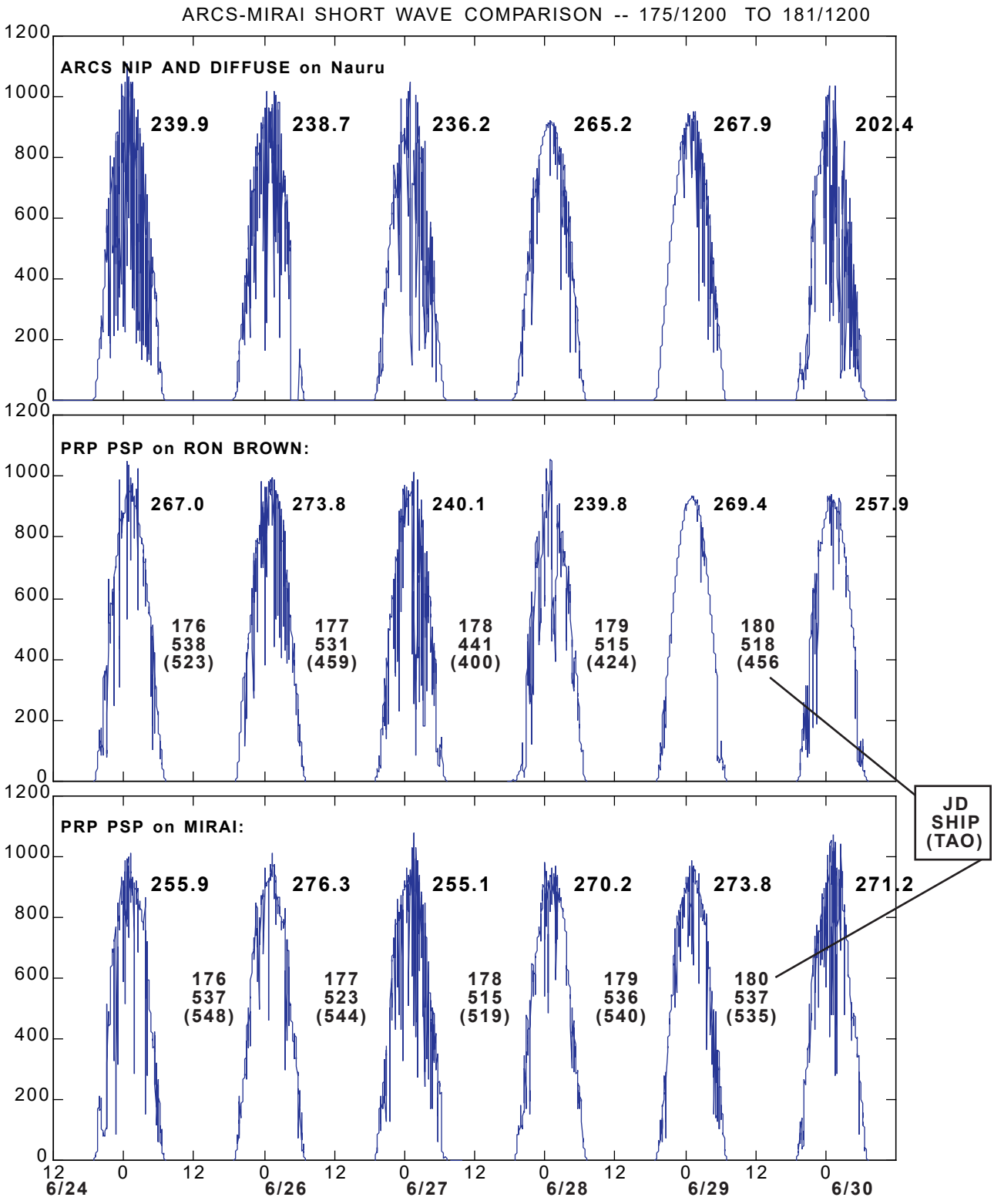

Figure 6.7-7. Shortwave Solar insolation comparisons between MIRAI, RON BROWN, and ARCS during the Large Trinangle operation. Comparisons to the TAO buoys are also shown.

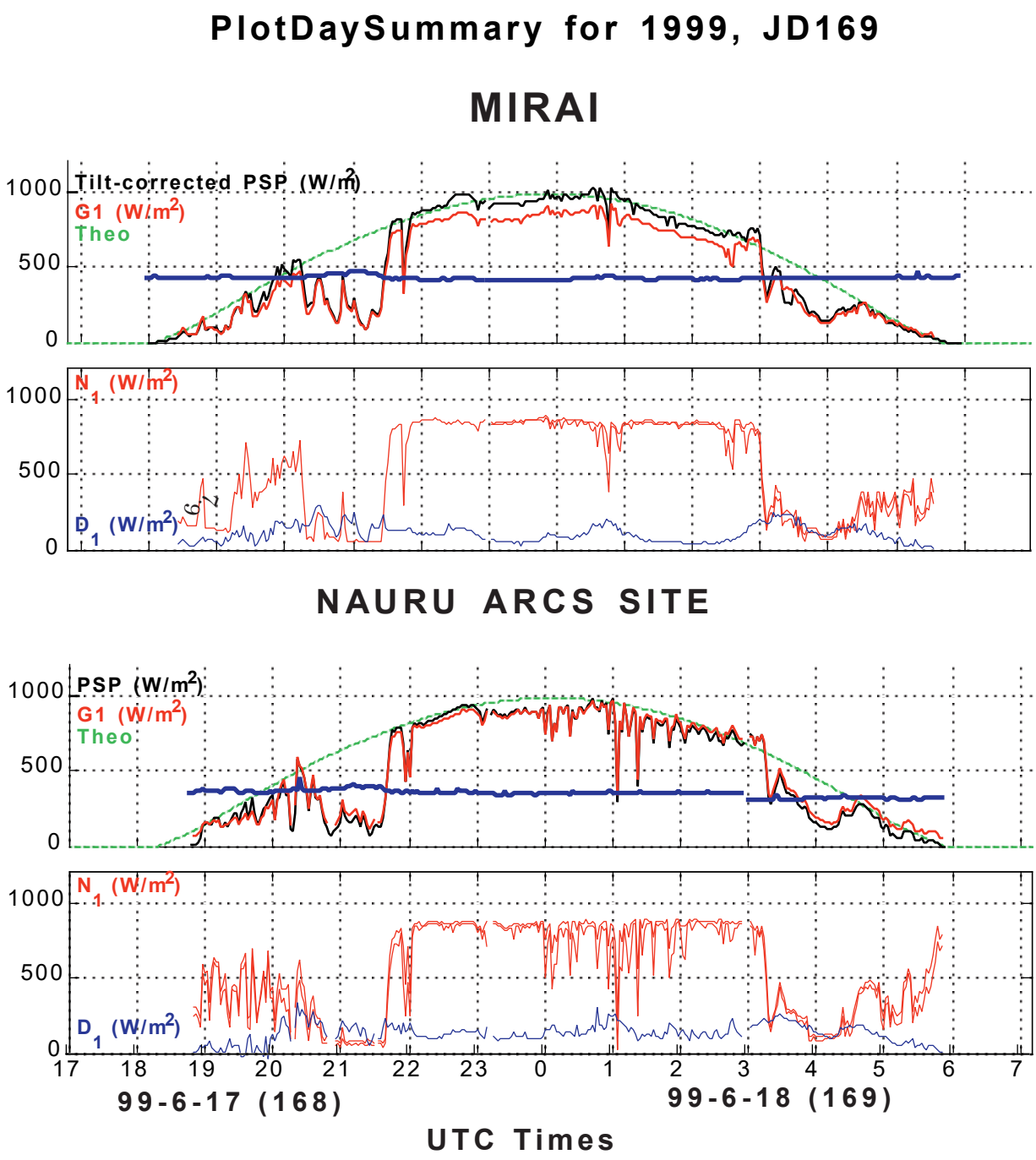

Figure 6.7-8. Comparison of Portable Radiation Package (PRP) measurements of global, direct normal, and diffuse shortwave irradiance for J169 during the MIRAI-Nauru intercomparison period. The black curve in the upper panels is the PRP measurement. The corresponding red curve is the global measurement from the FRSR which uses silicon cell detectors with different pass bands than the PSP.

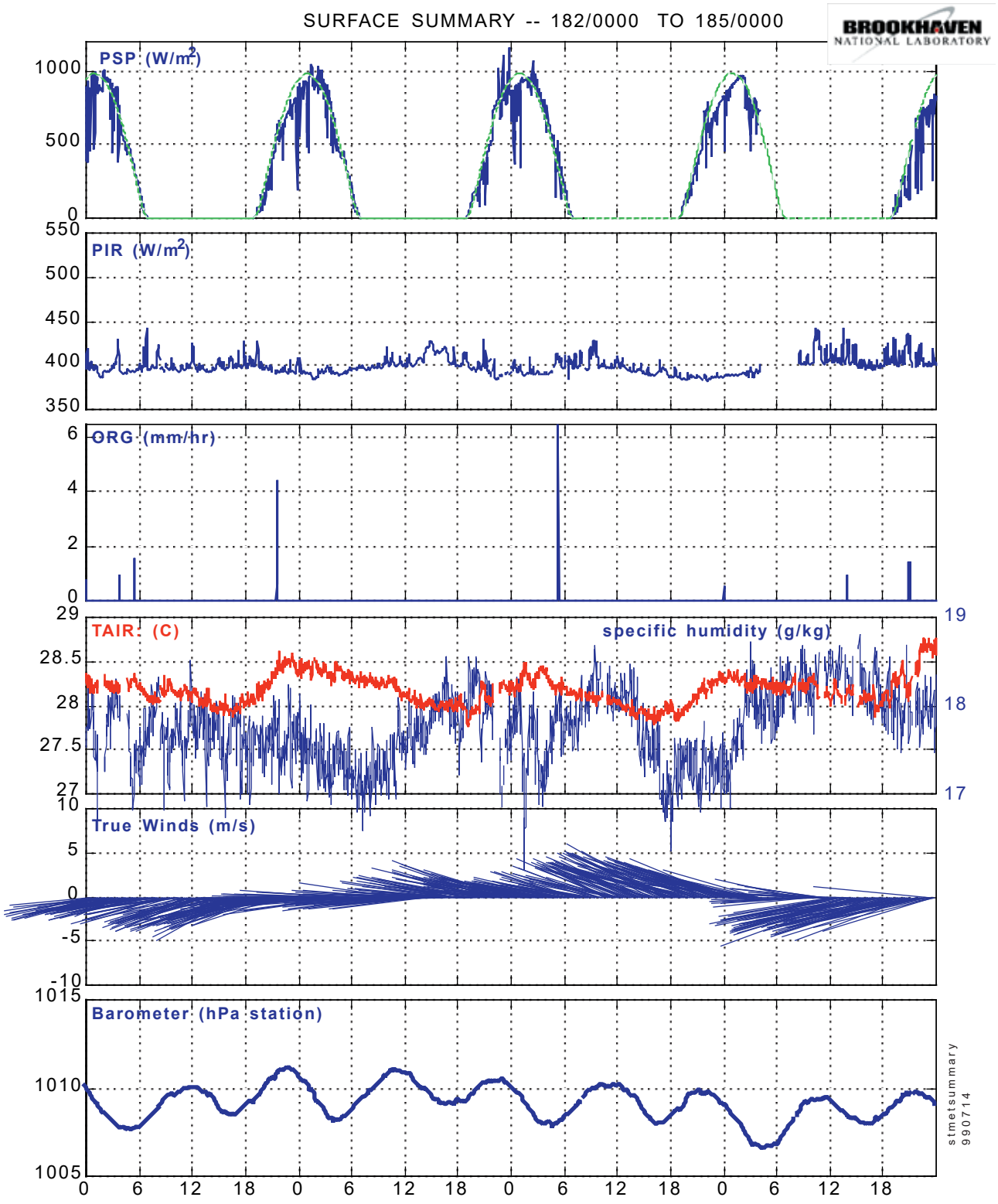

Fig. 6.7-9: Meteorological conditions during the small triangle period.

6.8 Surface Turbulent Flux Measurement

(1) Personnel

Osamu Tsukamoto (Okayama University): Principle Investigator
Hiroshi Ishida (Maritime University of Kobe): Principle Investigator
Tetsuya Takemi (Osaka University)
Tooru Iwata (Okayama University)
Satoshi Takahashi (Okayama University)

(2) Objectives

For the understanding of air-sea interaction, accurate measurements of surface heat and fresh water budgets are necessary as well as the momentum exchange through the sea surface. The surface turbulent fluxes of momentum, sensible heat and latent heat (water vapor) were measured with the eddy correlation method. These flux measurement data are combined with radiation and CTD measurements to lead the surface energy budget.

(3) Parameter

Turbulent fluctuations (up to 20 Hz) of
- Three components of wind velocity
- Air temperature
- Humidity

Sea surface temperature
Ship motions (Pitching, Rolling and Yawing angular accelerations and velocities, 3 axis accelerations)

(4) Methods

A three dimensional sonic anemometer-thermometer (Kaijo, DA-600) and an infrared hygrometer (Kaijo, AH-300) were mounted on the top of the foremast. These turbulence instruments output signals of turbulent fluctuations of three components of wind velocity, air temperature and specific humidity. The anemometer measures relative wind velocities effected by the ship motion. The motions were measured with the motion sensors, such as an inclinometer (Applied Geomechanics, Model-900), accelerometers (Kyowa, AS-2TG, ASV-5GA) and rate gyros (Murata, ENV-05A).

These signals were sampled at 10 Hz or 20 Hz in two kinds of PC based data logging system. The turbulent fluxes of momentum, sensible heat and latent heat (water vapor) are calculated with the eddy correlation method including the ship motion correction. This complicated data processing is carried out after the cruise.

(5) Results

The continuous measurements of turbulent fluctuations were carried out from Yokahama to Chuuk. The second continuous measurements were also carried out from Chuuk to Nauru. Three-hourly flux observation started during the first and second IOPs in the sea area adjacent to Nauru as a sequence of the radio sonde sounding and CTD cast. The time of the flux measurements is listed in Table 6.8-1.

(6) Data archives

The raw data of turbulent fluctuation time series were archived in MO disks. All raw data are submitted to JAMSTEC DMO. The processed data of turbulent fluxes will be archived in Okayama University and open to public after the data processing and quality check.

Table 6.8-1: List of Turbulent Flux Measurements

Run No	Date(UTC) (day-Mon)	Time(UTC) (hr:min)	Duration (hrs)	Remarks and Memo
1	8-Jun	2:24	6.5	Leaving Yokohama for Chuuk
2		9:04	7	sailing south
3		16:15	7	
4		23:36	8	
5	9-Jun	7:16	7.5	cloudy
6		14:59	8	sailing south
7		23:00	8	
8	10-Jun	7:03	8	fine
9		14:59	8	sailing south
10		23:02	8	
11	11-Jun	7:03	8	fine and cloudy
12		14:58	8	sailing south
13		23:00	8	
14	12-Jun	7:02	7	fine and cloudy
15		14:04	8	
16		22:03	7.5	Arriving Chuuk
17	14-Jun	0:10	6	Leaving for Nauru
18		6:05	7	cloudy
19		13:11	7	
20		21:02	8	
21	15-Jun	5:04	7	cloudy
22		12:12	7.5	
23		20:00	6	
24	16-Jun	4:03	8	cloudy
25		12:00	8	
26		20:02	6	fine
27	17-Jun	3:08	1	cloudy. IOP starts
28		6:21	1	fine and cloudy
29		9:03	1	cloudy
30		12:10	1	fine
31		15:11	1	fine
32		18:06	1	cloudy
33		20:45	0.5	cloudy. Nauru govern. staff visit.
34		23:55	0.5	fine
35	18-Jun	3:05	0.5	fine
36		6:00	1	cloudy
37		9:04	1	cloudy
38		12:02	1	fine
39		15:06	1	cloudy
40		18:17	1	cloudy
41		20:58	0.5	fine. Nauru obs. Staff visit
42	19-Jun	1:15	0.5	fine
43		3:00	1	fine
44		8:30	3.5	Leaving for ATLAS buoy position
45		12:01	8	cloudy
46		17:58	1	Arriving ATLAS buoy position
47		20:44	1	fine

48		23:45	1	fine
49	20-Jun	2:48	1	fine
50		5:56	1	fine
51		8:43	1	fine
52		12:18	1	fine
53		14:43	1	fine
54		18:09	1	fine
55		20:39	1	fine
56		23:47	1	fine
57	21-Jun	3:03	1	fine
58		5:52	1	fine
59		8:42	1	fine
60		12:10	1	fine
61		14:58	1	fine
62		17:53	1	cloudy
63		20:40	1	fine
64		23:51	1	fine
65	22-Jun	2:55	1	fine
66		6:06	1	cloudy
67		8:48	1	fine
68		12:11	1	fine
69		14:45	1	fine
70		17:50	1	fine
71		20:41	1	fine
72		23:55	1	fine
73	23-Jun	2:46	1	fine
74		5:50	1	fine
75		8:40	1	fine
76		11:55	1	fine
77		14:46	1	fine
78		17:58	1	fine
79		20:49	1	fine
80	24-Jun	0:20	1	fine
81		2:49	1	fine
82		5:58	1	fine
83		8:49	1	fine
84		11:55	1	fine
85		12:56	6	cloudy
86		20:47	1	cloudy and shower
87	25-Jun	0:47	1	cloudy
88		2:44	1	fine
89		5:49	1	cloudy
90		8:40	1	fine
91		12:00	1	fine
92		12:53	6	fine
93		20:42	1	fine
94	26-Jun	0:13	1	fine
95		3:20	1	fine
96		5:48	1	fine
97		8:41	1	fine
98		11:53	1	fine

99		12:53	6	fine
100		20:43	1	fine
101	27-Jun	0:05	1	fine
102		2:44	1	fine
103		6:05	1	fine and shower
104		8:42	1	cloudy and shower
105		11:52	7	fine
106		20:44	1	cloudy
107	28-Jun	0:02	1	fine
108		2:45	1	fine
109		5:47	1	cloudy
110		8:40	1	cloudy
111		11:52	7	cloudy
112		20:41	1	cloudy
113	29-Jun	0:12	1	fine
114		3:00	1	fine
115		5:46	1	fine
116		8:41	1	cloudy
117		11:47	7	fine
118		20:40	1	fine
119	30-Jun	0:09	1	fine
120		4:48	1	fine
121		5:50	1	fine
122	31-Jun	21:25	1	fine
123	1-Jul	0:11	1	fine
124		2:45	1	fine
125		6:05	1	fine
126		8:54	1	fine
127		11:50	7	cloudy
128		20:46	1	fine
129	2-Jul	0:13	1	fine
130		2:48	1	fine
131		5:48	1	fine
132		8:41	1	fine
133		11:49	7	fine
134		20:40	1	fine
135	3-Jul	0:03	7	fine. Intercom. with R.H.Brown.
136		6:03	1	fine
137		8:36	1	fine
138		11:47	7	fine. Final observation.

6.9 Solar Radiation and Aerosols Measurement

(1) Personnel

Hiroshi Ishida (Maritime University of Kobe): Principle Investigator
Masayuki Sasaki (Meteorological Research Institute, Japan Meteorology Agency)
Kunimitsu Ishida (Toba National College of Maritime Technology)
Masanao Kusakari (Maritime University of Kobe)

(2) Objectives

Aerosols in the atmosphere scatter, reflect, and absorb the solar radiation as an incoming energy to the atmosphere-ocean system of the earth, and they have a large effect on the incoming and outgoing solar radiation energy balance. The solar radiation and aerosols observations are required to understand the characteristics of the sky radiation and atmospheric absorption due to aerosols over the equatorial Pacific ocean.

(3) Measured Parameters

Optical thickness of aerosol
Angstrom coefficient
Degree of Polarization
Total amount of water vapor
Ocean color
Ions of the atmospheric deposition

(4) Methods

Sunphotometer (Eiko Seiki Corp., MS120) measures the solar radiance at four wavelengths of 368, 500, 675 and 778 nm, and obtains the characteristics of the atmospheric absorption due to atmospheric absorption, that is the aerosol optical thickness and Angstrom coefficient. Polarization spectral radiometer (Opto Research Corp., FPR5000) measures the atmospheric absorption of the solar radiation and the Polarization degree at the 90 degrees from the sun direction at six wavelengths of 443, 490, 565, 670, 765, and 865 nm. Multi-spectral radiometer (Opto Research Corp., MSR7000) measures polarized solar radiance at every 1nm wavelength from 400 to 1000 nm, and also does the ocean color. Water Vapor Radiometer (Radiometric Corp., WVR-1100) measures total amount of water vapor. The atmospheric depositions and rain were also sampled on board to analyze chemical components. These data will be analyzed after the cruise.

(5) Preliminary Results

The measurements of solar radiation were made on the fine weather during the whole cruise. And the atmospheric deposition was sampled once a day. The results of each observation are shown in the following tables and figures.

Table 6.9-1 List of each observation parameter

DATE	MSR-7000		FPR-5000		WVR-1100	MS-120	REMARKS
	SKY	SEA	SKY	SEA			
06/08/99	O		O		O		
06/09/99					O		
06/10/99	O		O		O		
06/11/99	O		O		O		
06/12/99	O		O		O	O	
06/13/99							Chuuk Island
06/14/99	O		O		O	O	
06/15/99	O		O		O		
06/16/99	O		O		O	O	
06/17/99	O	O	O		O	O	Nauru Intercomparison
06/18/99	O	O	O	O	O	O	
06/19/99	O	O	O		O	O	
06/20/99	O	O	O		O	O	TAO BUOY (Equater,165E)
06/21/99	O	O	O	O	O	O	
06/22/99	O	O	O		O	O	
06/23/99	O	O	O		O	O	
06/24/99	O	O	O		O	O	
06/25/99	O	O	O		O	O	
06/26/99	O	O	O	O	O	O	
06/27/99	O	O	O		O	O	
06/28/99	O	O	O		O	O	
06/29/99	O	O	O	O	O	O	
06/30/99	O	O	O	O	O	O	
07/01/99	O	O	O		O	O	small triangle
07/02/99	O	O	O		O	O	
07/03/99	O	O	O		O	O	
07/04/99	O	O	O		O	O	

Fig. 6.9-1 Water vapor by WVR-1100

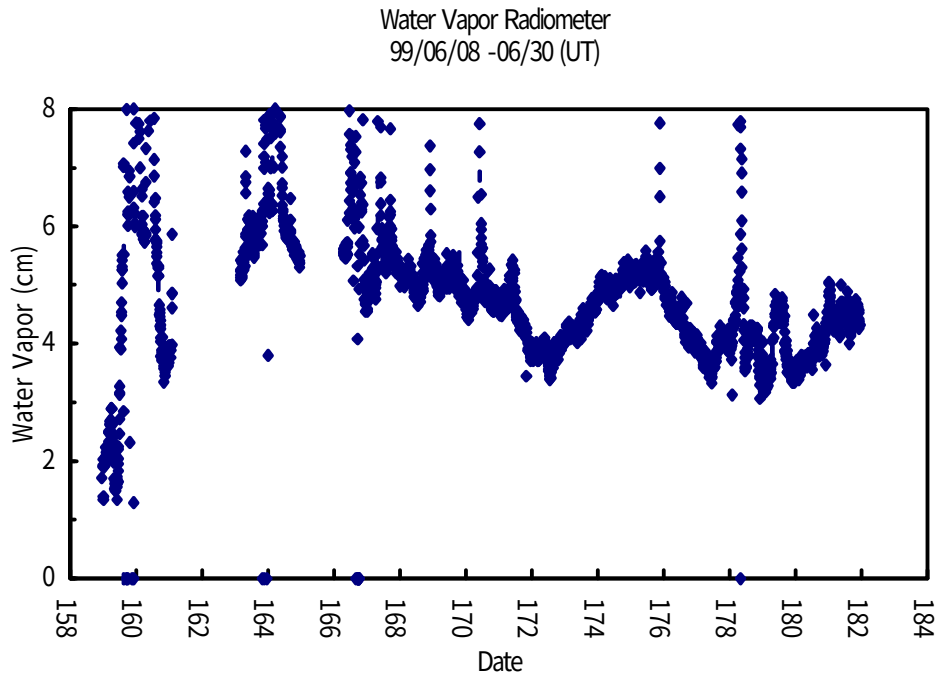

Fig. 6.9-2 Optical thickness by FPR-5000 at 565nm

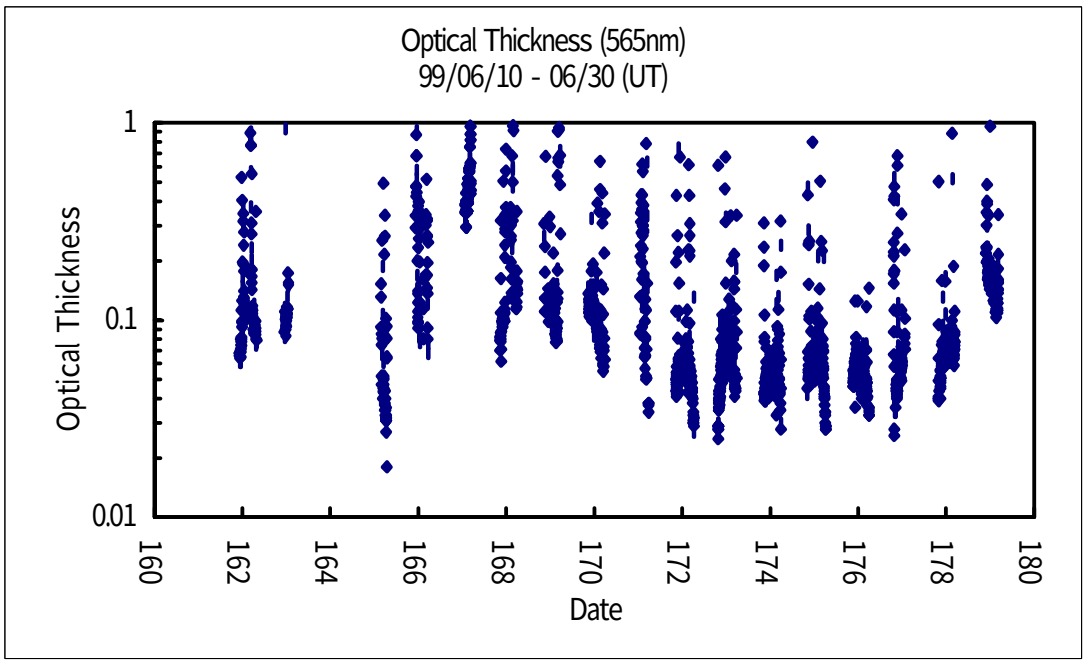

Fig. 6.9-3: Degree of polarization at 90 angle from the solar direction in the principal plane as function of wave length by FPR-5000.

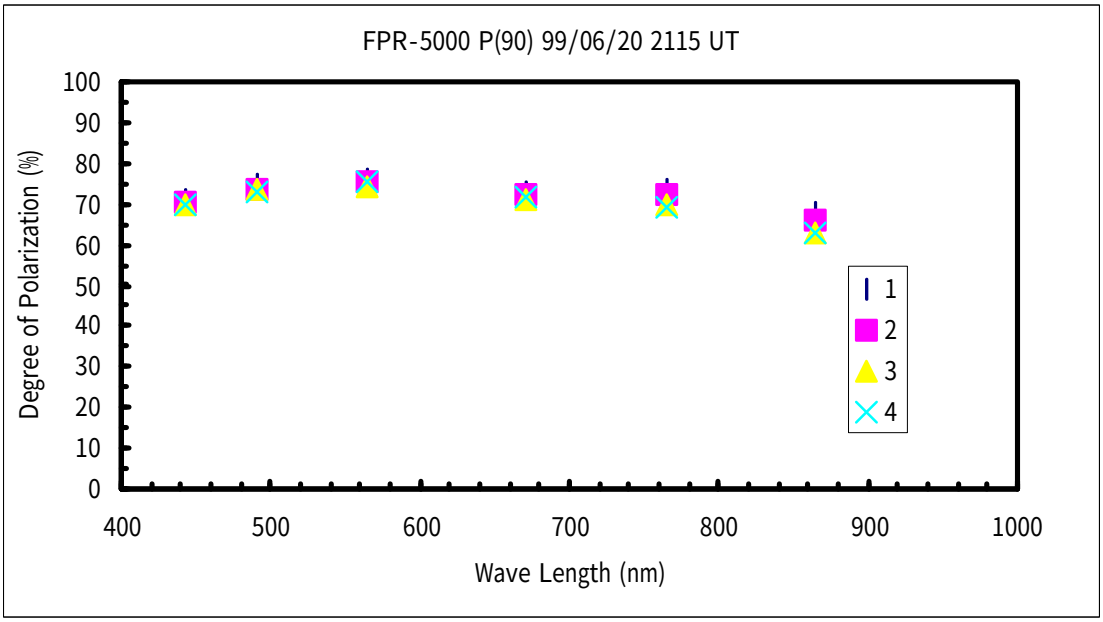

Fig. 6.9-4 Degree of polarization at 90 angle from the solar direction in the principal plane as function of wave length by MSR-7000.

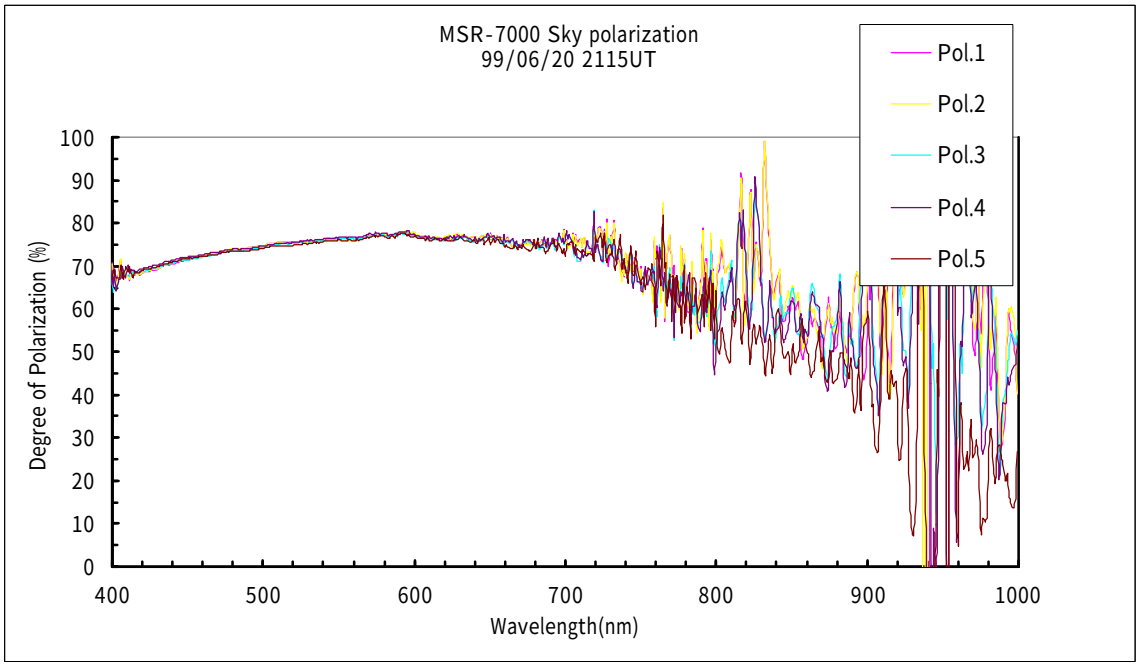

Fig. 6.9-5 Radiance at 90 angle from the solar direction in the principal plane as function of wave length by FPR-5000.

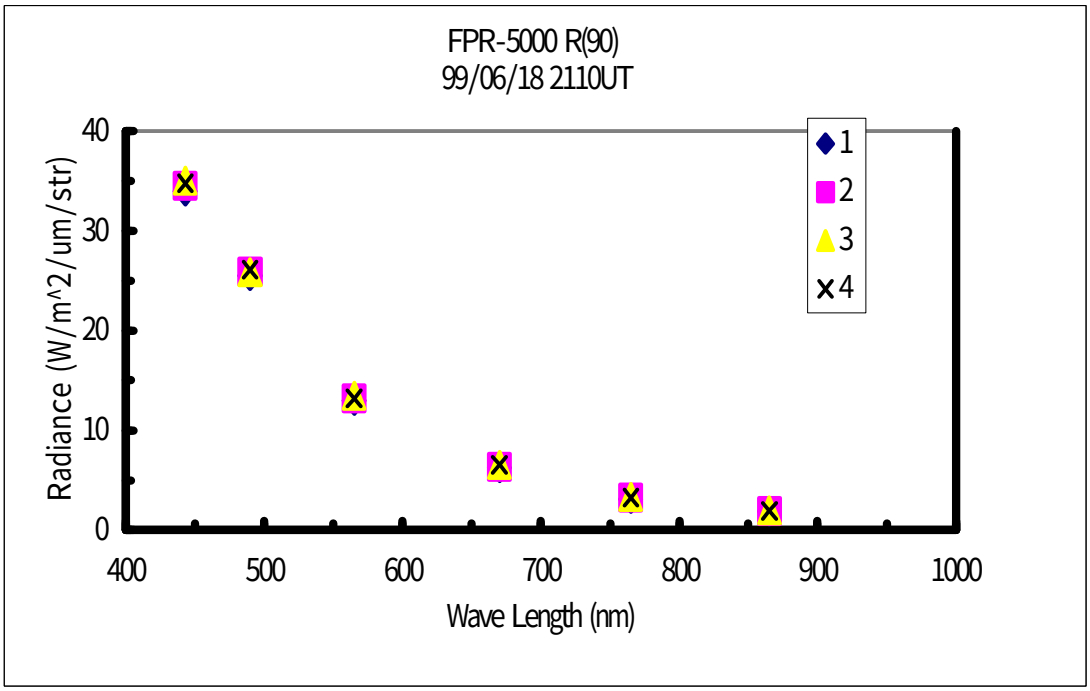

Fig. 6.9-6 Radiance at 90 angle from the solar direction in the principal plane as function of wave length by MSR-7000.

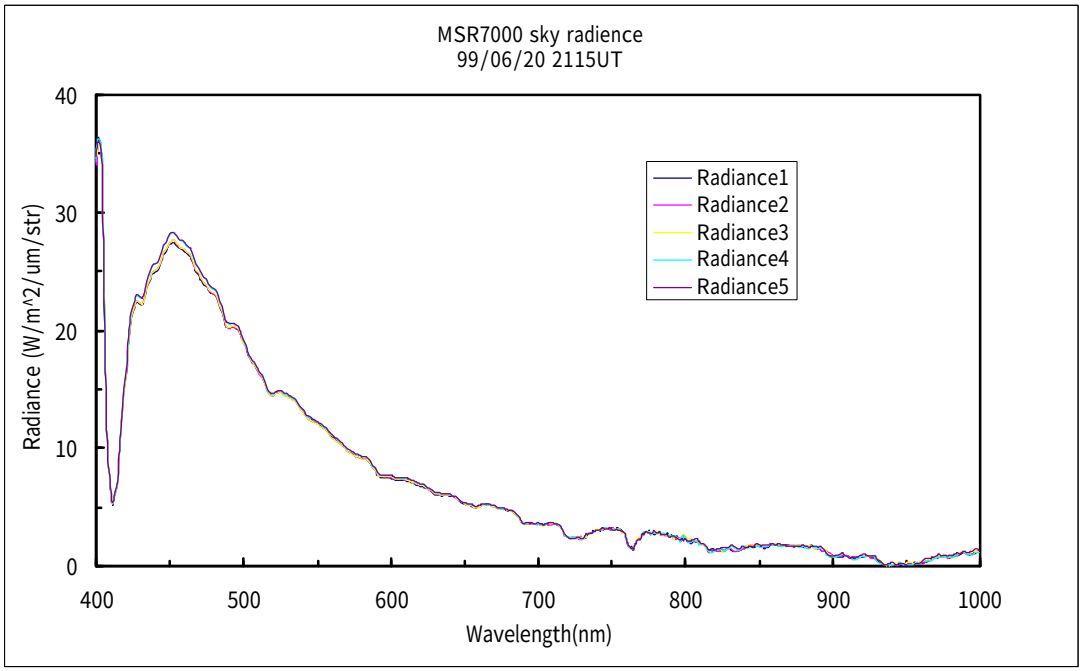

Fig. 6.9-7 Radiance at sea surface to solar direction as function of wave length by FPR-5000.

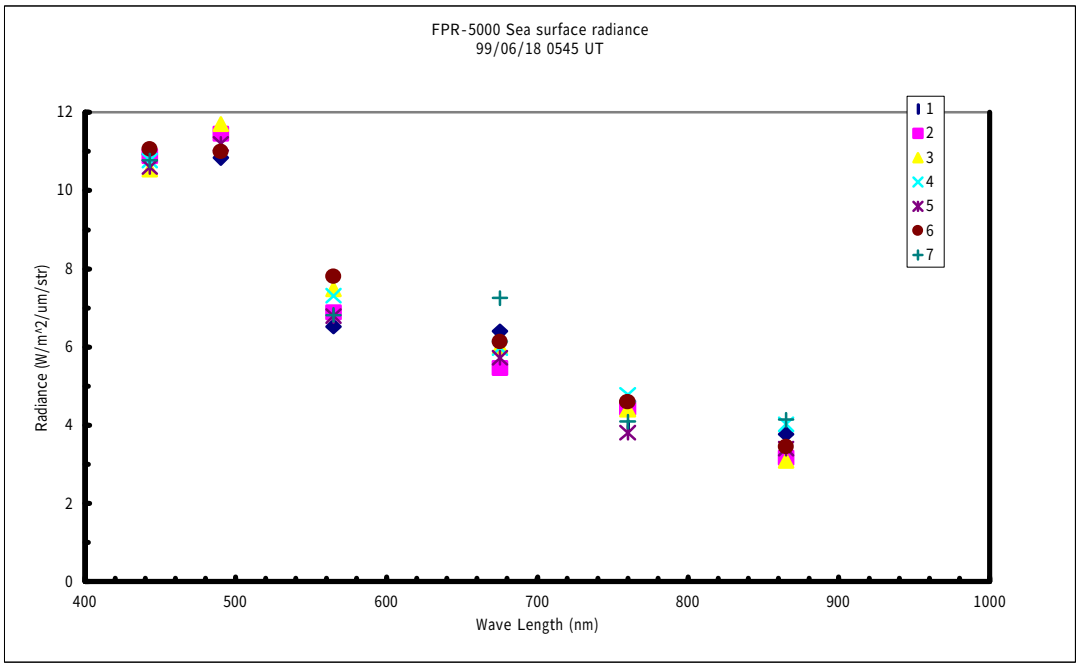

Fig. 6.9-8 Radiance at sea surface to solar direction as function of wave length by MSR-7000.

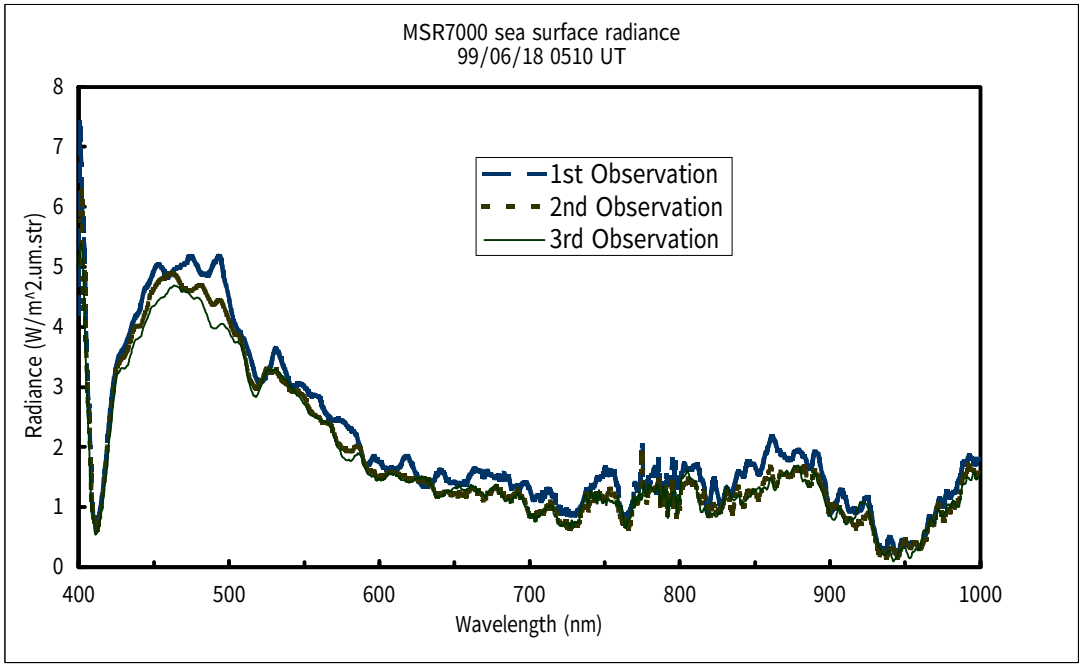

(6) Data archives

The raw data of the solar radiation are archived in a floppy disk. Samples of atmospheric deposition are analyzed on their chemical components etc., and the results are archived in a floppy disk. After the quality check of those data, they will be published an open to public. All data will be archived at Maritime University of Kobe. The data and sample inventory information are submitted to JAMSTEC DMO.

6.10 SSST Measurement

(1) Personnel

Bill Brown (NCAR)
Jennifer Hanafin (RSMAS)
Tim Nightingale (RAL)
R. Michael Reynolds (BNL)

(2) Objectives

Observation of temperature structure at the air/sea boundary and its dependence on surface heat fluxes. Validation of satellite SST products, in particular those from ERS-2/ATSR-2, NOAA-14/AVHRR and NOAA-15/AVHRR.

(3) Parameters

Upwelling radiance (10.8μm), 48° from nadir
Downwelling radiances (10.8μm), 8°, 48° and 60° from zenith
Upwelling spectral radiance (5μm – 20μm), 55° from nadir
Downwelling spectral radiances (5μm – 20μm), 10° and 55° from zenith
Skin Sea Surface Temperature (~50μm depth)
Bulk Sea Surface Temperature (~2cm – 10cm depth)
Air temperature

(4) Methods

(4.1) The Marine-Atmosphere Emitted Radiance Interferometer (M-AERI)

The RSMAS M-AERI (S/N MAERI-01) measures upwelling radiation emitted by the sea surface and downwelling atmospheric radiation in the wavelength range 5μm – 20μm at a spectral resolution of 4 cm^{-1}. It consists of three main parts, the scanning mechanism which directs infrared radiation into the main chamber containing the optics and detectors and a system of electronics which process the signal received at the detectors.

A mirror is aligned at an angle of 45° to a horizontal motor shaft. The mirror is gold-plated to avoid polarisation effects. As the shaft rotates, the mirror directs radiation emitted in the field of view into the main chamber. Each sequence of measurements consists of two atmospheric scene views and one ocean scene view sandwiched between two sets of blackbody views so that each measurement is calibrated. A sequence is completed every 11 minutes, of which the ocean view constitutes about 2 minutes. Two high emissivity blackbody cavities are used, one at 60°C and the second floating at the ambient air temperature. The ocean view is taken at 55° from nadir. One sky view is taken at 55° from zenith to give a complementary view for correction of the ocean view and the second is at 10° from zenith. Radiation directed into the main chamber enters an array of optics and then the interferometer where an interferogram is produced. This signal is then detected using an InSb/MCT sandwich detector the temperature of which is maintained at 75 – 76K with a Stirling cycle cooler.

The interferogram thus produced is calibrated, corrected for non-linear effects and Fourier transformed to give a spectrum of infrared radiance emitted in the field of view. Sea surface temperature is calculated using the upwelling radiance measured at 7.7μm, with an correction for atmospheric reflection from the complementary view 7.7μm measurement and a second correction for the radiance emitted by the air in the path between the instrument and the sea surface. Air temperature is calculated using a number of different

wavelengths which have very short optical paths and measure radiance emitted by the atmosphere approximately 9m from the instrument.

(4.2) The Scanning Infrared Sea Surface Temperature Radiometer (SISTeR)

The RAL SISTeR (S/N "Alice") is a compact and flexible chopped, self-calibrating infrared filter radiometer, specially designed for research in a maritime environment. Developed to validate the second Along Track Scanning Radiometer (ATSR-2), the instrument presently contains filters at 3.7μm, 10.8μm and 12.0μm, built to the ATSR-2 filter specifications. All external radiance measurements are referred to two internal black bodies, one of which is heated. The direction of external views can be programmed in fine increments at angles in a range spanning 180° from nadir to zenith. The instrument contains a small PC and all aspects of the instrument can be interrogated or controlled with a simple C program.

The instrument is divided into three compartments. The foreoptics compartment contains a TGS detector and preamplifier, a black rotating chopper and coaxial six-position filter wheel, and an off-axis ellipsoid mirror. It is sealed and separated from the calibration compartment by a coated ZnSe window. Within the calibration compartment is a 45° gold-plated scan mirror which rotates about the optical axis of the ellipsoid mirror. The scan mirror folds the optical beam through 90° and directs it either to an external view, or to one of two identical high-accuracy black bodies. Each contains an embedded RhFe thermometer, traceable to the ITS-90 temperature scale. One black body floats at ambient temperature and the other at approximately 10K above ambient. The remaining compartment contains a PC and the signal processing and control electronics required to operate the instrument.

All Nauru99 SISTeR radiances are sampled every 0.8s with the 10.8μm filter. The NEdT of a single 0.8s sample at typical SSTs is approximately 30mK. The radiometric accuracy of the instrument is also approximately 30mK or better. The Nauru99 measurement cycle contains 128 samples, made up of 76 ocean samples at 48° from nadir, 4 sky samples each at 60°, 48° and 8° from zenith, and 8 samples each of the hot and ambient black bodies. The remaining sample intervals are taken up by scan mirror movements. Skin SSTs are calculated from the ocean samples, corrected for the small reflected sky radiance term with the complementary sky samples.

(4.3) The Sea Snakes

The BNL and NCAR sea snake SST sensors are similar in design. A temperature sensor is fixed into the end of a long length of tygon tubing and allowed to float on the surface of the water. Because there are no changes from the cylindrical shape, the sea snake pulls through the water with minimal drag even at ship speeds as high as 10 – 12 knots. The BNL sensor used a platinum temperature sensor and a 4 – 20 mA PRT converter encapsulated into the end of the tubing. The current loop was routed to the Zeno data logger (See section 6.7) where the measurement was logged and sent to the SCS computer. The NCAR sea snake used a platinum element sealed into a brass cylinder. A 4-wire connection to the NCAR data logger enabled precise low-noise resistance measurements.

(4.4) The "Hard Hat"

The RSMAS "hard hat" is a well-calibrated thermistor, mounted on a float made from the shell of a hard hat. The "hard hat" is designed for deployment at low ship speeds (2 knots or less).

(4.5) The CASOTS Black Body

The Leicester University CASOTS black body (S/N CAS002) is a thin-walled copper black body cavity of high emissivity, immersed in a well-stirred water bath whose temperature is monitored by an immersible platinium thermometer (S/N A1113A/1) with an ASL F-250 AC resistance bridge (S/N 3010-011-1402).

The cavity is used to validate the calibration of the SISTeR radiometer and the water bath alone is used to intercompare the calibrations of the sea snake and hard hat thermometers.

(4.6) Deployment

The M-AERI and SISTeR instruments were mounted on the lower foremast platform of the R/V Mirai, looking forward over the port and starboard sides of the bow respectively. The two sea snakes were trailed in undisturbed water in front of the ship's wake, from booms projecting forward over the point of the bow. The "hard hat" was deployed from the light crane on the port side of the forward deck. Data was taken continuously from all instruments throughout the observation period, with the following exceptions:

(a) The M-AERI and SISTeR instruments did not collect data while it was raining.
(b) The "hard hat" was not deployed while the ship was under way at speeds greater than 2 knots.
(c) The sea snake and "hard hat" sensors were taken out of the water on two occasions on the 12th and 22nd – 23rd of June for calibration intercomparisons in the CASOTS black body water bath.

Data is also available from the M-AERI and SISTeR instruments on the transects to and from the observing regions at Nauru and at 165°E, 0°S.

(5) Results

(5.1) Ocean Observations

Preliminary SSTs for the entire "large triangle" observation period are shown in Figure 7.1-1. The diurnal cycle is clearly visible in all measurements and increases in amplitude during a period of relatively clear skies on days 173 – 176. Figure 7.1-2 Shows a 24 hour cycle in greater detail, starting at midnight, local time on day 174. In the absence of solar heating, the surface layer is a little colder than the underlying water and a cold skin with a magnitude of about 0.3K has formed. A little after dawn, all the SSTs begin to rise. Insolation preferentially heats the surface layer and its temperature rises above that of the deeper water. The skin however remains 0.2K – 0.3K cooler than the surface water. At dusk, the warm layer collapses and the night-time pattern resumes.

(5.2) Calibrations and Intercomparisons

The "hard hat" and sea snake sensors were intercompared and calibrated in the CASOTS water bath on the 12th and 22nd – 23rd of June. On each occasion the water bath temperature was raised approximately 15K over a period of several hours, spanning the range of expected SSTs. The "hard hat" and BNL sea snake sensors both tracked the water bath temperature to 10mK or so, at the limit of the various thermometer calibration accuracies. The NCAR probe differed a little more, but this was expected, given the preliminary state of its calibration.

The SISTeR calibration was checked against the CASOTS black body cavity before and after shipping at the beginning of the cruise. The brightness temperature measured with the SISTeR agreed with the water bath temperature to approximately 10mK over a 15K interval spanning the expected range of SSTs.

Data from the M-AERI and SISTeR instruments were intercompared from several sections of the cruise. SISTeR 0.8s SSTs were binned into the M-AERI SST measurement intervals. The mean bias between the two data sets was very low, of order 20mK or less, with a standard deviation typically of 40mK – 50mK.

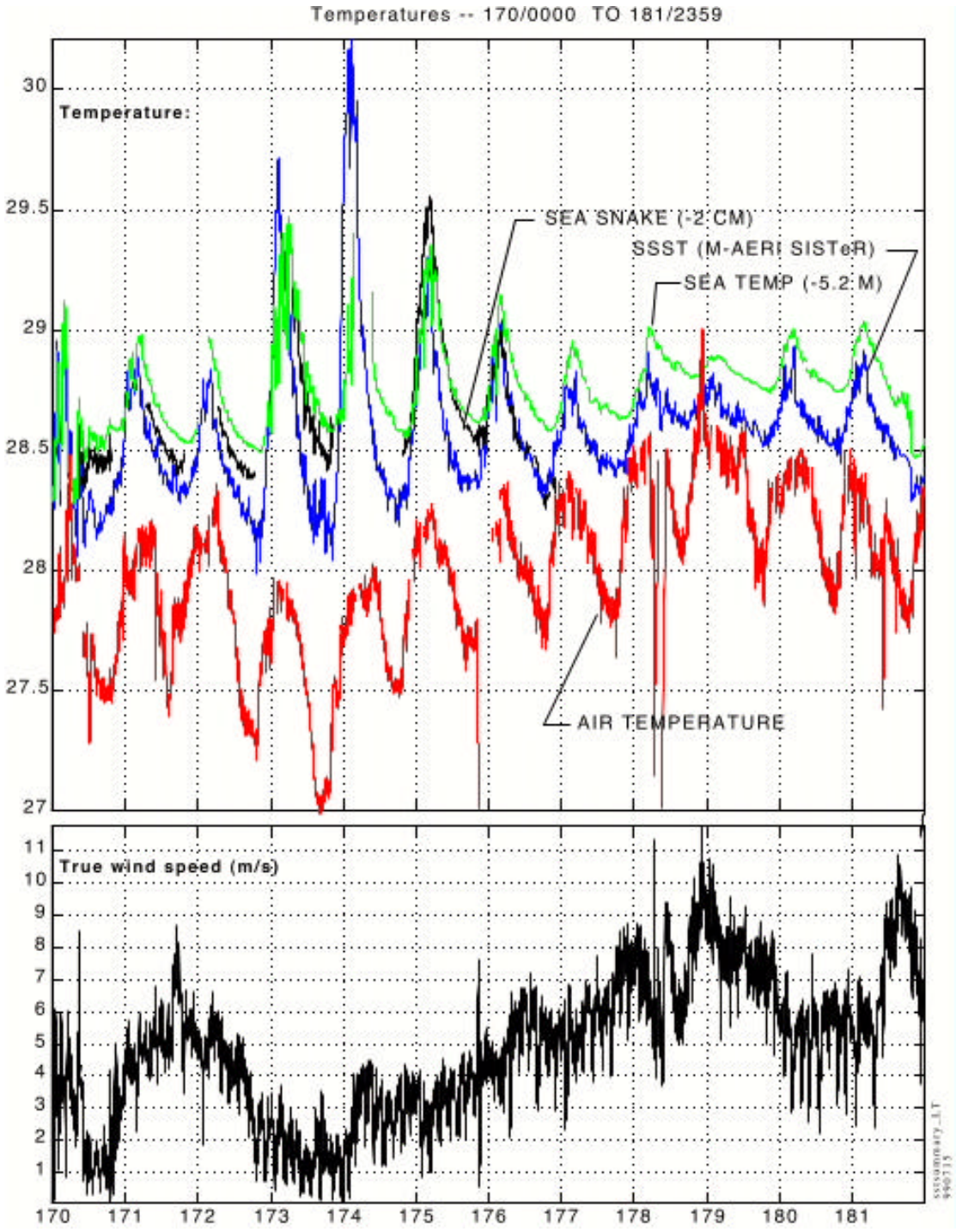

Figure 7.1-1: A comparison of three different measures of sea surface temperature and the corresponding air temperature and true wind speed. Data for the "large triangle period".

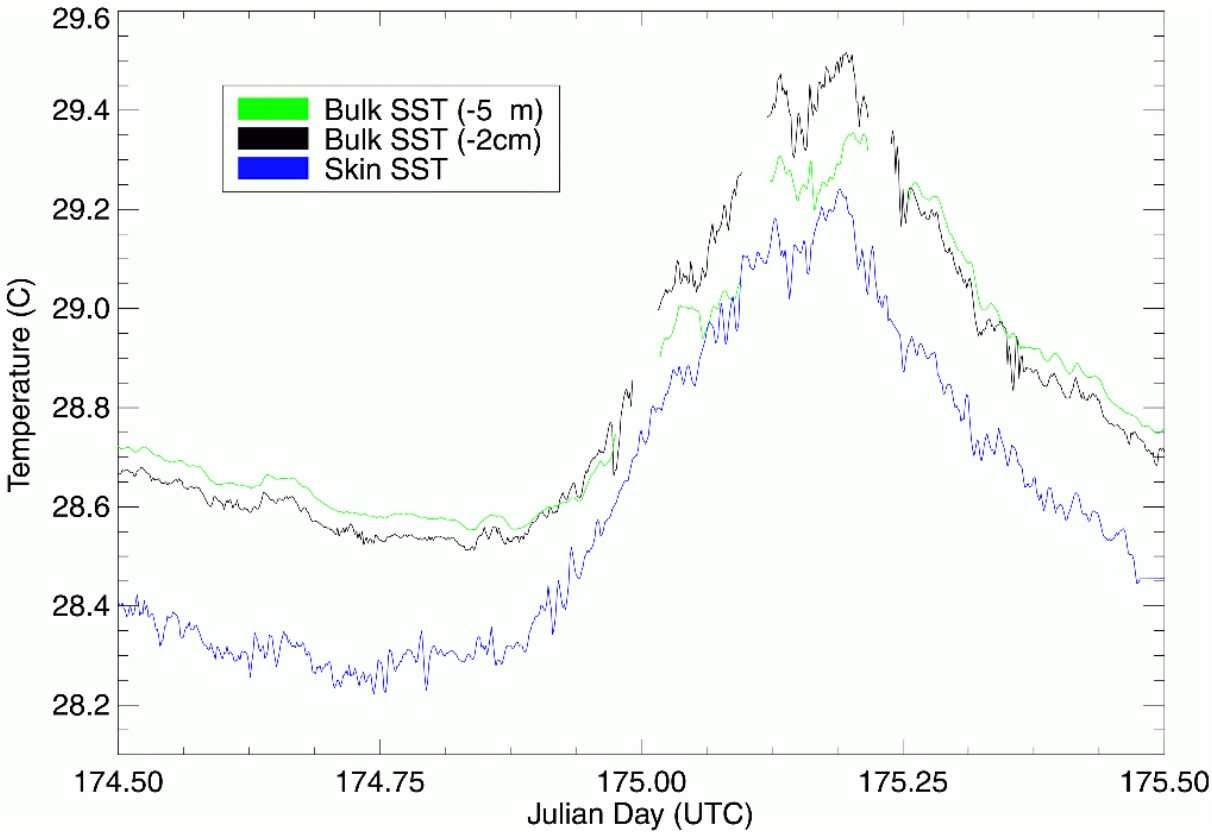

Figure 7.1-2: A diurnal temperature cycle in SST measurements, starting at 12:00 UTC on day 174 (midnight, local time).

(6) Other Remarks

The SST data should be treated with some caution. In general, it can be used with confidence only from periods when the R/V Mirai was under way. When the R/V Mirai was on station, the bow thrusters tended to disrupt both the skin layer and the thermocline beneath it. Consequently, skin and bulk SST measurements during these periods cannot be considered representative of conditions in undisturbed water. Also, depending on wind direction, the M-AERI SST product may sometimes have been influenced by the elevated temperature of air heated as it moved across the ship's structure. Measurements from the BNL sea snake after the 22nd – 23rd June intercomparison were improved by the addition of a reflective shield. The SST investigators strongly recommend that interested groups should contact them for advice before using the SST data.

7. Oceanographic Observations

7.1 CTD

7.1.1 CTD Observation

(1) Personnel

Satoshi Ozawa (MWJ): Operation Leader
Shinichiro Yokogawa (MWJ)
Katsunori Sagishima (MWJ)
Mizue Hirano (MWJ)
Ai Yasuda (MWJ)
Mikio Kitada (MWJ)
Keisuke Wataki (MWJ)
Masanari Sato (MWJ)

(2) Objectives

Investigation of the oceanic structure and its time variation by measuring vertical profiles of temperature and salinity.

(3) Measured Parameters

Pressure
Temperature
Conductivity
Dissolved Oxygen

(4) Methods

We observed vertical profile of temperature and salinity by CTD/RMS (Conductivity Temperature Depth profiler / Rosette Multi-bottle array water sampling system). The sensor attached on CTD were temperature sensor, conductivity sensor, pressure sensor, oxygen sensor and altimeter sensor. Salinity was calculated by measurement values of pressure, conductivity and temperature. The CTD/RMS was deployed from starboard on working deck. Descending rate and ascending rate were kept 1.2 m/s respectively.

The CTD raw data was acquired in real time by using by the SEASAVE utility from SEASOFT software (ver.4.232) provided by SBE and stored on the hard disk of an IBM personal computer.

Water samplings were made during up-cast by sending a fire command from the computer. In ordinary cast we sampled water at 1000 m to calibrate salinity data. In several casts sea water at 12 layer were sampled for PCO2 analysis.

Basically during the stationary observation, CTD casting was conducted every 3hours (00, 03, 06, 09, 12, 15, 18, 21 UTC). Measurement depth was 1000 m at 00 UTC, 500 m at 06, 12, 18 UTC and 250 m at others. In total, 129 castings were carried out.(see Table 7.1.1-1)

Specifications of the sensors are:

Under water unit: CTD 9plus (S/N 09P9833-0357, Sea-Bird Electronics, Inc)
Temperature Sensor: SBE3-04/F (S/N 031524, Sea-Bird Electronics, Inc)
Conductivity Sensor: SBE4-04/0 (S/N 041203, Sea-Bird Electronics, Inc)
Oxygen sensor: MODEL 13-04-B (S/N 130338, Sea-Bird Electronics, Inc)

Altimeter sensor: MODEL 2110-2 (S/N 206, Benthos, Inc)
Deck unit: SBE 11plus (S/N 11P8010-0308, Sea-Bird Electronics, Inc).

(5) Results

Vertical profiles at each CTD cast are attached in the following APPENDIX. Time variations of the vertical profile of temperature, salinity and oxygen at Large and Small Triangle are shown in Figs. 7.1.1-1 and 7.1.1-2, respectively.

Note that the data correction on salinity using sampled water (see Section 7.1.2) is not applied in these figures.

(6) Data archive

All raw and processed CTD data files were copied onto magnetic optical disks (MO) and submitted to JAMSTEC Data Management Office (DMO) and will be under their control.

Table 7.1.1-1 CTD Cast Table

Leg	Cast No.	Cast name	Latitude	Longitude	Date (UTC)	Time (UTC)	Depth (m)
Phase 1	01	061703	00-31.2547 S	166-54.3619 E	17 June '99	02:26	250
	02	061706	00-31.1645 S	166-54.3309 E	17 June '99	05:47	250
	03	061709	00-31.1121 S	166-54.3943 E	17 June '99	08:27	250
	04	061712	00-30.0034 S	166-54.3638 E	17 June '99	11:34	250
	05	061715	00-31.0669 S	166-54.3899 E	17 June '99	14:25	250
	06	061718	00-31.2855 S	166-54.3062 E	17 June '99	17:25	250
	07	061721	00-31.1511 S	166-54.4003 E	17 June '99	20:12	250
	08	061800	00-31.2837 S	166-54.0972 E	17 June '99	23:29	250
	09	061803	00-31.1427 S	166-54.3097 E	18 June '99	02:29	250
	10	061806	00-31.1480 S	166-54.3954 E	18 June '99	05:16	250
	11	061809	00-31.1597 S	166-54.4143 E	18 June '99	08:20	250
	12	061812	00-31.2108 S	166-54.3242 E	18 June '99	11:22	250
	13	061815	00-31.2860 S	166-54.2983 E	18 June '99	14:27	250
	14	061818	00-31.2584 S	166-54.3097 E	18 June '99	17:34	250
	15	061821	00-31.2022 S	166-54.3348 E	18 June '99	20:24	250
	16	061900	00-31.0759 S	166-54.1236 E	18 June '99	23:25	250
	17	061903	00-31.7500 S	166-54.3046 E	19 June '99	02:23	250
	18	061906	00-31.2887 S	166-54.2879 E	19 June '99	05:29	250
Phase 2	19	062006	00-01.3691 N	164-59.5164 E	20 June '99	05:27	500
	20	062009	00-01.1150 N	164-59.4425 E	20 June '99	08:26	250
	21	062012	00-01.1349 N	164-59.6097 E	20 June '99	11:27	250
	22	062015	00-01.0857 N	164-59.4377 E	20 June '99	14:28	250
	23	062018	00-00.8094 N	164-59.1772 E	20 June '99	17:28	250
	24	062021	00-00.1418 S	164-59.4220 E	20 June '99	20:24	250
	25	062100	00-00.1310 S	164-59.2579 E	20 June '99	23:26	1030
	26	062103	00-00.1727 S	164-59.3283 E	21 June '99	02:26	250
	27	062106	00-00.2242 S	164-59.3086 E	21 June '99	05:25	520
	28	062109	00-00.3887 S	164-59.2271 E	21 June '99	08:26	250
	29	062112	00-00.5346 S	164-59.8423 E	21 June '99	11:24	520
	30	062115	00-00.2600 S	164-59.6658 E	21 June '99	14:23	250
	31	062118	00-00.9008 S	165-00.0730 E	21 June '99	17:27	520
	32	062121	00-00.8351 S	165-00.2125 E	21 June '99	20:26	250
	33	062200	00-00.8903 S	165-00.2648 E	21 June '99	23:23	1030
	34	062203	00-01.1223 S	165-00.1543 E	22 June '99	02:26	250
	35	062206	00-00.1400 S	164-59.2294 E	22 June '99	05:26	520
	36	062209	00-00.3103 S	164-59.2809 E	22 June '99	08:24	250
	37	062212	00-00.2316 S	164-59.2686 E	22 June '99	11:28	520
	38	062215	00-00.2183 S	164-59.0965 E	22 June '99	14:31	250
	39	062218	00-02.0142 S	165-00.4017 E	22 June '99	17:33	520
	40	062221	00-00.8077 S	164-59.3692 E	22 June '99	20:30	250
	41	062300	00-00.2632 S	164-59.7436 E	22 June '99	23:24	1030
	42	062303	00-00.5124 S	165-00.4414 E	23 June '99	02:27	250
	43	062306	00-00.1141 S	164-59.6023 E	23 June '99	05:23	520
	44	062309	00-00.3060 S	164-59.9081 E	23 June '99	08:24	250
	45	062312	00-00.5411 S	164-59.7616 E	23 June '99	11:29	520
	46	062315	00-00.5756 S	164-59.8378 E	23 June '99	14:27	250
	47	062318	00-00.8881 S	164-59.8915 E	23 June '99	17:31	520
	48	062321	00-00.7309 S	164-59.7068 E	23 June '99	20:24	250
	49	062400	00-00.4318 S	165-00.1855 E	23 June '99	23:26	1030
	50	062403	00-00.7872 S	165-00.5052 E	24 June '99	02:26	250
	51	062406	00-00.2119 S	164-59.8413 E	24 June '99	05:26	520
	52	062409	00-00.3758 S	164-59.5024 E	24 June '99	08:31	250
	53	062412	00-00.4371 S	164-59.2411 E	24 June '99	11:29	520
	54	062415	00-00.2625 S	164-59.6540 E	24 June '99	14:30	250
	55	062418	00-00.6243 S	164-59.8114 E	24 June '99	17:26	520
	56	062421	00-00.7318 S	165-00.0400 E	24 June '99	20:29	250
	57	062500	00-00.2132 S	164-59.0042 E	24 June '99	23:26	1030
	58	062503	00-00.6017 S	165-00.2114 E	25 June '99	02:25	250
	59	062506	00-00.5328 S	164-59.4128 E	25 June '99	05:25	520
	60	062509	00-00.8572 S	164-59.6802 E	25 June '99	08:24	250
	61	062512	00-00.7301 S	164-59.8578 E	25 June '99	11:27	520
	62	062515	00-00.8734 S	165-00.0148 E	25 June '99	14:27	250

Leg	Cast No.	Cast name	Latitude	Longitude	Date (UTC)	Time (UTC)	Depth (m)
Phase 2	63	062518	00-00.9023 S	165-00.0074 E	25 June '99	17:29	520
	64	062521	00-00.9332 S	165-00.9590 E	25 June '99	20:24	250
	65	062600	00-00.9910 S	165-00.2830 E	25 June '99	23:25	1030
	66	062603	00-00.7430 S	164-59.8120 E	26 June '99	03:05	250
	67	062606	00-00.7690 S	164-59.6899 E	26 June '99	05:24	520
	68	062609	00-00.7835 S	164-59.7896 E	26 June '99	08:25	250
	69	062612	00-00.8167 S	164-59.8990 E	26 June '99	11:29	520
	70	062615	00-00.5661 S	164-59.7905E	26 June '99	14:34	250
	71	062618	00-00.4647 S	164-59.9137 E	26 June '99	17:28	520
	72	062621	00-00.5830 S	164-59.7832 E	26 June '99	20:26	250
	73	062700	00-00.7164 S	164-59.9228 E	26 June '99	23:23	1030
	74	062703	00-00.7063 S	164-59.8547 E	27 June '99	02:24	250
	75	062706	00-00.6607 S	164-59.7854 E	27 June '99	05:23	520
	76	062709	00-00.6090 S	164-59.4147 E	27 June '99	08:24	250
	77	062712	00-00.7342 S	164-59.4940 E	27 June '99	11:25	520
	78	062715	00-00.8763 S	165-00.1578 E	27 June '99	14:25	250
	79	062718	00-00.5383 S	165-00.0260 E	27 June '99	17:29	520
	80	062721	00-00.5481 S	164-59.7705 E	27 June '99	20:26	250
	81	062800	00-00.7196 S	164-59.9560 E	27 June '99	23:24	1030
	82	062803	00-00.6201 S	164-59.9489 E	28 June '99	02:27	250
	83	062806	00-00.7920 S	164-59.7930 E	28 June '99	05:23	520
	84	062809	00-00.6300 S	164-59.6554 E	28 June '99	08:23	250
	85	062812	00-00.7880 S	164-59.6548 E	28 June '99	11:28	520
	86	062815	00-00.7158 S	165-00.0328 E	28 June '99	14:34	250
	87	062818	00-00.5095 S	164-59.1089 E	28 June '99	17:29	520
	88	062821	00-00.5210 S	164-59.8457 E	28 June '99	20:24	250
	89	062900	00-00.6837 S	164-59.8633 E	28 June '99	23:24	1030
	90	062903	00-00.3214 S	164-59.1265 E	29 June '99	02:44	250
	91	062906	00-00.4890 S	164-59.7225 E	29 June '99	05:23	520
	92	062909	00-00.4969 S	164-59.3112 E	29 June '99	08:24	250
	93	062912	00-00.4312 S	164-59.4872 E	29 June '99	11:23	520
	94	062915	00-00.5243 S	164-59.9817 E	29 June '99	14:25	250
	95	062918	00-00.4783 S	164-59.8345 E	29 June '99	17:28	520
	96	062921	00-00.3757 S	164-59.8943 E	29 June '99	20:25	250
	97	063000	00-00.4500 S	164-59.4838 E	29 June '99	23:24	1030
	98	063003	00-00.4532 S	164-59.9146 E	30 June '99	02:25	250
	99	063006	00-00.4977 S	165-00.3891 E	30 June '99	05:23	520
Phase 3	100	063021	00-10.8026 S	165-51.0381 E	30 June '99	20:22	250
	101	070100	00-10.8939 S	166-50.8357 E	30 June '99	23:23	1030
	102	070103	00-10.9551 S	166-50.7078 E	01 July '99	02:28	250
	103	070106	00-11.2073 S	166-50.1470 E	01 July '99	05:25	520
	104	070109	00-11.2749 S	166-50.1241 E	01 July '99	08:22	250
	105	070112	00-11.2456 S	166-49.8556 E	01 July '99	11:26	520
	106	070115	00-11.5874 S	166-49.6975 E	01 July '99	14:22	250
	107	070118	00-10.8928 S	166-50.9785 E	01 July '99	17:29	520
	108	070121	00-10.9601 S	166-51.0674 E	01 July '99	20:23	250
	109	070200	00-10.9305 S	166-51.3191 E	01 July '99	23:24	1030
	110	070203	00-10.9644 S	166-51.2270 E	02 July '99	02:26	250
	111	070206	00-10.9769 S	166-51.2797 E	02 July '99	05:24	520
	112	070209	00-10.8552 S	166-50.9955 E	02 July '99	08:25	250
	113	070212	00-10.8865 S	166-50.9437 E	02 July '99	11:24	520
	114	070215	00-10.8245 S	166-51.1425 E	02 July '99	14:25	250
	115	070218	00-10.8143 S	166-51.2127 E	02 July '99	17:29	520
	116	070221	00-10.9391 S	166-51.2133 E	02 July '99	20:23	250
	117	070300	00-11.0417 S	166-51.1056 E	02 July '99	23:34	1030
	118	070303	00-12.2448 S	166-53.2601 E	03 July '99	02:30	250
	119	070306	00-11.9034 S	166-52.1083 E	03 July '99	05:34	520
	120	070309	00-10.8678 S	166-51.1025 E	03 July '99	08:23	250
	121	070312	00-10.9405 S	166-50.9790 E	03 July '99	11:25	520
	122	070315	00-10.7683 S	166-51.0622 E	03 July '99	14:25	250
	123	070318	00-10.8119 S	166-51.7890 E	03 July '99	17:25	520
	124	070321	00-10.9118 S	166-51.2226 E	03 July '99	20:23	250
	125	070400	00-10.8335 S	166-51.1123 E	03 July '99	23:24	1030
	126	070403	00-10.7805 S	166-51.2238 E	04 July '99	02:15	250
	127	070406	00-10.9360 S	166-51.1064 E	04 July '99	05:23	520
	128	070409	00-10.8394 S	166-51.1652 E	04 July '99	08:23	250
	129	070412	00-10.8516 S	165-51.1485 E	04 July '99	11:27	520

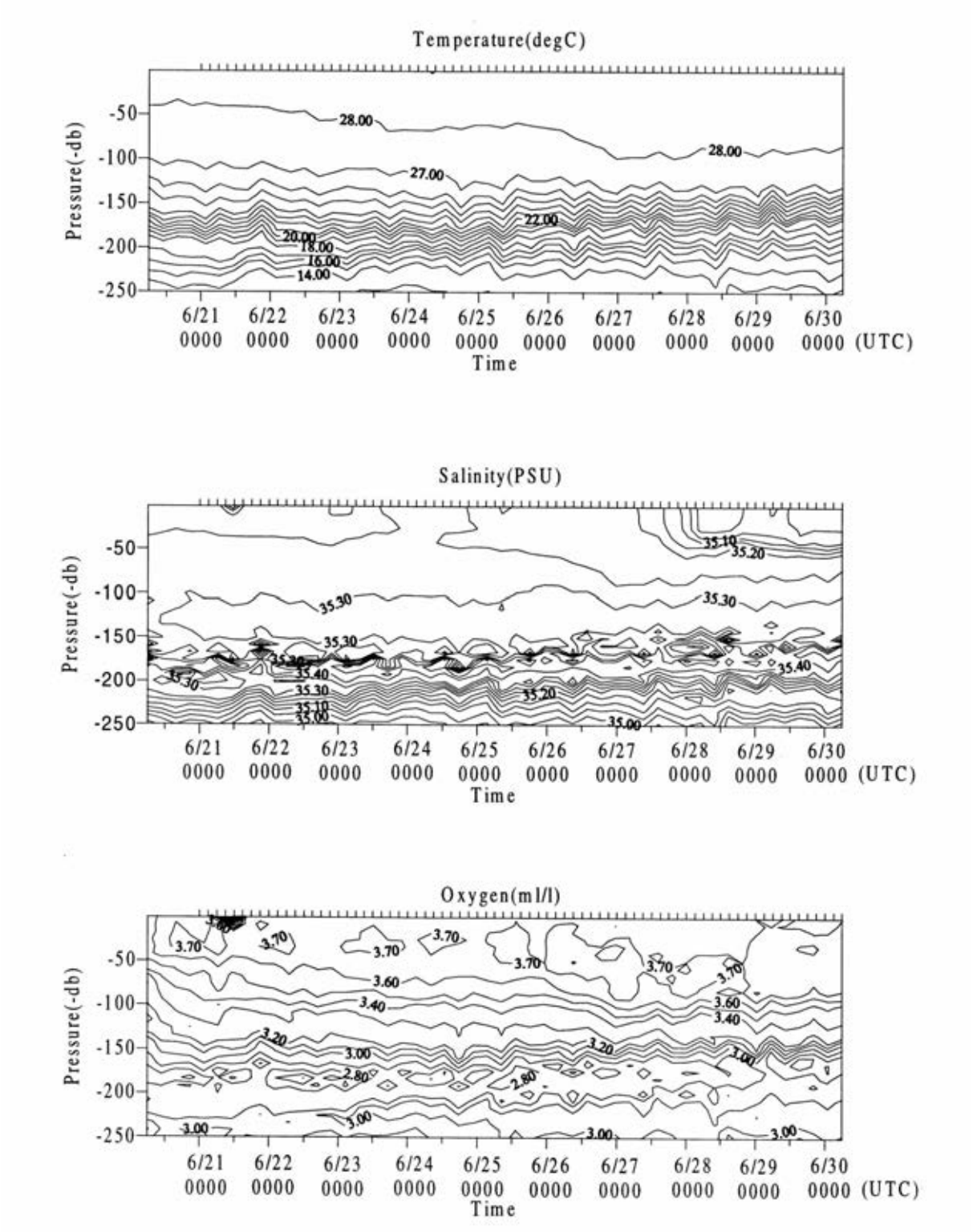

Fig. 7.1.1-1: Time-depth cross section of temperature, salinity and dissolved oxygen in phase 2 “Large Triangle”, for 0 – 250 m.

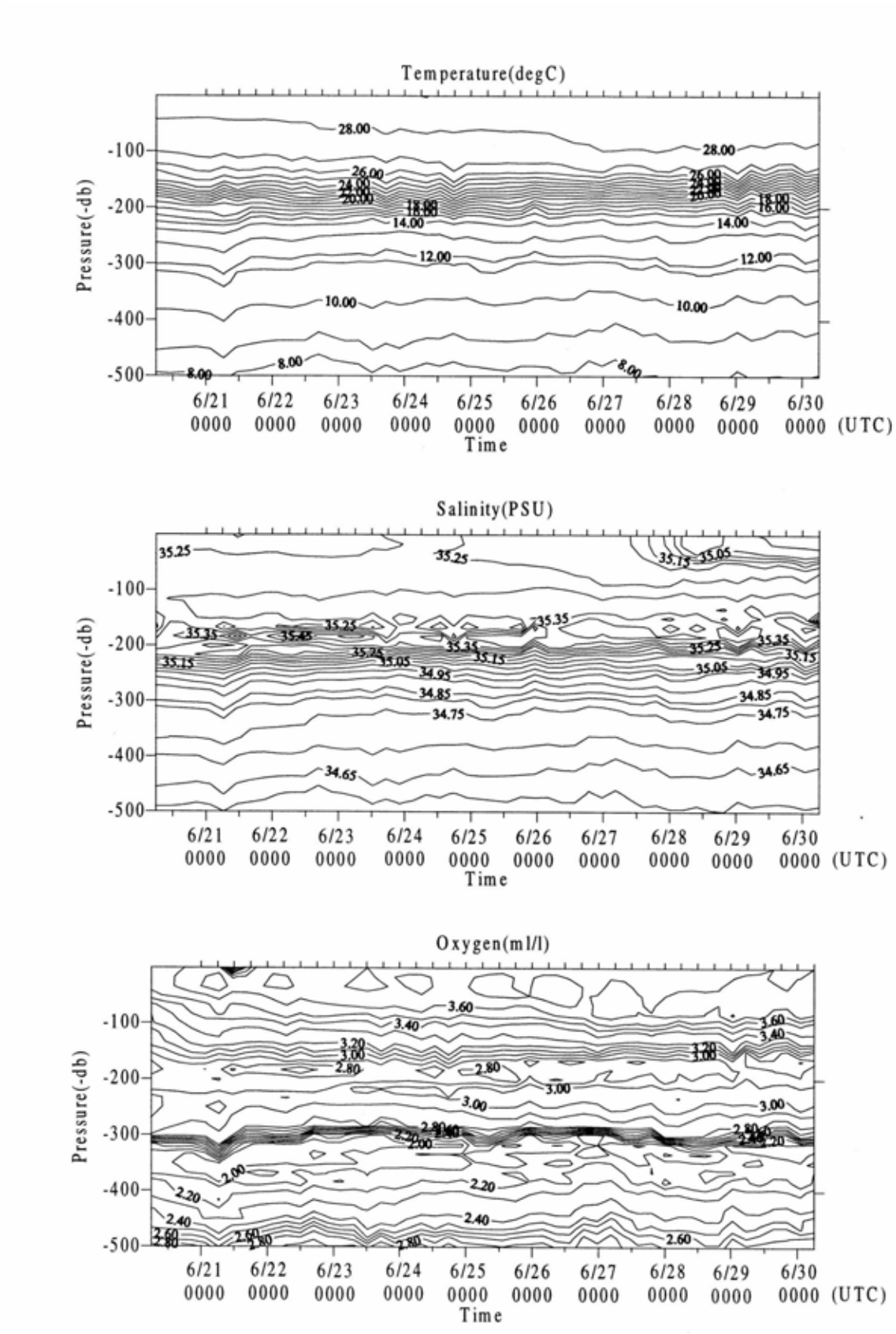

Fig. 7.1.1-2: Same as Fig. 7.1.1.-1, except for 0 – 500 m.

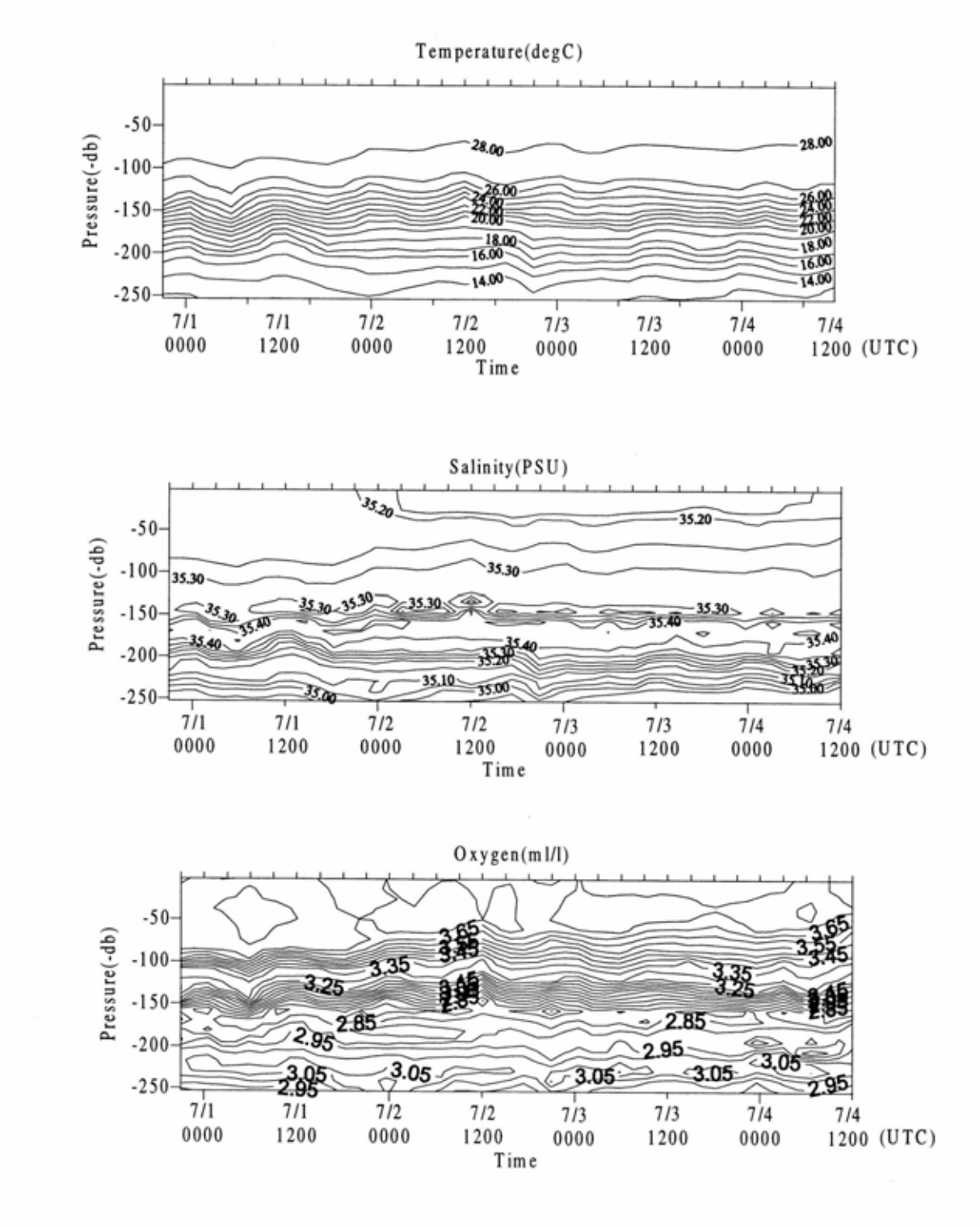

Fig. 7.1.1-3: Time-depth cross section of temperature, salinity and dissolved oxygen in phase 3 “Small Triangle”, for 0 – 250 m.

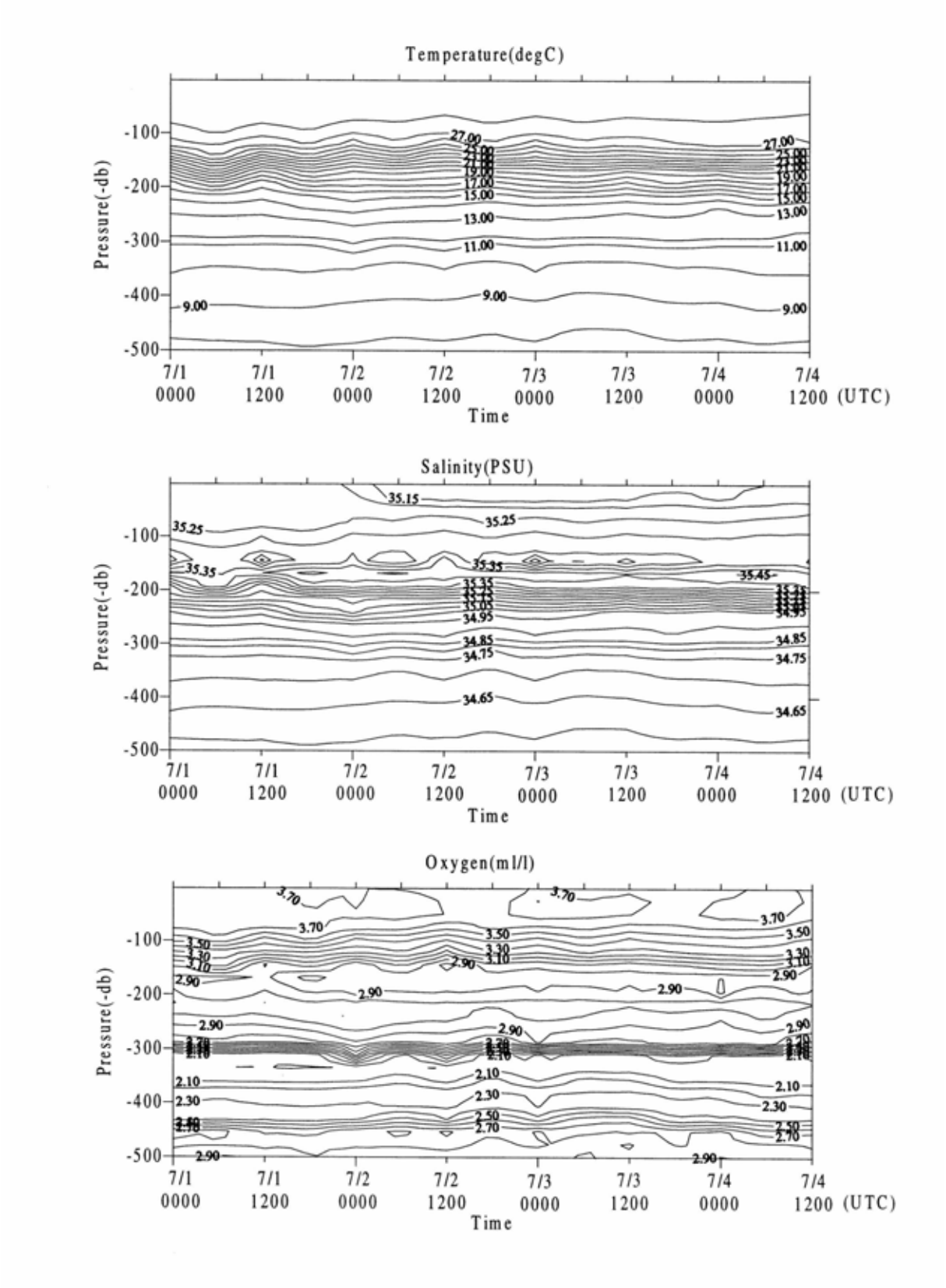

Fig. 7.1.1-4: Same as Fig. 7.1.1-3, except for 0 – 500 m.

7.1.2 Salinity and Sea Surface Temperature Measurements by Direct Water Sampling

(1) Personnel

Satoshi Ozawa (MWJ): Operation Leader
Shinichiro Yokogawa (MWJ)
Mizue Hirano (MWJ)

(2) Objectives

Calibration of the salinity data obtained by CTD.
Monitoring of the variation of Sea Surface Temperature (SST) and Salinity (SSS).

(3) Measured Parameters

Salinity of sea water at 250-m depth
Temperature and salinity of sea surface water

(4) Methods

Salinity was measured by a Guildline Autosal salinometer(model 8400B) with an Ocean Science International peristaltic-type sample intake pump and Hewlett Packard quartz thermometer(model 2804A) with two quartz probes(18111A). One probe measured at room temperature and another measured at a bath temperature. The resolution of the quartz thermometer was set to 0.001 ºC. Data of both the salinometer and the temperature was collected simultaneously by a personal computer. A double conductivity ratio was defined as median of 31 times readings of the salinometer. Data collection started after 5 seconds and it took about 10 seconds to collect 31 reading by a personal computer. We measured conductivity until they showed constant values.

The salinometer was operated in the air-conditioned ship's laboratory at bath temperature of 24ºC. Room temperature varied from approximately 24 ºC to 26 ºC, while a variation of bath temperature was almost within +/- 0.004 ºC.

1. Salinity Sample Bottles
   The salinity samples are collected and stored in 250 ml brown glass bottles with screw caps.
2. Salinity Sample Collection and Temperature Equilibration
   Each bottle was rinsed twice with sample water and was filled to the shoulder of the bottle. Its cap was also thoroughly rinsed. Salinity samples were stored more than 24 hours in the same laboratory where the salinity measurement was done.
3. Standardization
   Autosal salinometer was standardized before and after sequence of measurements by use of IAPSO Standard Seawater batch P134 whose conductivity ratio was 0.99989.
4. Sub-Standard Seawater
   We also used deep-sea water filtered by pore size of 0.45 micrometer and stored in a 20 liter cubical made of polyethylene and stirred for at least 24 hours before measuring as sub-standard seawater. It was measured every 10 samples in order to check and correct the trend.

(5) Preliminary Results

The difference of salinity data (at 1000 db) between CTD and directly sampled water are shown in Table 7.1.2-1. The average of difference is 0.0036 PSU(CTD value is lower than that of direct sampling) with its standard deviation 0.0012 PSU. Note that maximum and minimum values of difference are not

used for the calculation of average(i.e. eleven points are used in this case).

The variation of SST and SSS are shown in Fig. 7.1.2-1.

Table 7.1.2-1: Difference of salinity data between CTD and sampled water

Cast No.	File Name	Depth(m)	Sal.(PSU)				Avg.	CTD Sal.	Difference
25	062100	1000	34.5516	34.5514			34.5515	34.5474	0.0041
33	062200	1000	34.5500	34.5484	34.5502		34.5501	34.5483	0.0018
41	062300	1000	34.5492	34.5490			34.5491	34.5474	0.0017
49	062400	1000	34.5492	34.5480	34.5490		34.5491	34.5463	0.0028
57	062500	1000	34.5486	34.5486			34.5486	34.5452	0.0034
73	062700	1000	34.5476	34.5457	34.5457		34.5457	34.5435	0.0022
81	062800	1000	34.5498	34.5492	34.5498		34.5498	34.5445	0.0053
89	062900	1000	34.5586	34.5574	34.5574		34.5574	34.5518	0.0056
97	063000	1000	34.5539	34.5543			34.5541	34.5520	0.0021
101	070100	1000	34.5590	34.5588			34.5589	34.5547	0.0042
109	070200	1000	34.6234	34.6234			34.6234	34.5467	0.0767
117	070300	1000	34.5529	34.5541	34.5533	34.5543	34.5542	34.5498	0.0044
125	070400	1000	34.5535	34.5539			34.5537	34.5495	0.0042

(6) Data archive

These data are stored on a magnetic optical disk which will be kept on Ocean Research Department in JAMSTEC.

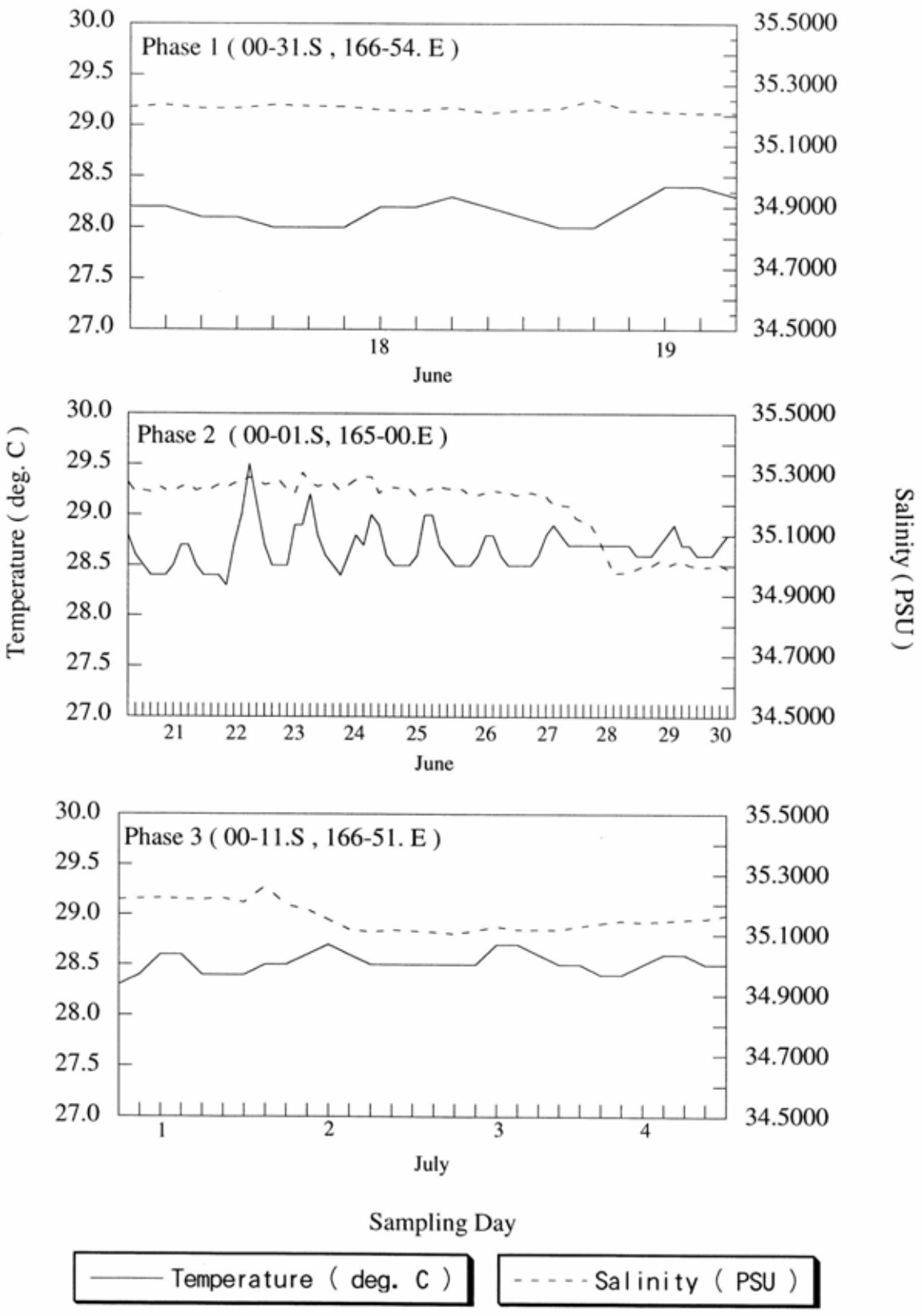

Fig. 7.1.2-1: Sea surface temperature and salinity, measured on the direct water sampling.

7.2 Sea Surface Water Monitoring

(1) Personnel

Shinichiro Yokogawa (MWJ): Operation leader

Katsunori Sagishima (MWJ)

(2) Objectives

Measuring sea surface temperature, salinity and dissolved oxygen along the ship's track using integrated monitoring system of surface seawater.

(3) Parameters

Temperature

Salinity

Dissolved oxygen

(4) Methods

This system can measure temperature, salinity and dissolved oxygen of surface water continuously in real time. It is located in the sea surface monitoring laboratory on this ship. Sea surface water was pumped up to the laboratory and flowed through a vinyl-chloride pipe. The flow rate was controlled by several valves.

This system is connected to shipboard LAN-system. Data was stored in a hard disk of computer every one minute.

The measurement is from 8 June, 1999 to 4 July, 1999. The flow rate of the system is checked everyday.

Specifications of the sensors were listed below.

a) Temperature and Salinity sensor

SEACAT THERMOSALINOGRAPH

Model: SBE-21, SEA-BIRD ELECTRONICS, INC.

Serial number: 2113117-2088

(Temperature sensor is first, Salinity is second)

Measurement range: -5 to +35 ℃, 0 to 6.5 S/m

Accuracy: 0.01 ℃/6month, 0.001 S/m/month

Resolution: 0.001℃, 0.0001S/m

b) Dissolved Oxygen sensor

Model: 2127, Oubisufair Laboratories Japan INC.

Serial number: 31757

Measurement range: 0 to 14 ppm

Accuracy: ±1 % at 5 ℃of correction range

Stability: 1 %/month

c) Flow meter

Model: EMARG2W, Aichi Watch Electronics LTD.

Serial number: 8672

Measurement range: 0 to 30 l/min

Accuracy: ±1 %

Stability: ±1 %/day

(5) Preliminary Results

Preliminary data along the ship's track are shown in Figs. 7.2-1 ～ 7.2-4. They show the respective trend of temperature, salinity and dissolved oxygen distributions on the ship's track every 30 minutes. Fig. 7.2-1 is the graph between Yokohama and Chuuk. Fig.7.3-2 is the graph between Phase 1. Fig. 7.2-3 is the graph between Phase 2. Fig. 7.2-4 is the graph between the date in the following time is the data in devices maintenance between Phase 3.

(6) Data archive

The data were stored on a magnetic optical disk, which will be kept in Ocean Research Department, JAMSTEC.

(7) Other remarks

Note that the followings on the use of raw data.

1. The instruments are in maintenance for the following periods.

File name	Time(JST)	Time(UTC)
Da990619	6/19 17:27～20:59 (JST)	[6/19 08:27～11:59 (UTC)]
Da990620-1	6/20 06:31～16:29 (JST)	[6/19 21:31～6/20 07:29 (UTC)]
Da990623-2	6/23 05:34～18:59 (JST)	[6/23 15:54～18:59 (UTC)]

2. The header in the raw data is Japanese notation. English notation example is written to Reading example File.

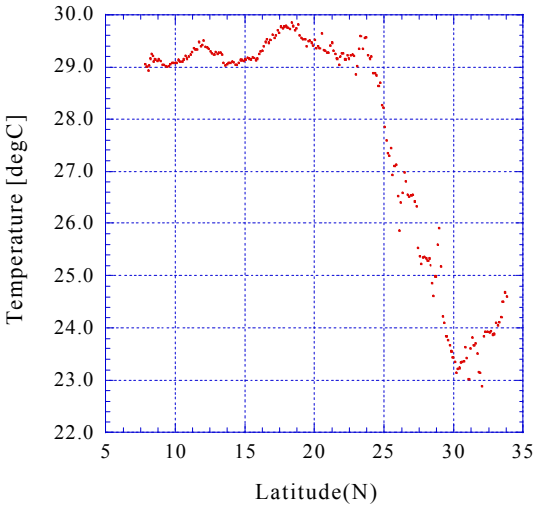

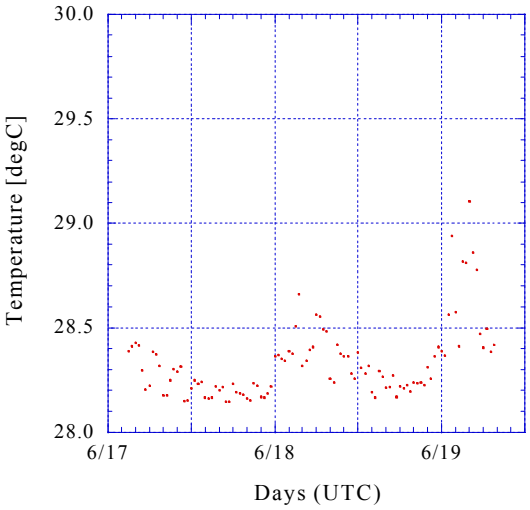

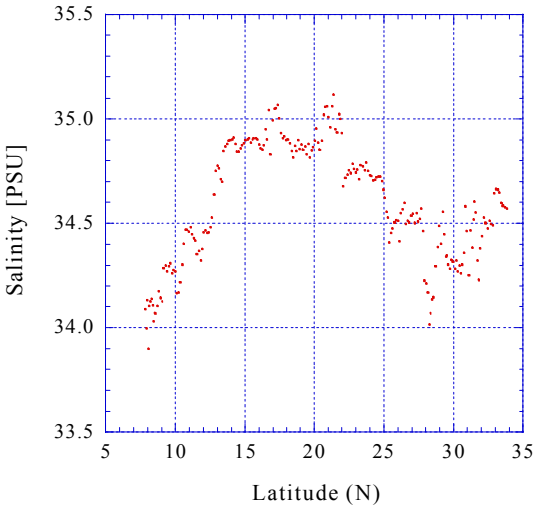

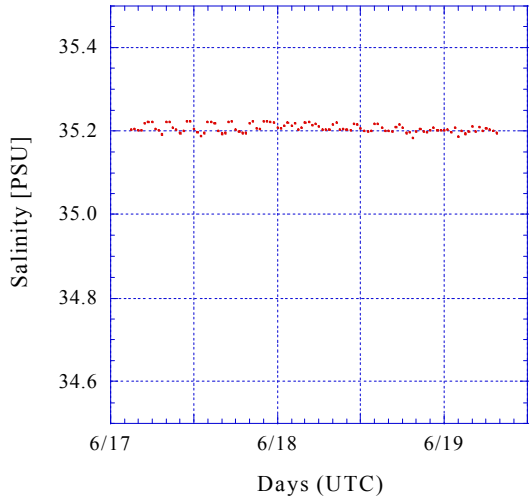

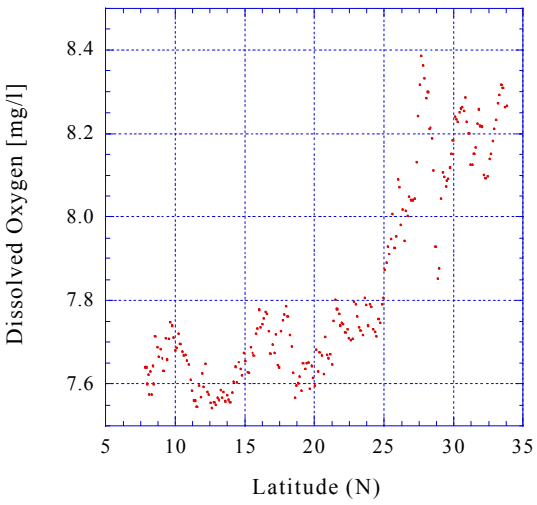

Fig7.2-1: Latitudinal distribution of sea surface temperature, salinity, and dissolved oxygen from Yokohama to Chuuk.

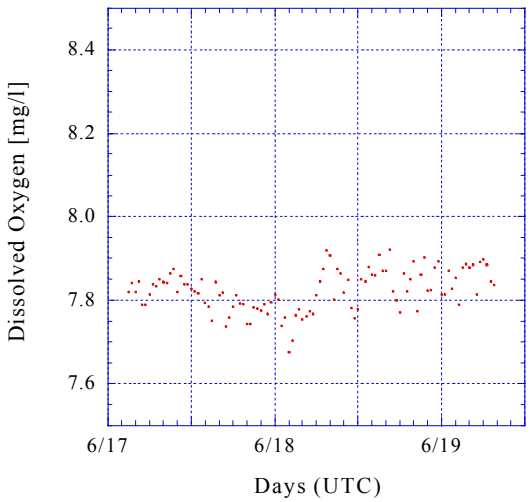

Fig7.2-2: Temporal variation of sea surface temperature, salinity, and dissolved oxygen at phase 1.

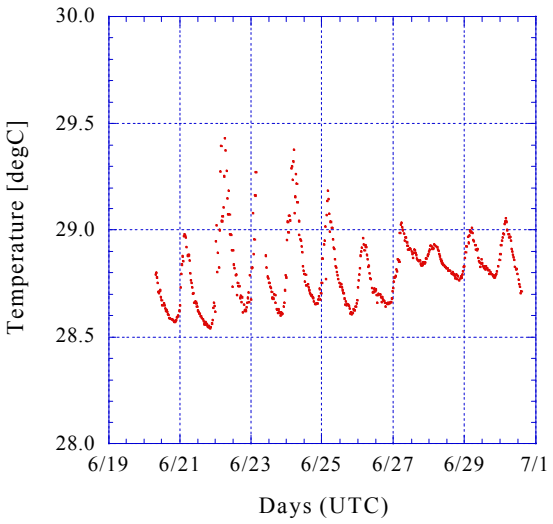

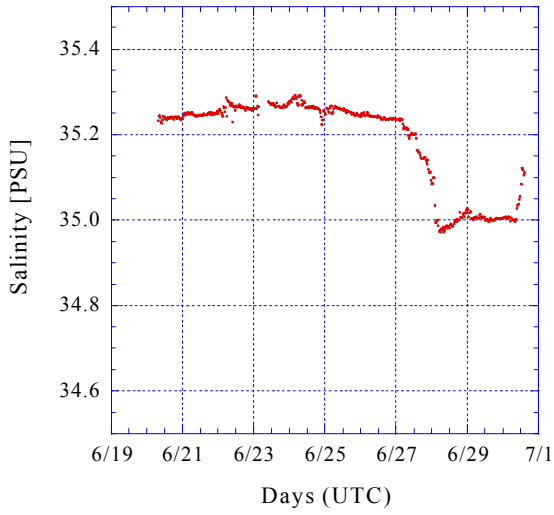

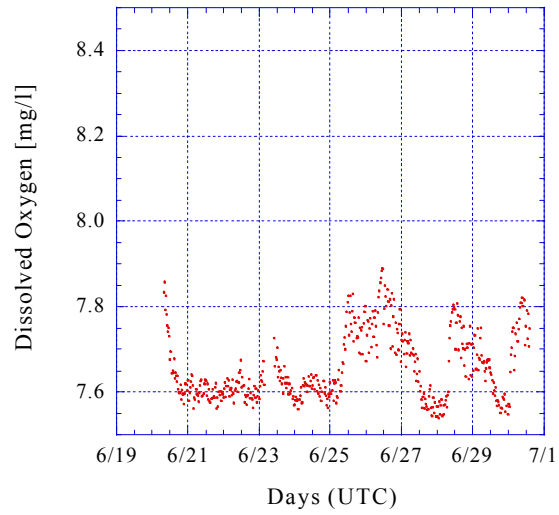

Fig7.2-3: Temporal variation of sea surface temperature, salinity, and dissolved oxygen at phase2.

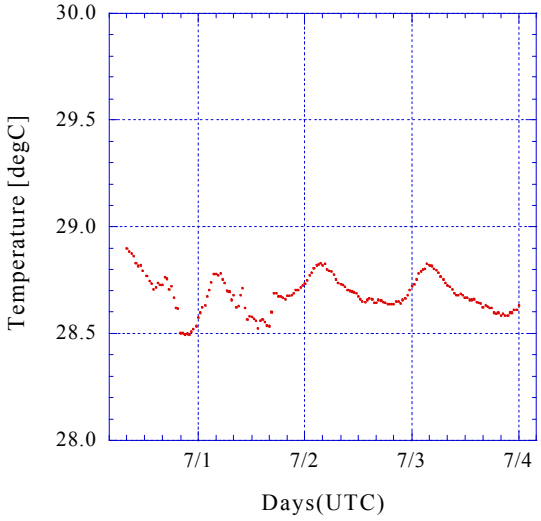

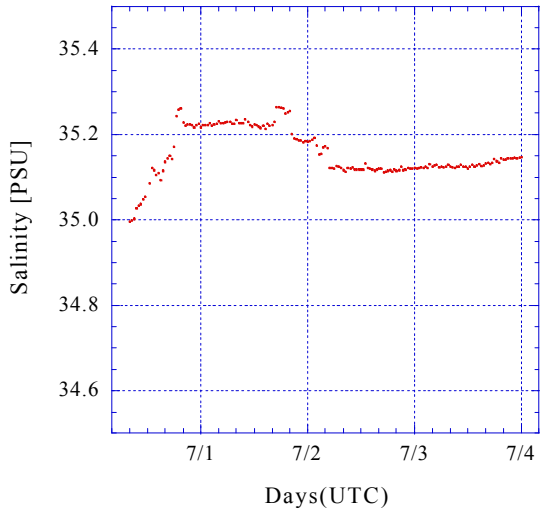

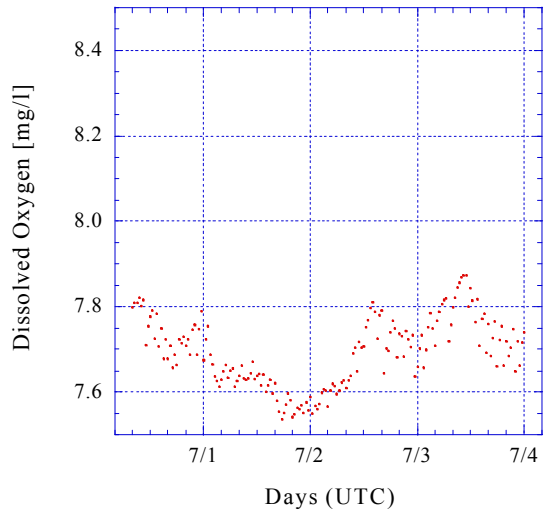

Fig.7.2-4: Temporal variation of sea surface temperature, salinity, and dissolved oxygen at phase 3.

7.3 CO2/pCO2 Measurement

7.3.1 MRI method

(1) Personnel

Mikio Kitada (MWJ)

(2) Objectives

Continuous measurement of partial pressure of CO_2 in the atmosphere and surface sea water .

(3) Measured Parameters

Carbon dioxide in the atmosphere (PCO_2)

Carbon dioxide in the seawater (pCO_2)

(4) Methods

Concentrations of CO_2 in the atmosphere and the sea surface were measured continuously during the entire cruise by the automated system with a non-dispersive infrared (IR) analyzer (BINOS 4.1 S/N 20309801017). It runs on one and half-hourly cycle during which four standards, an ambient air sample, and a head space sample from the equilibrator were analyzed.

The ambient air sample taken from the bow is introduced into the IR through a mass flow controller which controls the air flow rate at about 0.5 L/min, a cooling unit, a parma pure dryer, and a desiccant holder ($Mg(ClO_4)_2$).

The equilibrator has shower head space in the top through which surface water is forced at a rate of 5-8 L/min. Air in the head space is circulated with an air pump at 0.5-0.8 L/min in a closed loop through two cooling units, a perma pure dryer, and the desiccant holder.

For calibration, compressed gas standards with nominal mixing ratios of 264,320,348,395ppmv (parts per millions by volume) were used.

(5) Preliminary Results

Distribution of PCO_2 and pCO_2 from Yokohama to Chuuk are shown in Fig.7.3-1.

Variation of PCO_2 and pCO_2 at Phase-1 to 3 are shown in Fig.7.3-2 to Fig.7.3-4.

(6) Data Archives

The datasets are stored on a magnet optical disks which will be kept on Ocean Research Department, JAMSTEC.

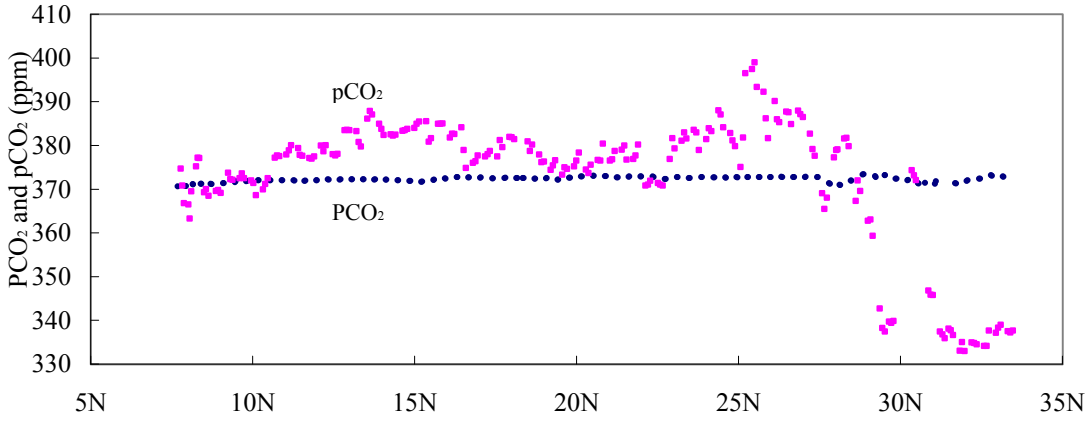

Fig.7.3.1-1: Latitudinal distribution of PCO2 and pCO2 from Yokohama to Chuuk.

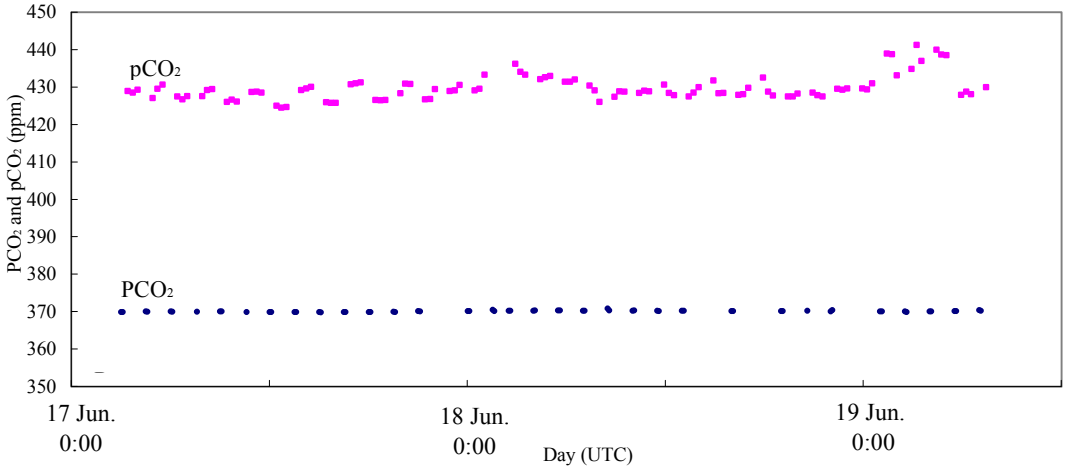

Fig.7.3.1-2 Temporal variation of PCO2 and pCO2 on Phase 1.

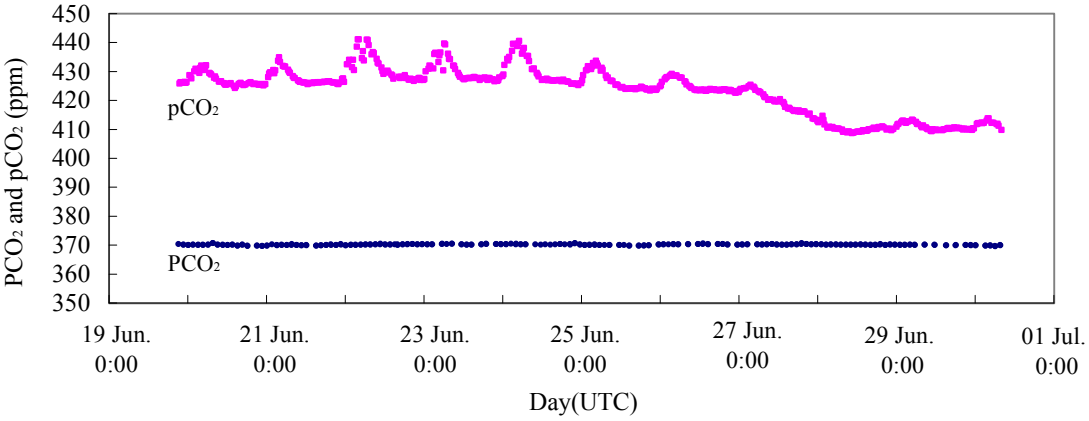

Fig.7.3.1-3 Temporal variation of PCO_2 and pCO_2 on Phase 2.

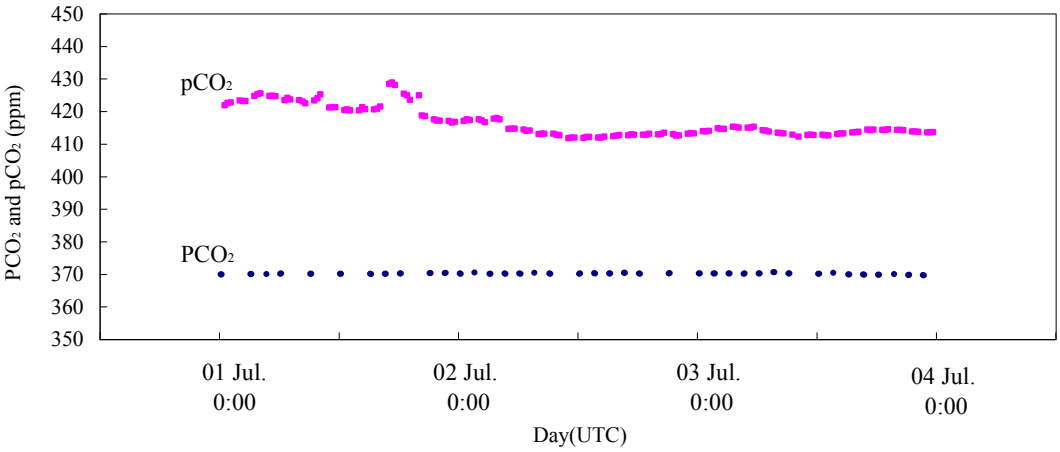

Fig.7.3.1-4 Temporal variation of PCO_2 and pCO_2

7.3.2 Okayama University of Science Group Method

(1) Personnel

Eiji Yamashita (Okayama University of Science): Principle Investigator
Takehiko Kono (Okayama University)
Naoki Nakatani (Osaka Prefecture University)

(2) Objectives

Latitudinal distribution of pCO2 and PCO2 during Yokohama to equatorial station
Vertical distribution of pCO2 at equatorial station
Diurnal variation of pCO2 at equatorial station

(3) Measured Parameters

Carbon dioxide in the sea water (pCO2)
Carbon dioxide in the atmosphere (PCO2)

(4) Methods

Carbon dioxide in the sea water and carbon dioxide in the atmosphere were measured using the measurement system which is made by the S-ONE company.

This system can measure carbon dioxide in the sea water and carbon dioxide in the atmosphere every 30 minutes and can measure carbon dioxide in the sea water only 500 ml seawater sample.

It located in the sea surface laboratory on this ship.

Sea surface water was pumped up to the laboratory and deep sea water was obtained by CTD-RMT sea water sampling system. Sample air was introduced from foremast. We had measured from 9 June, 1999 to 2 July, 1999. We checked the system everyday.

Specification of the carbon dioxide measurement system was listed below.

Unit 1: CO2 analyzer
Model: LI-6252 LI-COR ,INC.
Serial number: IR-62-286
Measurement range: 0-5V
Unit 2: Gas mixing unit
Model: SO96NL-T, S-ONE, INC.
Unit 3: Equilibrumeter
Model: SO96NL-T, S-ONE, INC.
Unit 4: Data processing equipment (Personal computer)

(5) Preliminary Results

Latitudinal distribution of pCO2 and PCO2 during Yokohama to Chuuk from 9 June to 19 June, 1999, is shown in Fig .7.3.2-1. The pCO2 concentration was from 335.7 to 398.9 ppmv in the ocean. The PCO2 concentration was from 366.7 to 373.4 ppmv in the atmosphere. The pCO2 concentration is higher than PCO2 from 32.41N to 28.35N, from 28.21N to 23.06N, from 13.51N to 12.25N and 7.27N (Chuuk island) . Then, the pCO2 concentration is higher than PCO2 from 4.33N to equatorial station (00.00S, 165.00E).

Fig .7.3.2-2 shows vertical distribution of pCO2, DO and pH in seawater on June 21, 1999 at 00.00S, 165.00E station. It shows that the value of pCO2 became high when the water depth became deep and the value of DO and pH became lower when the water depth became deep.

Fig .7.3.2-3 shows diurnal variation of pCO2 from 26 June to 29 June, 1999, at 00S, 165E station. The raw pCO2 concentration shows that low value in nighttime and high value in daylight hours.

(6) Data archive

The raw data were stored on a magnetic optical disk which will be kept on Ocean Research Department, JAMSTEC. The raw data were corrected and will be published.

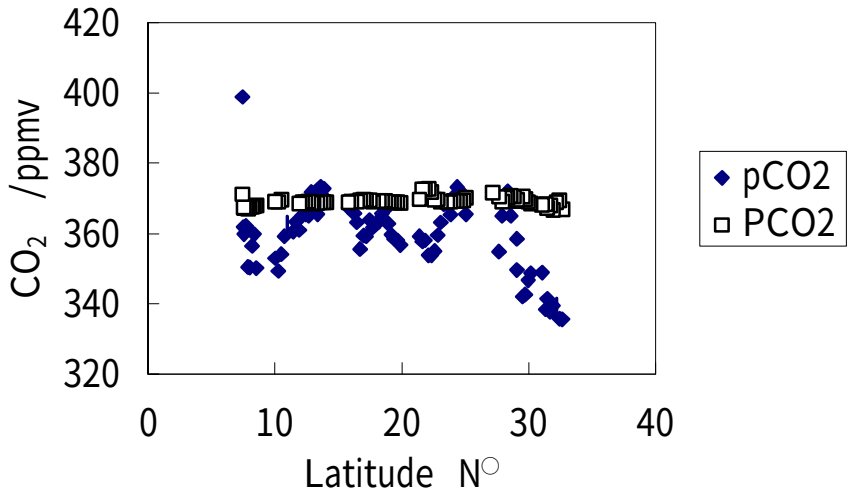

Fig .7.3.2-1: Latitudinal distribution of pCO2 and PCO2 during Yokohama to Chuuk, from 9 June to 19 June, 1999 .

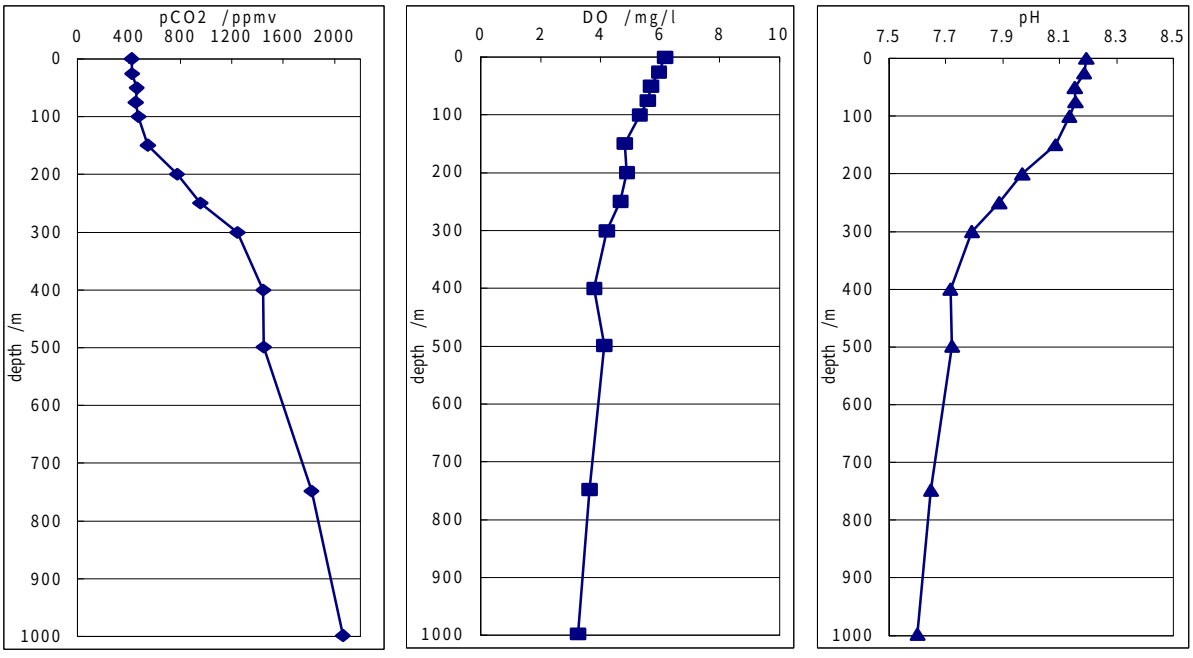

Fig .7.3.2-2: Vertical distribution of pCO2, DO and pH in seawater on 21 June, 1999 at equatorial station (0S, 165E).

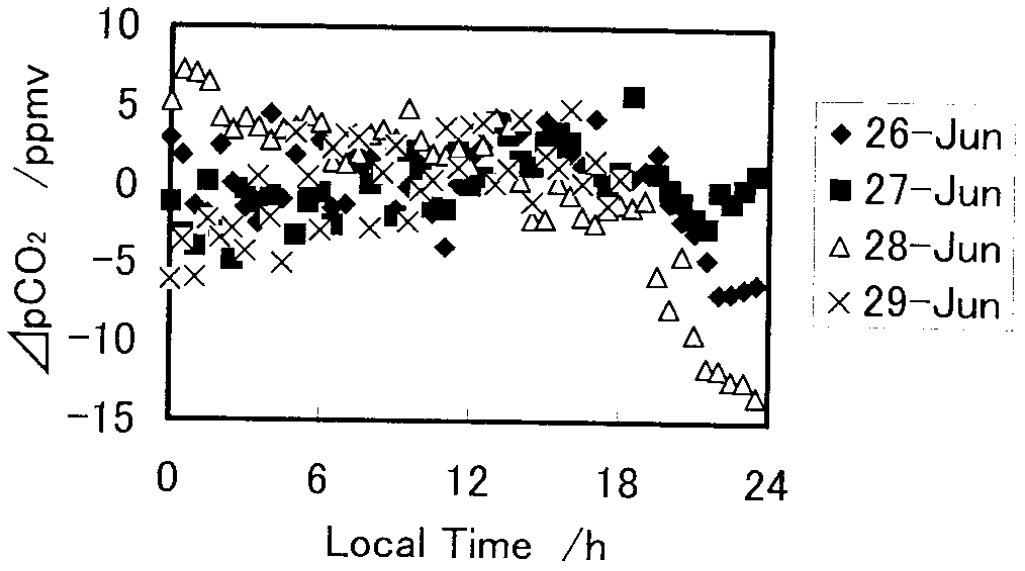

Fig .7.3.2-3: Diurnal variation of pCO2 from 26 June to 29 June, 1999 at equatorial station (00S, 165E). ⊿pCO2 is deviation from the average value on 1 day.

7.4 Greenhouse Effect Gasses (N2O / CH4) Measurement

(1) Personnel

Hiroshi Ishida (Maritime University of Kobe): Principle Investigator
Mitsuru Hayashi (Maritime University of Kobe)
Tomoko Iwamoto (Maritime University of Kobe)
Kazuyoshi Kikuchi (University of Tokyo)

(2) Objectives

N2O (Nitrous oxide) and CH4 (Methane) gasses play an important role and function of the global warming as well as CO2 (Carbon dioxide).It is required to get more accurate information of those gasses exchanges between the sea and atmosphere in order to understand the mechanism of the global warming process. The measurements of these gas densities in the atmosphere and sea water were made in the equatorial Western Pacific area for a about two weeks from 14 June to 5 July.

(3) Measured Parameters

N2O density in the atmosphere and sea water
CH4 density in the atmosphere and sea water

(4) Methods

The sample air was intaken at the foremast about 11m height above the sea level, and surface sea water was intaken at about 5-m depth.

N2O / CH4 densities in the atmosphere were measured using N2O / CH4 analyzer. N2O / CH4 densities in sea water were obtained by the babbling method.

Specification of analyzer is as follows;

N2O analyzer
MODEL: 46C (Thermo Environmental Instruments Inc.)
Accuracy: 2 % of full scale < 50 ppm (using 1ppm scale)

CH4 analyzer
MODEL: APHA-360 (HORIBA Ltd.)
Accuracy: 1.0 % of full scale (using 5ppm scale)

(5) Preliminary Results

The three-hourly time series of N2O densities in the atmosphere and sea water during the phase-2 are shown in Fig 7.4-1. N2O density in sea water changed larger than that in the atmosphere. N2O density in sea water was higher than that in the atmosphere in daytime, and in night N2O density in sea water was about equal or lower than that in the atmosphere.

The data will be analyzed in detail later.

(6) Data archives

The data are archived in MO disks and will have a quality check in Maritime University of Kobe, and will be distributed to public later. The raw data is submitted to JAMSTEC DMO.

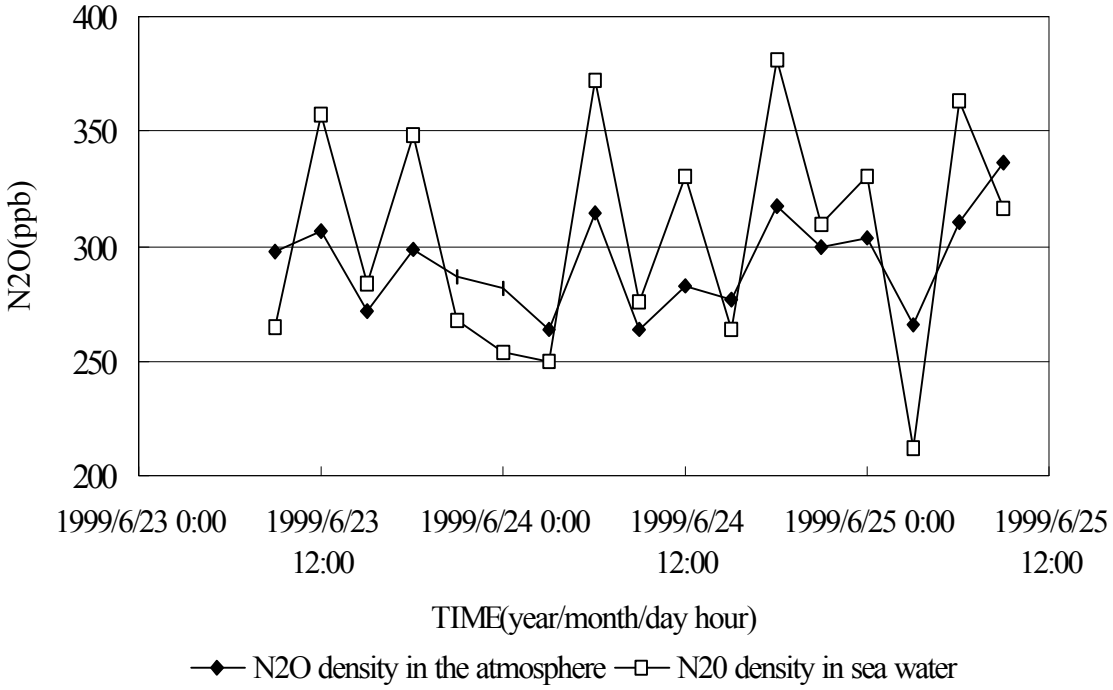

Fig 7.4-1: Three-hourly time series of N2O density in the atmosphere and sea water.

7.5 Shipboard ADCP

(1) Personnel

Masaki Hanyu (GODI) : Operation Leader
Kiyotake Kouzuma (GODI)
Fumitaka Yoshiura (GODI)
Satoshi Okumura (GODI)

(2) Objectives

The ocean current profiles are measured for the use of large fields of oceanography, as the basic dataset.

(3) Measured Parameters

N-S (North-South) and E-W (East-West) velocity components of each depth cell [cm/s]
Echo intensity of each depth cell [dB]

(4) Methods

We measured current profiles by VM-75 (RD Instruments, Inc. U.S.A.) shipboard ADCP (Acoustic Doppler Current Profiler) throughout MR99-K03 cruise from the departure of Yokohama, Japan on 8 June 1999 to the arrival of Sekinehama, Japan on 20 July 1999 via Chuuk, Majuro, Guam and Tsuruga.

Major parameters for the measurement configuration are as follows;

Frequency :	75 kHz
Averaging :	every 300 sec
Depth cell length :	1600 cm
No. of depth cells :	40
First depth cell position :	30.9 m
Last depth cell position :	654.9 m
Ping per ADCP raw data :	16

(5) Preliminary Results

Hourly current vectors of 2-hour running mean averaged data are plotted along the ship's track for 30.9m-layer (Fig.7.5-1) and 206.9m-layer (Fig.7.5-2) respectively. Fig.7.5-3, Fig.7.5-4 and Fig.7.5-5 show the vertical profiles during the IOP phase-1, phase-2 and phase-3 respectively.

(6) Data Archives

ADCP data obtained in this cruise will be submitted to the DMO (Data Management Office), JAMSTEC and will be under their control.

(7) Remarks

From 13 to 14 June, ADCP data was not recorded because of errors on the MO disk drive.

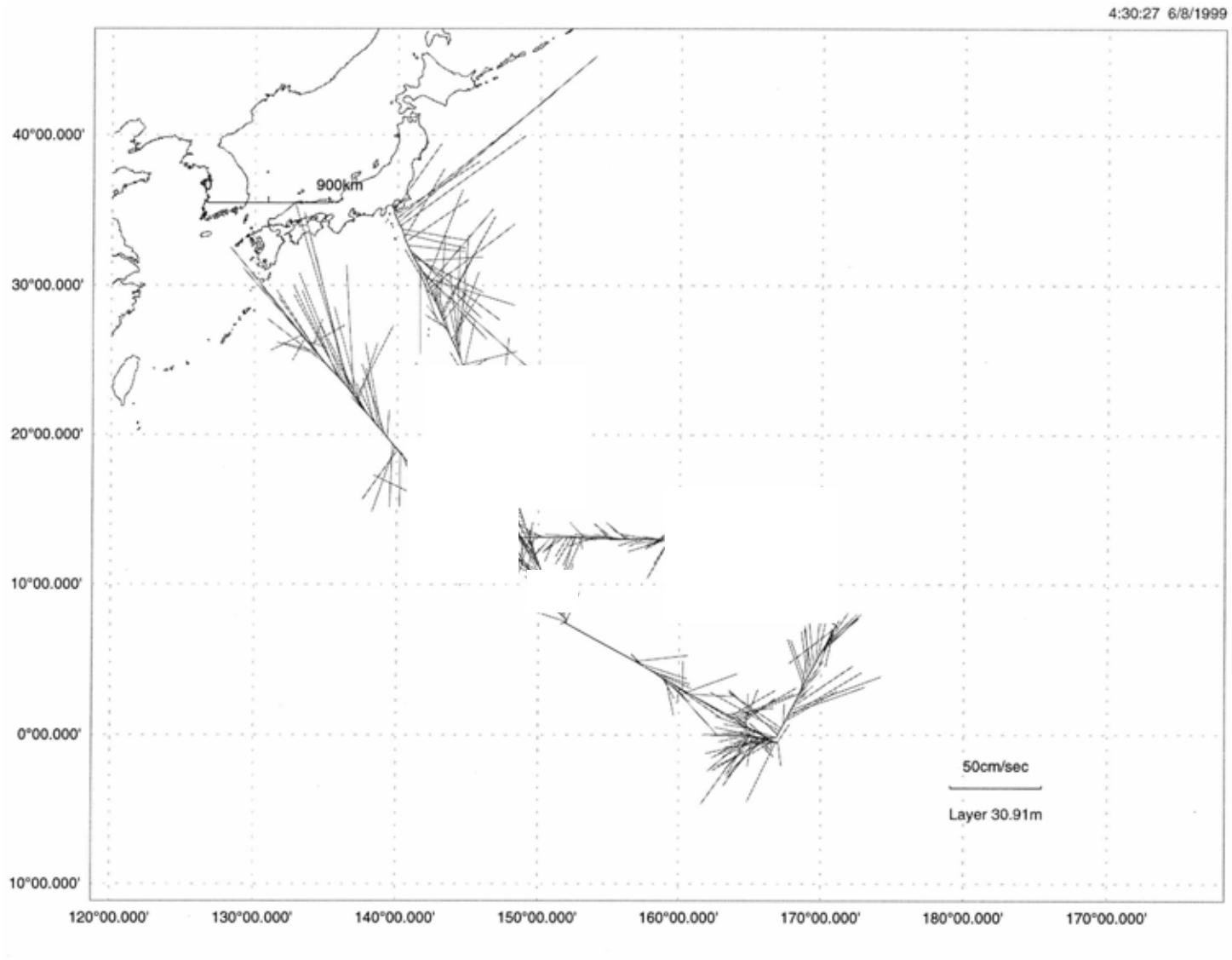

Fig. 7.5-1: Two hour averaged current vectors for every hour along the ship track, at 30-m depth.

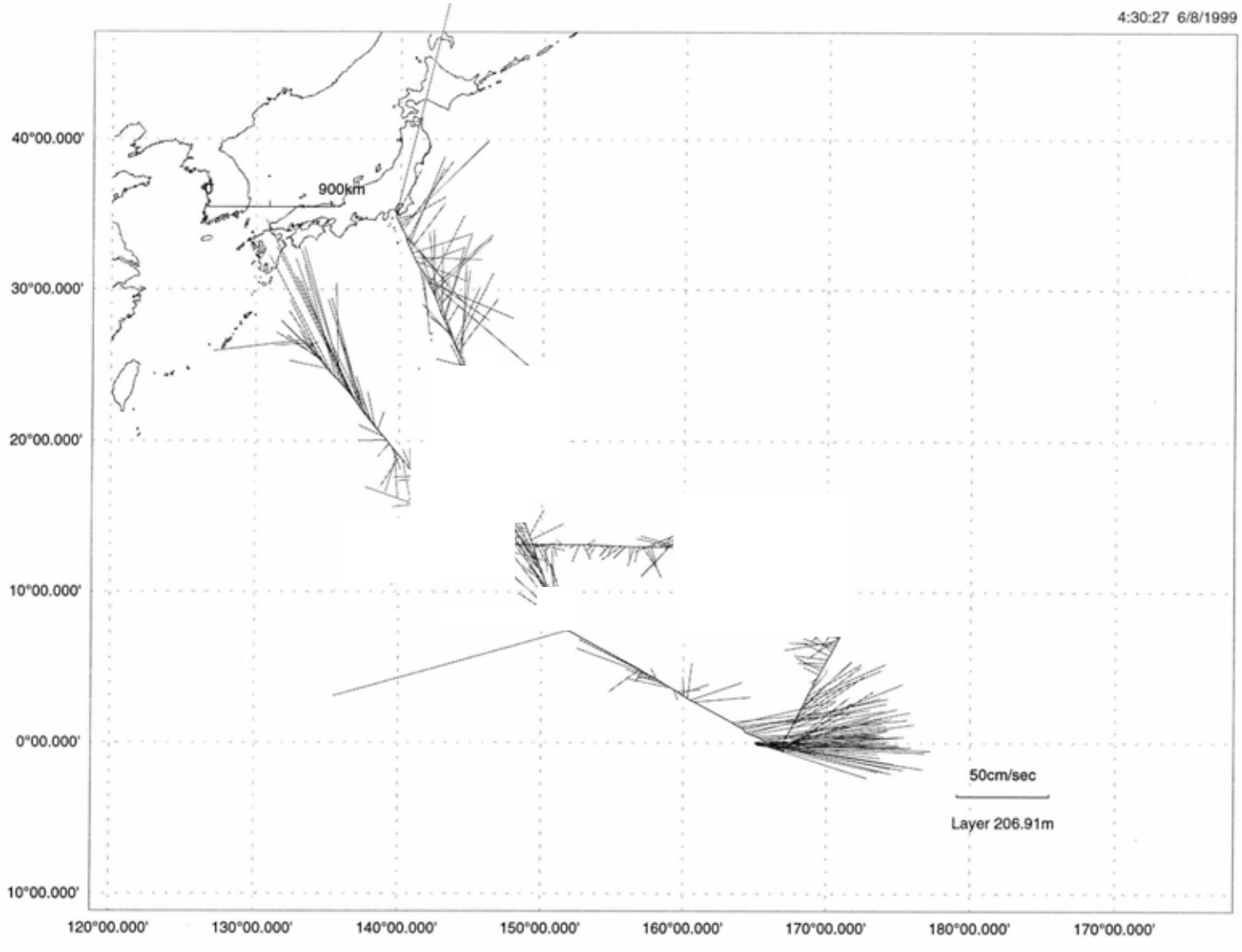

Fig. 7.5-2: Same as Fig.7.5-1, except at 207-m depth.

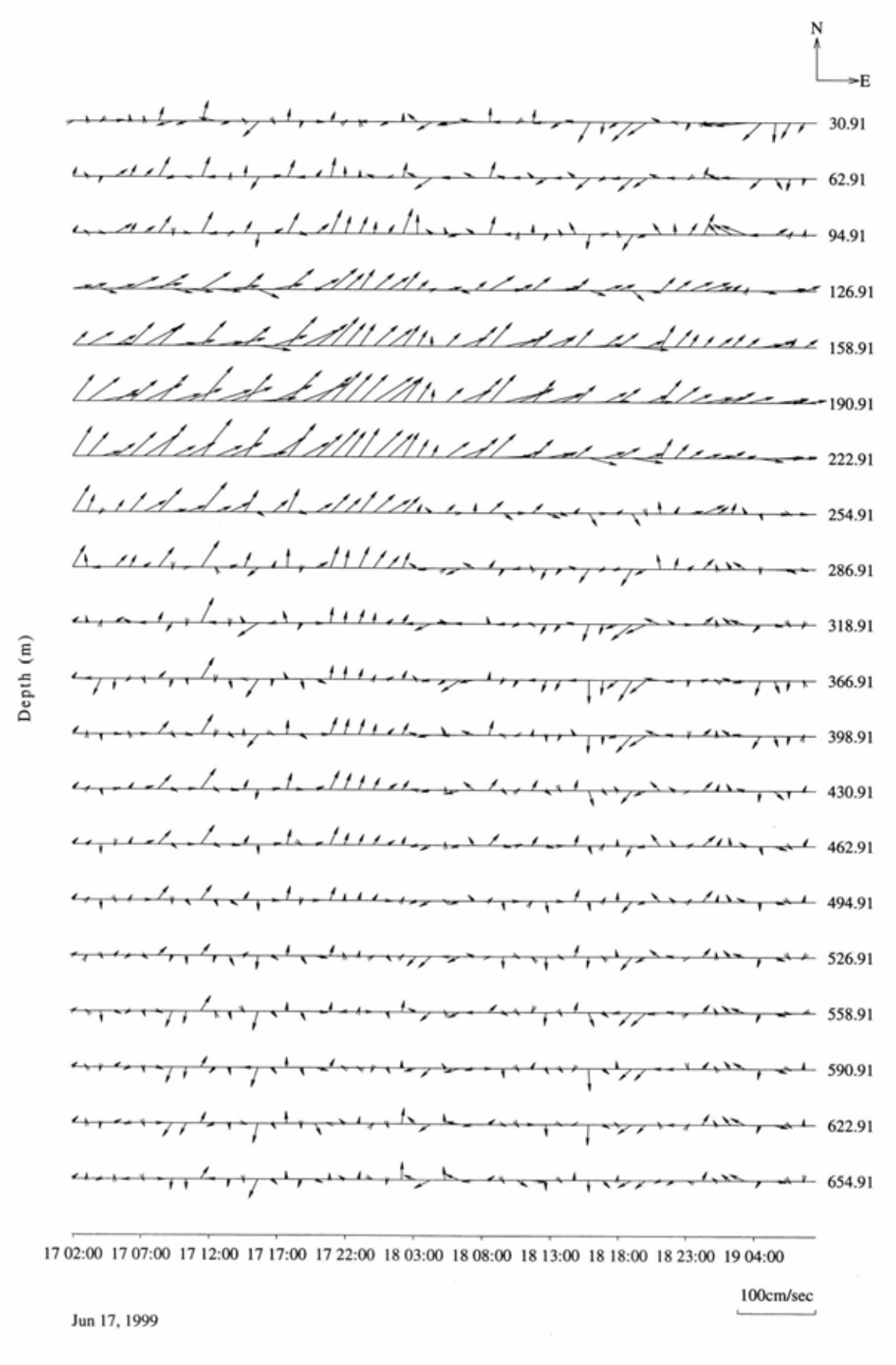

Fig. 7.5-3: Vertical profile of the current during IOP phase 1.

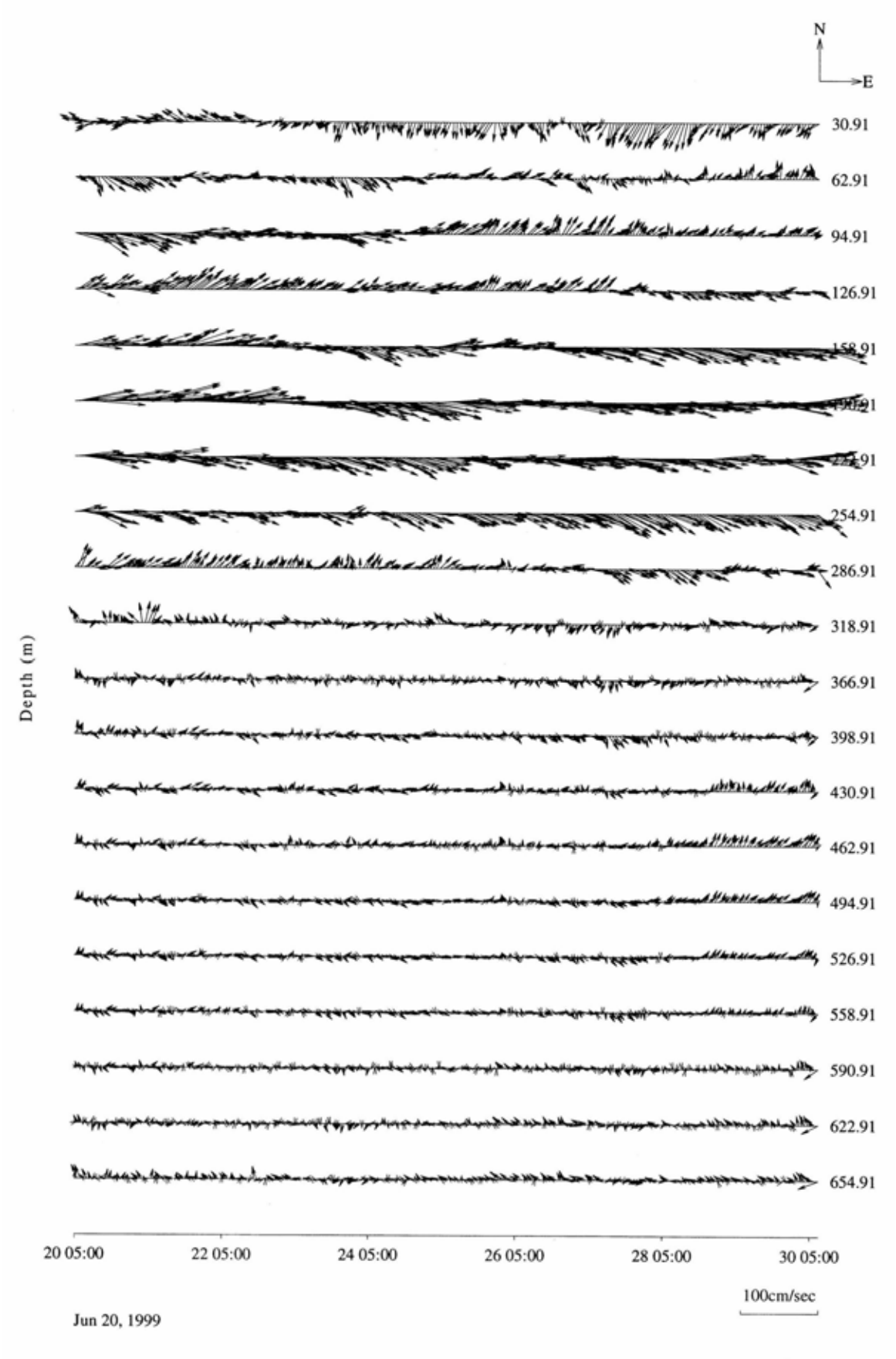

Fig. 7.5.4: Same as Fig. 7.5-3, except during IOP phase 2.

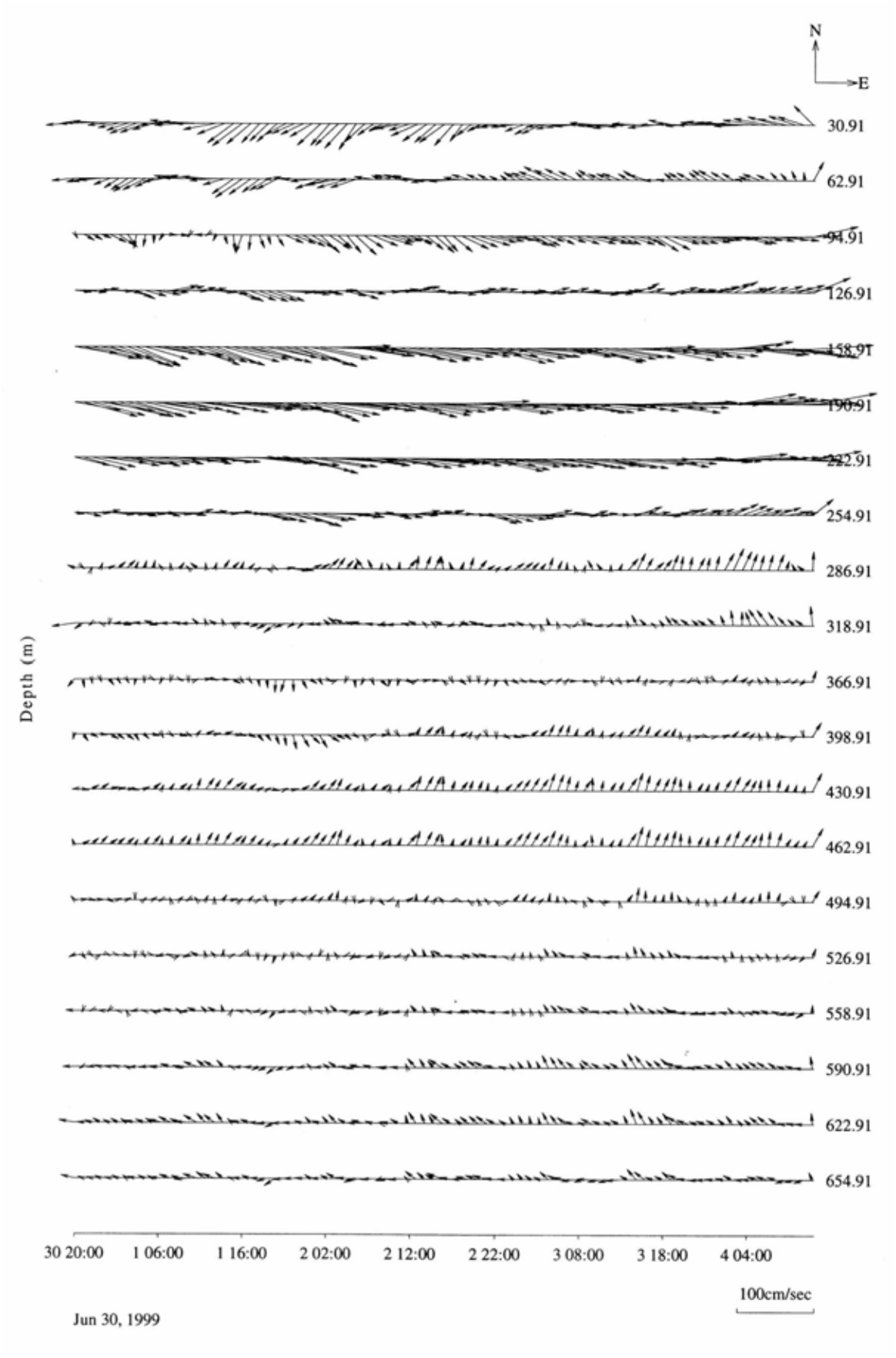

Fig. 7.5-5: Same as Fig. 7.5-3, except during IOP phase 3.

8. Underway Geophysical Observation

(1) Personnel

Masaki Hanyu (GODI) : Operation Leader
Satoshi Okumura (GODI)
Kiyotake Kouzuma (GODI)
Fumitaka Yoshiura (GODI)

(2) Objectives

The spatial and temporal variation of the parameters at / below the sea bottom, gravity, magnetic force or sea bottom depth, are basic data for the many fields of geophysics. However, the chance to measure these parameters by shipborne instruments is rare. The observation in this cruise is carried out to accumulate these data to fill the basic dataset for the geophysics.

(3) Measured Parameters

Gravity [mGal]
Magnetic force [nT]
Sea bottom depth [m]

(4) Methods

All of the observations are carried out for Japanese territorial sea, Japanese EEZ and the open seas.

The sea surface gravity was measured by S-116 (LaCoste-Romberg, U.S.A.) gravity meter. For the calibration, the shore side gravity was measured at Yokohama and Tsuruga using CG-3M (Scintrex) portable gravity meter. Table xx shows the results of these measurements.

The magnetic force was measured by 3-component magnetometer (Tera Technica, Japan) at the sampling rate of 8 Hz.

The bathymetry was measured by SeaBeam2100 (SeaBeam, U.S.A.) Multi Narrow Beam Echo Sounding System (MNBESS).

(5) Preliminary Results

The results will be public after the analyses.

(6) Data Archives

All dataset which obtained in this cruise will be submitted to the DMO (Data Management Office), JAMSTEC and will be under their control.

9. Ship Operations

(1) Personnel

Captain Masaharu Akamine: Master of R/V"MIRAI"

And Ship's Crew

(2) Objectives

The ship's maneuvering should be carried out so as to satisfy various conditions demanded for Observation Strategy in NAURU99 and so as to achieve ship operation in safety and in a time limit. The main condition of it is to make the ship hold at a fixed point. The ship's maneuvering of a fixed point observation is done on manual basis on getting hold of the ship's movement by finding the value of vector of wind and current. The observation of ship's position and external force such as wind and current is carried out for the ship's handling.

(3) Measured Parameters

- Ship's position, course, speed,
- Direction of wind and current, Velocity of wind and current,
- Vector of wind and current, resultant force.

(4) Methods

(A) Conditions

Following conditions demanded for the observation were given careful consideration to manage the ship.

1) The Phase 1 (June 17-19, Off Nauru)

① To keep ship's position within o.6 miles of ARCS (0-31.26S, 166-54.96E) in Nauru Island during the operations other than the Flux measurement operation.

② To keep more than 1 miles away from Nauru Island to avoid the influence of Island's Blocking in case of the Flux measurement operation.

2) The Phase 2 (June 20-30, Off TAO buoy)

① To keep ship's position within 2 miles of TAO buoy (0-00N, 165-00E) during the operations except the Flux measurement operation.

② To keep more than 0.3 miles away from TAO buoy to avoid blocking between ship and buoy.

3) The Phase 3 (July 1-4, Off Nauru Island)

To keep ship's position within 2miles of a fixed point (0-10.8S, 166-51.2E) during the operation except the Flux measurement operation.

4) Conditions of each observation are as follows.

A) Radiosonde Operation

① To keep ship's head so as to get the wind from the port bow (more than 30 degrees).

② To maintain ship's speed with the wind velocity of under 3 knots by relative scale.

B) CTD/Sampling Seawater Operation

① To stop ship at a fixed point.

② To manage ship's movement so as to lead the CTD cable right below.

③ Not to churn sea surface at CTD observation area with discharged currents from a right propeller and stern thruster.

C) Flux measurement Operation

① To set ship's course so as to face the wind.

② To maintain ship's speed of 2-3 knots by ground.

③ To set up ship's speed on the high side of ② in case of breeze condition.

④ To navigate for 1 hour from a point that ship's speed run up to the required figures.

⑤ To keep a initial speed/course of ship even if there is any change in the weather/ wind.

D) Sea Surface Temperature Float (Helmet sensor) Operation

① To keep ship's speed of 3 knots and under.

② To avoid jumping up of The SST Float away from sea surface due to violent wave.

(B) Typical pattern of ship's handling

A) Radiosode Operation (The time required: about 25 minutes)

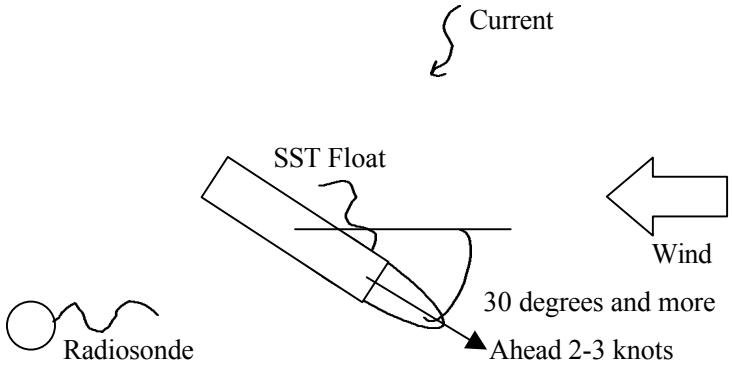

B) CTD/Sampling Seawater Operation (The time required: about 15 minutes)

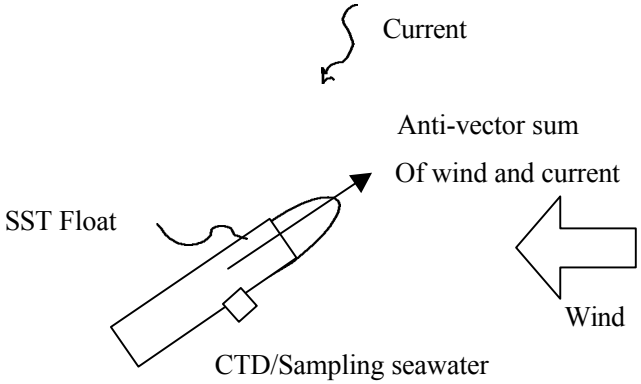

C) Flux Measurement Operation (The time required: about 60 minutes)

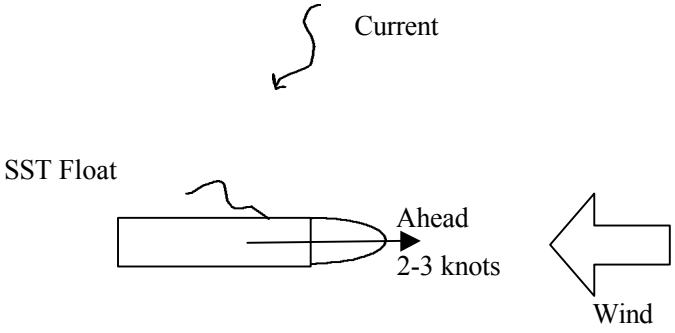

Return to the origin point after the flux measurement operation finished.

(The time required: about 60 minutes)

(C) Wind and Current

Data of Wind direction/speed were simultaneously measured by ship's LAN system (KOAC-7800 weather data processor and sensors assembled by Koshin Denki), Data of current direction/speed were continuously given by a Doppler sonar installed the bottom of the ship. Vector direction and speed was found by both data in real-time as follows.

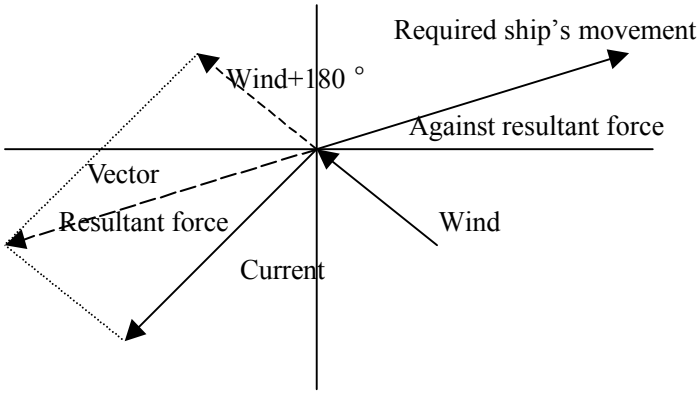

(5) Preliminary Results

All of the ship's position during CTD operations are in existence within required limits of each operation as indicated in Fig. 9-1, 9-2 and 9-3.

Her course and speed have to be adjusted so that the ship can stay in a fixed position under external forces i.e. wind and current. The adjustment of her course and speed is given by resultant force summed up vector value of wind and current. The difference between an actual ship's course and an anti-resultant force of wind / current vector is mostly less than 10 degrees (see Appendix). Accordingly the result shows that it was comparatively easy to handle the ship as the influence of external forces i.e. wind, current and wave was low. Meanwhile this means to be capable of a standard for setting ship's course in case the ship hold her position for the observation operation.

(6) Data archive

All data will be archived on board.

(7) Remarks

The above-mentioned standard is not finished yet because the quantity of drifting by the wind is incomplete for lack of the data. The data will be continuously accumulated through such observation voyage from now on.

As for the speed it is difficult to set a standard because the speed is required at all times in response to the ship's movement and a hanging angle of the CTD cable. This matter does not cause the ship's handling inconvenience particularly.

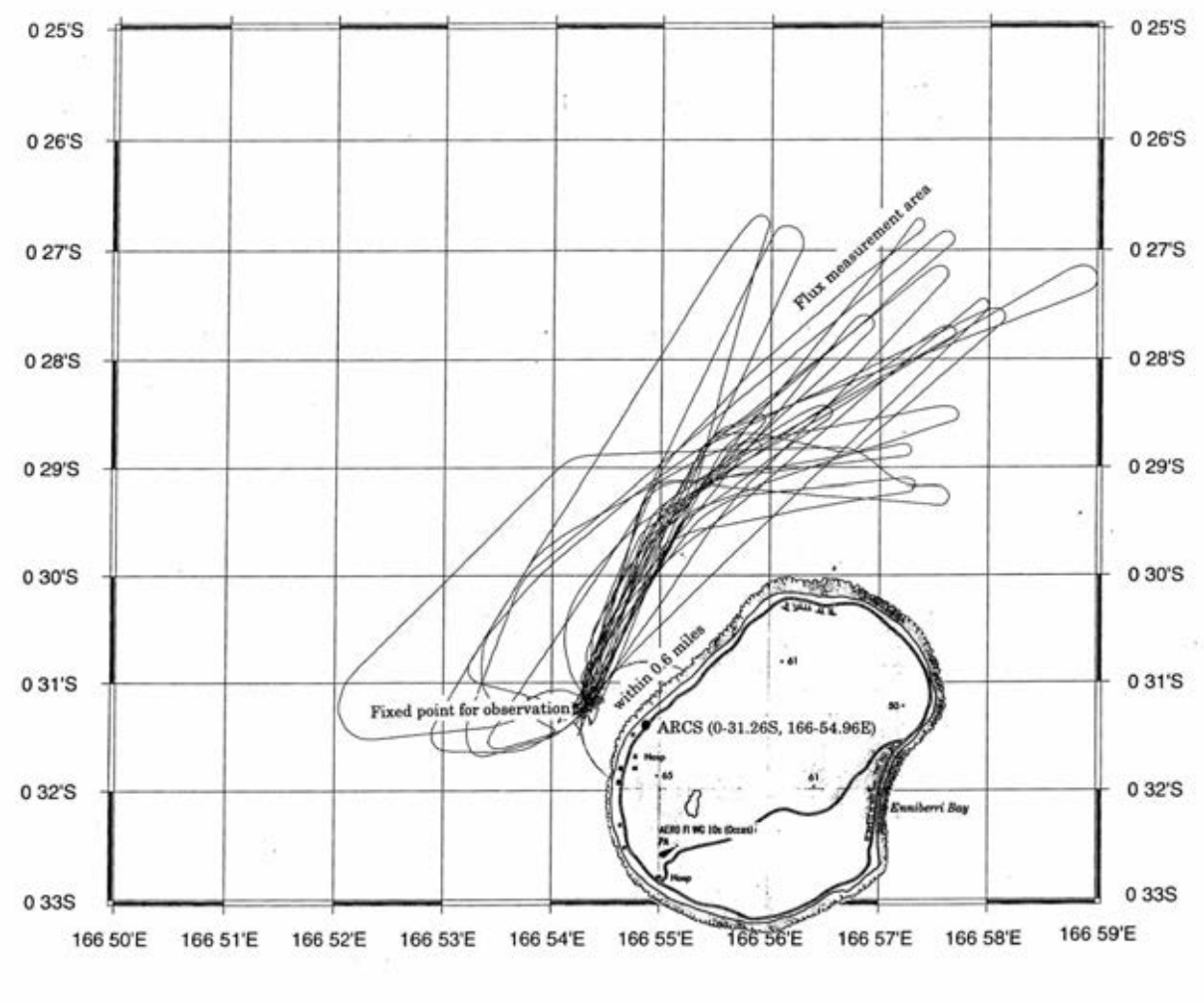

Fig. 9-1: Ship track in IOP phase 1.

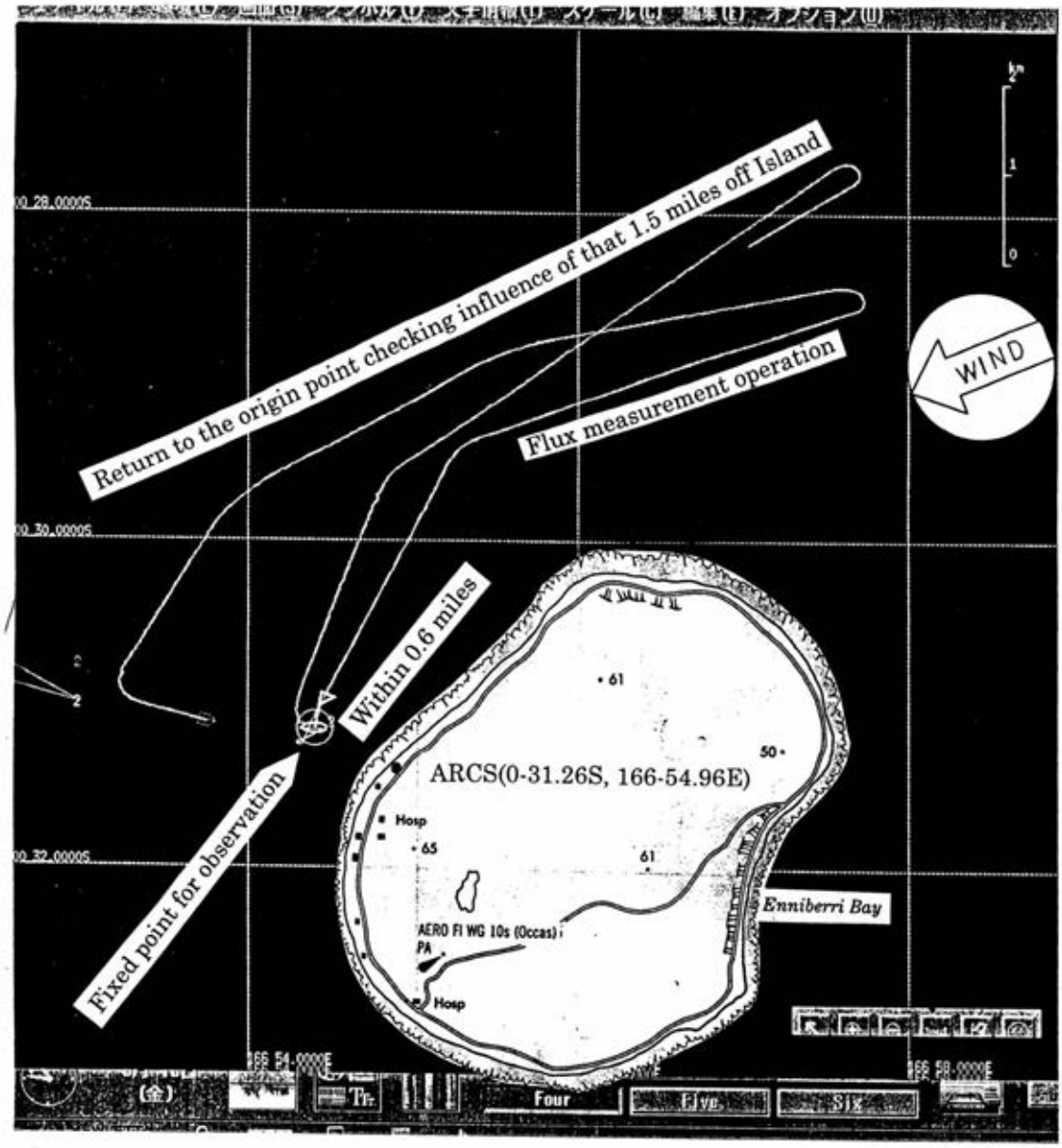

Fig. 9-2: Typical pattern of the operations off Nauru Island, in IOP phase 1.

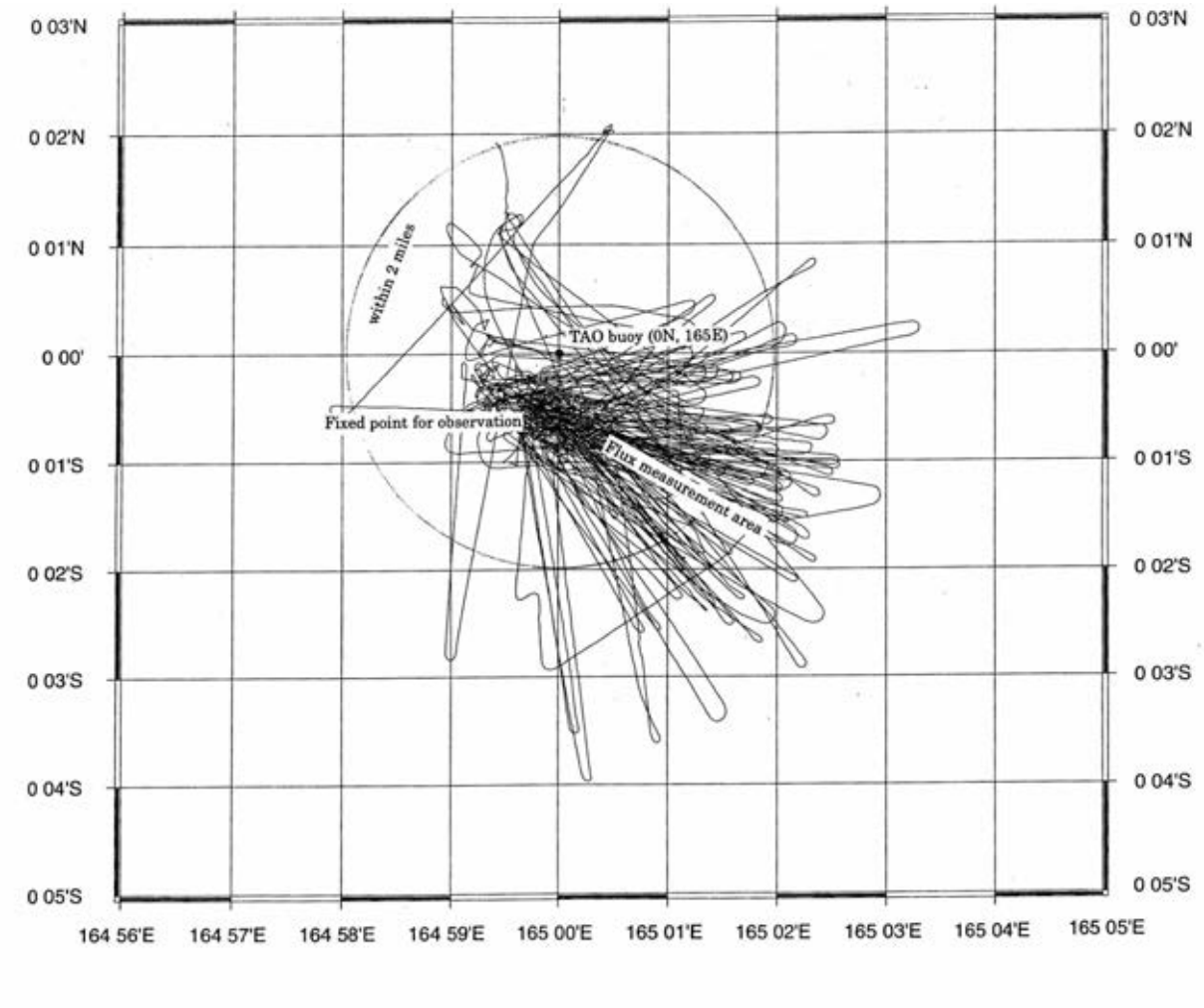

Fig. 9-3: Ship track in IOP phase 2.

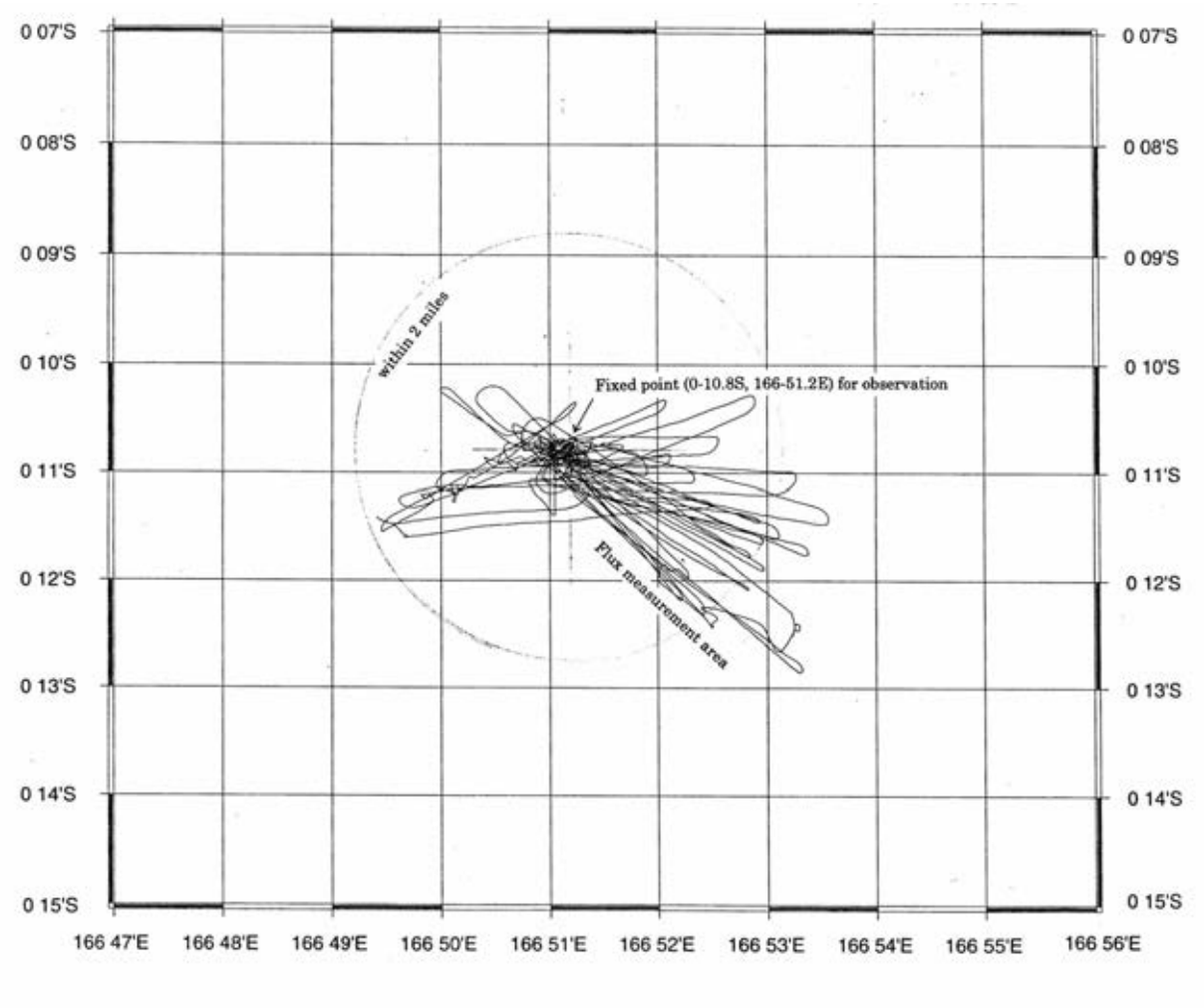

Fig. 9-4: Ship track in IOP phase 3.